Master Thesis

Analysis on Solar Retrofit in Combined Cycle Power Plants

ausgeführt zum Zwecke der Erlangung des akademischen Grades eines Master of Science
unter Anleitung von

Univ.Ass. Dipl.-Ing. Armin STEINER
Univ.Prof. Dipl.-Ing. Dr.tech. Markus HAIDER

E 302 - Institut für Energietechnik und Thermodynamik

erstellt an der

Technische Universität Wien
Fakultät für Maschinenwesen und Betriebswissenschaften von

Andrea MIGUEZ DA ROCHA

Wien, am 23.04.2010

Contents

1 Introduction

The objective of the thermodynamics studies of thermal power plants is the determination and maximization of the efficiency of combined cycle power plants. With other words, we wish to study and apply the methods for increasing the plant effectiveness by saving costs.

In the production of electricity the combined cycle power plants are largely known and developed. A combined cycle power plant is the combination of two cycles associated with the power production, Rankine and Brayton.

The Rankine cycle consists in a close steam cycle where the steam at high pressure is expanded in a turbine to produce power. The Brayton cycle is an open cycle in which air enters in a compressor for being mixed with fuel in a combustor chamber. The mixture of fuel and air, at high pressure and temperature, is expanded through a turbine which produces power. Both cycles are combined in a way that the energy in the exhaust gases of the gas turbine supports the steam cycle.

Gas Turbines are volumetric machines. At high ambient temperature the air and gas flow through the gas turbine decreases due to the lower air density. The gas turbine produces less power. The steam cycle is also over dimensioned due to the fact it is receiving less exhaust energy than in its design.

In this study we propose a solar retrofit for making up for the lack of input energy in the steam cycle from the gas turbine. Linear concentrating thermal technology is applied. The solar retrofit can deliver additional steam for the steam cycle without spending the investment costs of power island. Therefore the concept can be economically advantageous.

In the following process models of a single, two and three pressure combined cycle power plants will be developed and simulated with the software EBSILON® Professional 8.0. The different modes of operation will be analyzed. The performance of the three pressure combined cycle will be modeled under different load conditions.

Two different modes of boosting the combined cycle power plant will be studied and compared: boosting the steam cycle with saturated steam at high pressure (SHP) or with cold reheated steam (CRH). The chosen solution will be analyzed both technically and economically comparing two concentrating thermal technologies, Parabolic Trough Concentrators (PTC) and Pneumatic Pre-Stressed Concentrators (PPC).

2 Combined Cycle Power Plants

The combined cycle is one of the most efficient cycles in operation for power generation. Its thermal efficiency can reach 66%. In design conditions, the gas turbine supplies the 60% of the power, while the steam turbine delivers only the 34% of the energy.

The combined cycle exists in different configurations: single-shaft or multi-shaft. The difference is the number of gas turbines and heat recovery steam generators (HRSGs) delivering power to the steam turbine.

2.1 Gas Turbine

A gas turbine is an engine which allows the conversion of the energy of fuel in some form of useful power, such as mechanical power. The simplest cycle of a gas turbine is formed by a compressor, where the air is compressed until the required pressure; a combustion chamber, where the fuel and air at high pressure are mixed, and a turbine, where the mixture of gases are expanded after the combustion. In the turbine, the gases are expanded adiabatically generating a big amount of work. Part of the work obtained, between the 50% to 60%, is used to drive the compressor an the rest is delivered to the surroundings, Bathie [2].

The ideal Brayton cycle is shown in Figure2.1. The cycle efficiency is given by the following

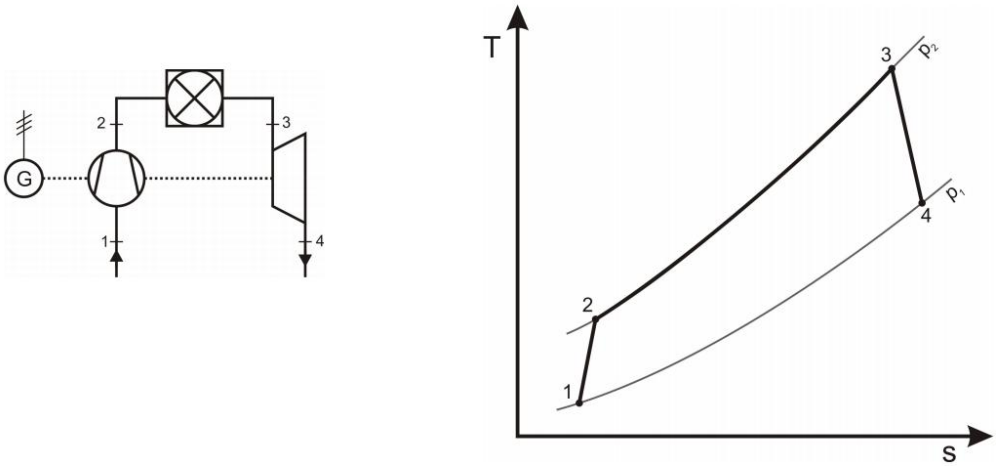

Figure 2.1: Simple Brayton cycle, [17]

relationship:

$$\eta = 1 - \left(\frac{1}{r}\right)^{\frac{(\gamma-1)}{\gamma}} \tag{2.1}$$

and depends only on the pressure ratio (r) and the nature of the gas (γ is the adiabiatic coefficient of the air).

By taking into account in the overall cycle efficiency, the efficiencies of the compressor (η_c) and the turbine (η_t) which work between the firing temperature (T_f) and the ambient tem-

perature (T_{amb}), we can obtain the following equation:

$$\eta_{cycle} = \left(\frac{\eta_t T_f - \frac{T_{amb} r^{\left(\frac{\gamma-1}{\gamma}\right)}}{\eta_c}}{T_f - T_{amb} - T_{amb}\left(\frac{r^{\left(\frac{\gamma-1}{\gamma}\right)}-1}{\eta_c}\right)} \right) \left(1 - \frac{1}{r^{\left(\frac{\gamma-1}{\gamma}\right)}}\right) \tag{2.2}$$

The Figure 2.2 shows how increases the cycle efficiency when the pressure ratio and the firing temperature increase. At a given firing temperature, the efficiency increases with higher pressure ratios; however, increasing the pressure ratio too much over a specific value can result in the opposite effect, lowering the overall efficiency.

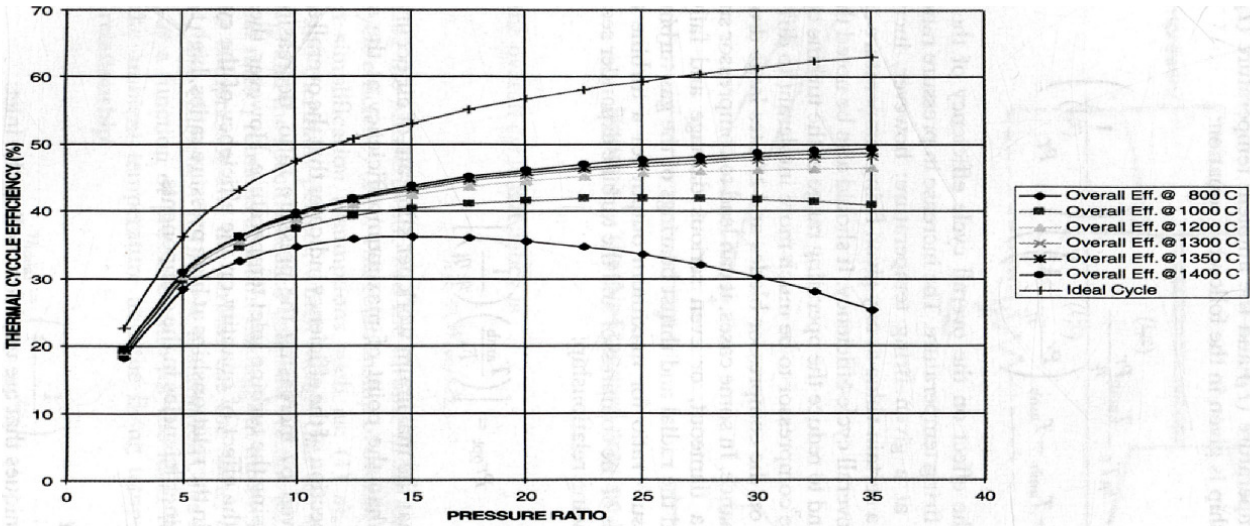

Figure 2.2: Overall Cycle Efficiency of the Pressure Ratio [3]

The optimum pressure ratio for getting the maximum power output of the turbine can be expressed by the following relationship:

$$r_{opt} = \left[\left(\frac{T_{amb}}{T_f} \right) \left(\frac{1}{\eta_c} \eta_t \right) \right]^{\frac{\gamma}{2-2\gamma}} \tag{2.3}$$

Comparing Figure 2.2 and Figure 2.3, we can come to the conclusion that the pressure ratio for reaching the maximum efficiency is much higher than for reaching the maximum work per kg of air.

It is necessary to be noted, that having a look at the efficiency equation we can conclude that the overall efficiency of the cycle can be improved by increasing the pressure ratio, decreasing the compressor inlet temperature or increasing the turbine inlet temperature.

2.1.1 Improvements for increasing the work output

There are many ways of improving the performance of the basic gas turbine and raising the cycle efficiency. We will discuss in the following three of the most common possibilities:

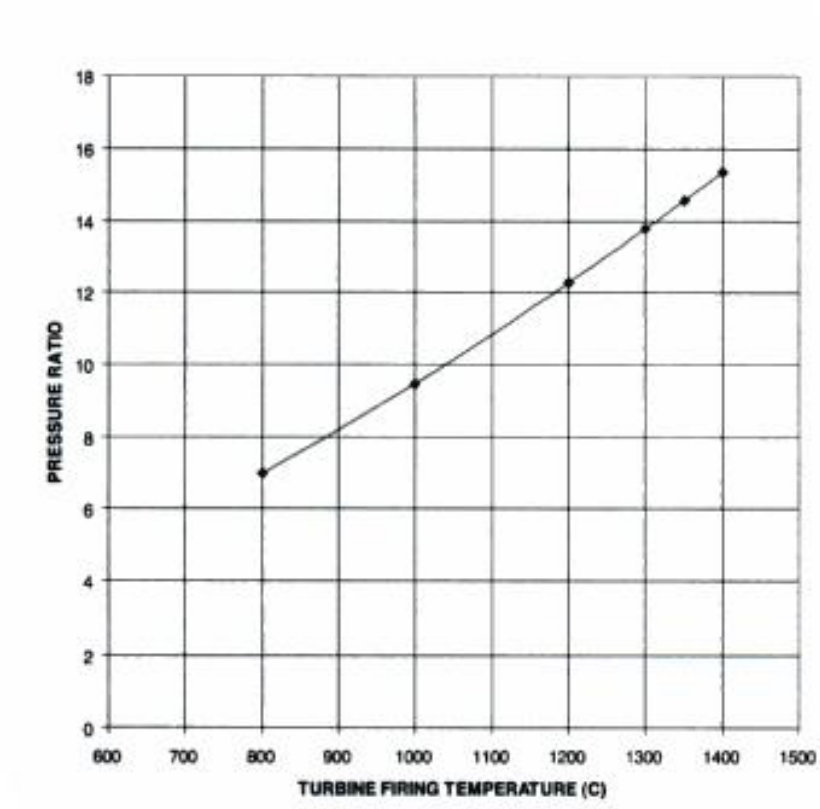

Figure 2.3: Pressure Ratio for Maximum Work per kg of Air[3]

Regeneration

The regeneration effect takes place by adding a heat exchanger which heats the air at its entrance reducing the fuel consumption. The efficiency can be increased because the flue-gas is hotter in the exhaust of the turbine than the air leaving the compressor. With the regeneration is possible to preheat the air before the combustion chamber so the necessary amount of fuel is smaller. This increases the cycle thermal efficiency without changing the work produced in the cycle, Bathie [2].

It is important to note that the higher effectiveness the regenerator the bigger heat exchanger, because the transferring area has to be also bigger. That means the pressure drop in the heat exchanger and the space required for the installation increase which lead to higher costs. It is necessary to find the equilibrium between increasing efficiency and lowering costs.

Intercooling

When the air enters the compressor a certain amount of work is needed to rise the pressure from the ambient to the turbine pressure. That amount of work can be reduced by dividing the compression process in two or more stages and cooling the air in between. Lowering the temperature of the air lowers the volume too and more mass of air can be compressed at the same time. Besides, dividing the process in more parts permits to approximate the

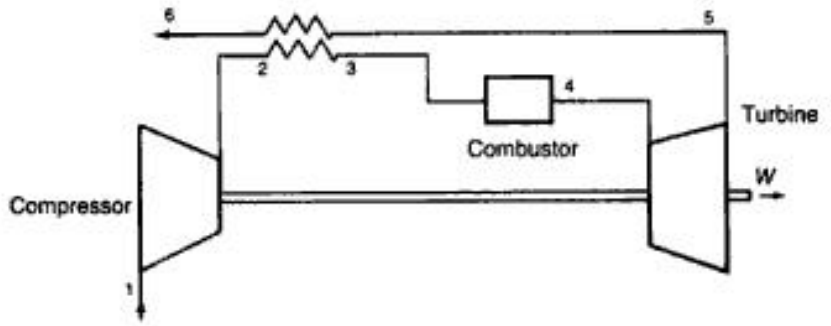

Figure 2.4: Regenerative Brayton cycle [4]

compression process to an isothermal process. The problem is with more stages the process becomes more expensive because more compressors are needed.

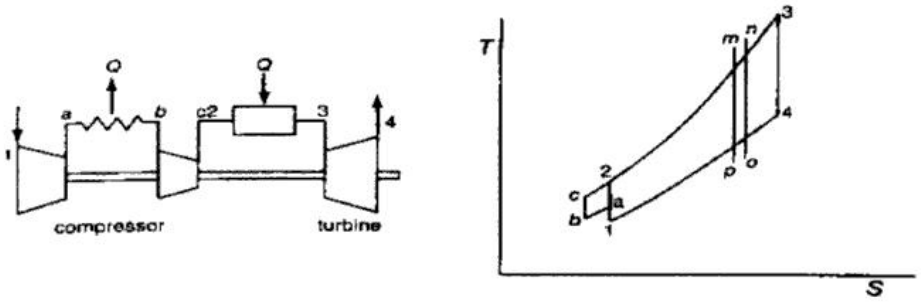

Figure 2.5: The Intercooled Gas Turbine Cycle [3]

Although the work given for the turbine does not increase, the work required for the compressor is lower. The result is, with intercooling more work can be delivered to the generator because the compression process needs less work.

It is important to say the work increases but does not occur the same with the efficiency of the cycle. Dividing the gas turbine cycle into a lot of cycles $(m-n-o-p-m)$ as in Figure 2.5 it is possible to simulate the Carnot cycle. The efficiency for the Carnot cycle is given by:

$$\eta_{CARNOT} = 1 - \frac{T_m}{T_p} \tag{2.4}$$

and when the specific heats are constant, we can assume

$$\frac{T_3}{T_4} = \frac{T_m}{T_p} = \frac{T_2}{T_1} = \left(\frac{P_2}{P_1}\right)^{\frac{\gamma-1}{\gamma}} \tag{2.5}$$

By joining all the Carnot cycles the gas turbine cycle can be simulated. But taking into account the additional part of the cycle due to intercooling $(a-b-c-2-a)$ the efficiency

will decrease because in that part the efficiencies of the Carnot cycles are smaller.

An intercooling regenerative cycle can increase the power output and the thermal efficiency. This combination provides an increase in efficiency of 12% and an increase in power output of about 30%, Boyce [3].

Reheat

The reheat is based in the same theory than the intercooling, but in this case the expansion is divided in stages in an intent to aproximate the expansion process to an isothermal process. For reheating, two turbines are necessary and between the first and the second stage the products of the combustion are reheated until the maximum temperature of the cycle. That permits to obtain more work during the second part of the expansion process.

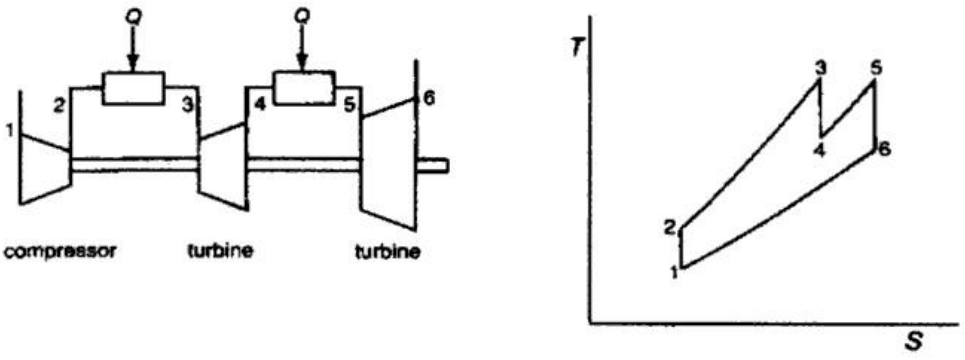

Figure 2.6: Reheat cycle and T-s diagram [3]

There is an intermediate pressure which divides the stages for both process, reheat and intercooling. The optimum value for that pressure is given by the following equation, Boyce [4].

$$p_i = \sqrt{p_1 p_2} \tag{2.6}$$

2.1.2 Part-load performance

The variation of thermal efficiency with reduction in power, sometimes referred to as *part-load performance*, is of major importance in applications where considerable running at low power settings is required, Saravanamuttoo [1].

When determining the off-design performance it is important to be able to predict not only the effect on thermal efficiency at part load, but also the effect of ambient conditions on maximum power output, the effects of high and low ambient temperatures and pressures must be considered. The variation of maximum power with ambient conditions is clearly of prime importance to the customer, and the manufacturer must be prepared to guarantee the performance available at any specified condition. Cold conditions are beneficial for power output and result in a modest increase in efficiency, while warmer conditions cause large

decrease in both power output and efficiency.

The start point for studying the flow rate behaviour of a multistage turbine is the investigation of the behaviour of a single stage. If we apply the continuity equation to a cross section in a nozzle, every unit of section is being crossed for an amount of flow:

$$\frac{\dot{m}}{A_{min}} = \rho c = \mu \rho_s c_s \tag{2.7}$$

where μ is the flow rate, ρ and c the medium magnitudes, and ρ_s and c_s, the isentropic medium values of density and velocity in the cross section. The flow rate depends of the efficiency and because of that depends also of Reynolds and Mach. In most of the practical cases the variation of μ is very small because Reynolds values are high enough.

The velocity in the outlet of the stage is calculated with the total pressure at the inlet, p_A, and the static pressure at the outlet, p_B:

$$c = \sqrt{\frac{2\kappa}{\kappa - 1} p_A v_A \left[1 - \left(\frac{p_B}{p_A}\right)^{\frac{\kappa-1}{\kappa}}\right]} \tag{2.8}$$

For the density $\rho = 1/v$

$$\rho_s = \frac{1}{v_A} \left(\frac{p_B}{p_A}\right)^{\frac{1}{\kappa}} \tag{2.9}$$

Combining equations 2.8 and 2.9, we obtain:

$$\dot{m} = \mu A \frac{p_A}{\sqrt{p_A v_A}} \sqrt{\frac{2\kappa}{\kappa - 1}} \sqrt{\left(\frac{p_B}{p_A}\right)^{\frac{2}{\kappa}} - \left(\frac{p_B}{p_A}\right)^{\frac{\kappa+1}{\kappa}}} = \mu A \sqrt{\frac{p_A}{v_A}} \xi \tag{2.10}$$

The capacity is described by the next function

$$\xi = \sqrt{\frac{2\kappa}{\kappa - 1} \left[\left(\frac{p_B}{p_A}\right)^{\frac{2}{\kappa}} - \left(\frac{p_B}{p_A}\right)^{\frac{\kappa+1}{\kappa}}\right]} \tag{2.11}$$

For the sound pressure ratio

$$\frac{p_{B\kappa}}{p_A} = \left(\frac{2}{\kappa + 1}\right)^{\frac{\kappa}{\kappa-1}} \tag{2.12}$$

it is possible to obtain the maximum value

$$\xi_{max} = \left(\frac{2}{\kappa + 1}\right)^{\frac{1}{\kappa-1}} \sqrt{\frac{2\kappa}{\kappa + 1}} \tag{2.13}$$

If the pressure ratio decreases below the critical value compare to the equation (2.12), the

capacity does not change, that means that the capacity function ξ remains at the maximum level. By leaving $\kappa = constant$, the relative capacity function:

$$\phi = \frac{\xi}{\xi_{max}} \tag{2.14}$$

which looks like in Figure (2.7).

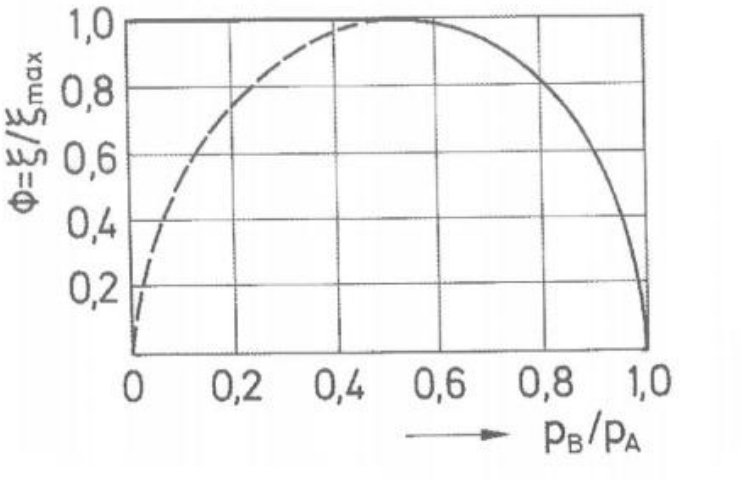

Figure 2.7: Relative flow rate function, [15]

The behaviour presented is associated with an ideal single nozzle. When we connect more nozzles in series, we can make an approximate statement for a complete turbine. The flow is in critical conditions in such a configuration, equation (2.12) has to be filled for at least one nozzle. The product of the pressure ratio of all nozzles has to be smaller than in equation (2.12), due to the fact that the pressure ratio, p_B/p_A, for the rest of nozzles have to be below the unity.

The point K in the Figure 2.8 slices to the left until finally, for a multi-stage turbine, we obtain an ellipse as the curve which describes the turbine behaviour.

For this case the function can be approximated for a circle,

$$\phi = \sqrt{1 - \left(\frac{p_B}{p_A}\right)^2} \tag{2.15}$$

Furthermore, the flow rate is influenced by the rotation of the turbine. Therefore the function $\bar{\mu}$ is formed. Now it is possible to describe the ratio of two flow rates by using equation (2.10), where the index "0" marks the design case.

$$\frac{\dot{m}}{\dot{m}_0} = \frac{\bar{\mu}}{\bar{\mu}_0} \frac{p_A}{p_{A0}} \sqrt{\frac{p_{A0}}{p_A} \frac{v_{A0}}{v_A}} \frac{\phi}{\phi_0} \tag{2.16}$$

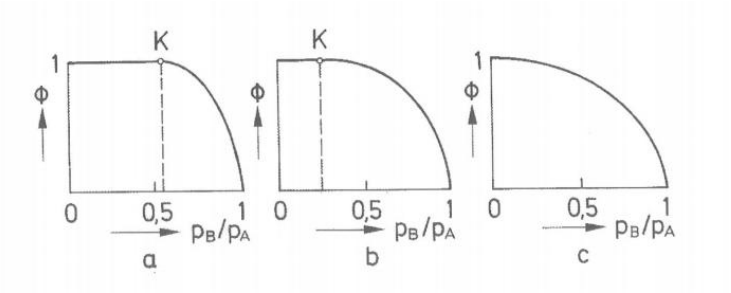

Figure 2.8: Relative flow rate function, [15]

Taking into account the caloric equation of state $p_A v_a = \frac{\kappa-1}{\kappa} h_A$, we get:

$$\frac{\dot{m}}{\dot{m}_0} = \frac{\bar{\mu}}{\bar{\mu_0}} \frac{p_A}{p_{A0}} \sqrt{\frac{h_A 0}{h_A}} \frac{\phi}{\phi_0} \tag{2.17}$$

For a multi-stage turbine the influence of the revolution speed is small, so we can state $\bar{\mu}/\bar{\mu_0} = 1$. Finally, we write the simplified equation as:

$$\frac{\dot{m}}{\dot{m}_0} = \sqrt{\frac{h_{A0}}{hA}} \sqrt{\frac{p_A^2 - p_B^2}{p_{A0}^2 - p_{B0}^2}} \tag{2.18}$$

In steam turbines the conditions at the entrance can be changed by the throttling, so it is possible to say that $h_A = h_{A0}$. If $h_A = h_{A0} = constant$ the equation (2.18) describes a cone cylindrical surface.

In steam turbines and stationary gas turbines the case of constant power output have a practical meaning. With $p_B = p_{B0} = constant$ and a fixed ratio h_A/h_{A0} the equation (2.18) describes a hyperbola. That is described in the Figure 2.9, with $\dot{m}$ as abscissas and p_A as ordinates. h_A/h_{A0} appears as parameter. For ratios $p_A/p_B > 4$ the hyperbola can be quite exactly replaced with its asymptote in the way that the flow ratio will be directly proportional to the initial pressure.

$$\frac{\dot{m}}{\dot{m}_0} = \sqrt{\frac{h_{A0}}{h_A}} \frac{p_A}{p_{A0}} \tag{2.19}$$

In the turbine condenser the final pressure has only a hundredth bar, that means that practically $p_B = p_{B0} = 0$ can be applied in the (2.19) for all the pressure range.

2.2 Steam Cycle

The steam turbine is an engine in which a steam flow, at high pressure and temperature, is expanded transforming its energy into kinetic energy, which is as well converted into work by moving the rotational parts of the turbine, Boyce [3]. The performance of the steam turbine is described by the Rankine cycle.

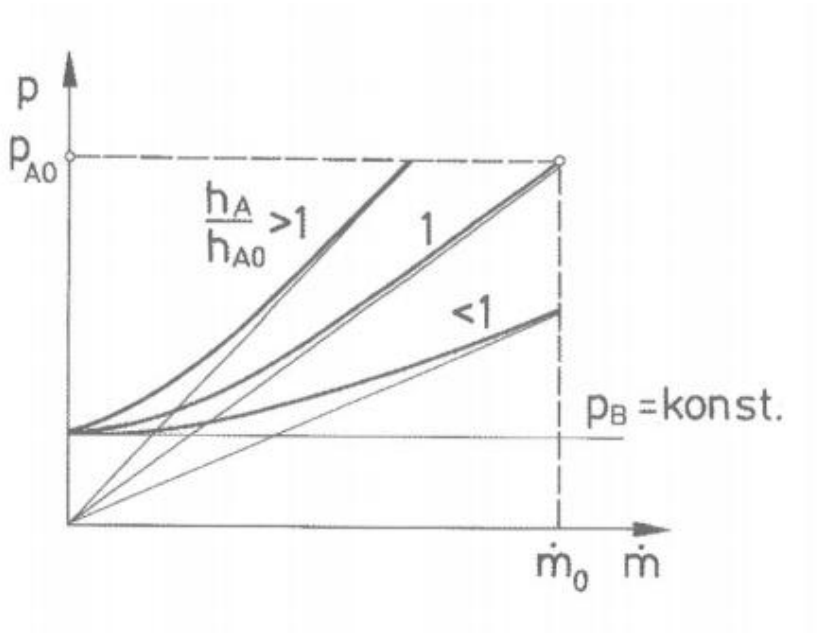

Figure 2.9: Ratio between mass flow and inlet pressure by leaving the outlet pressure constant, [15]

The Rankine cycle is the most common thermodynamic cycle utilized in the production of electrical power with water-steam as the working fluid and consists in two isobaric and two adiabatic processes. Pumped water from low to high pressure enters a boiler where it is heated at constant pressure by an external heat source to become a dry saturated steam. The saturated steam expands through a turbine, generating power and decreasing its temperature. The wet steam enters a condenser to become a saturated liquid.

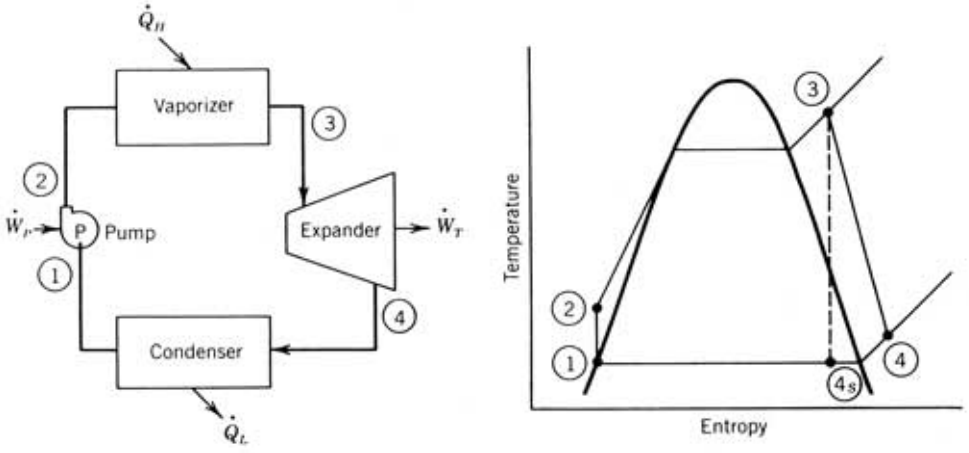

Figure 2.10: Rankine cycle

The thermal efficiency of the Rankine cycle is given by the following expression:

$$\eta = \frac{(\dot{W}_{turb} - \dot{W}_{pump})}{\dot{Q}_{in}} \approx \frac{\dot{W}_{turb}}{\dot{Q}_{in}} \tag{2.20}$$

The work required for pumping the water is very small compared with the work that the turbine produces, so is not taken into account at the time to estimate the efficiency.

In a real Rankine cycle, the compression in the pump and the expansion in the turbine are not isentropic. In other words, these processes are non-reversible and entropy is increased during the two processes. This increases the power required by the pump and decreases the power generated by the turbine.

In particular the efficiency of the steam turbine will be limited by water droplet formation. As the water condenses, water droplets hit the turbine blades at high speed causing pitting and erosion, gradually decreasing the life of turbine blades and efficiency of the turbine. The way used to avoid this problem is superheating the steam.

As for the gas turbine, there are improvements for increasing the efficiency of the cycle:

In the reheated cycle two turbines work in series and after the first expansion in the high pressure turbine the steam re-enters the boiler and is reheated almost until the maximum temperature of the cycle. Then pass through the second, lower pressure turbine. Among other advantages, this prevents the vapor from condensing during its expansion which can seriously damage the turbine blades, and improves the efficiency of the cycle.

In the regenerative Rankine cycle the water after emerging from the condenser (possibly as a subcooled liquid) is heated by steam tapped from the hot side of the cycle.

2.2.1 Types of Condensers

In the condenser the steam leaving the turbine in the steam turbine is condensate to water. The steam quality before entering the turbine is usually between 90% to 96% which means 10% to 4% of liquid in the mixture, Boyce [3].

The amount of heat removed ($\dot{Q}_c$)by the condenser is given by the next equation:

$$\dot{Q}_c = \dot{m}_s(h_s - h_c) \tag{2.21}$$

where $\dot{m}_s$ is the mass flow of steam through the condenser, h_s is the enthalpy of the steam leaving the steam turbine and h_c is the enthalpy of the liquid leaving the condenser.

In condensers, working with water or with air, the amount of heat extracted from the steam has to be the same that the cooling fluid receives.

$$\dot{m}_s(h_s - h_c) = \dot{m}_{air}(h_o - h_i) = \dot{m}_w C_{pw}(T_o - T_i) \tag{2.22}$$

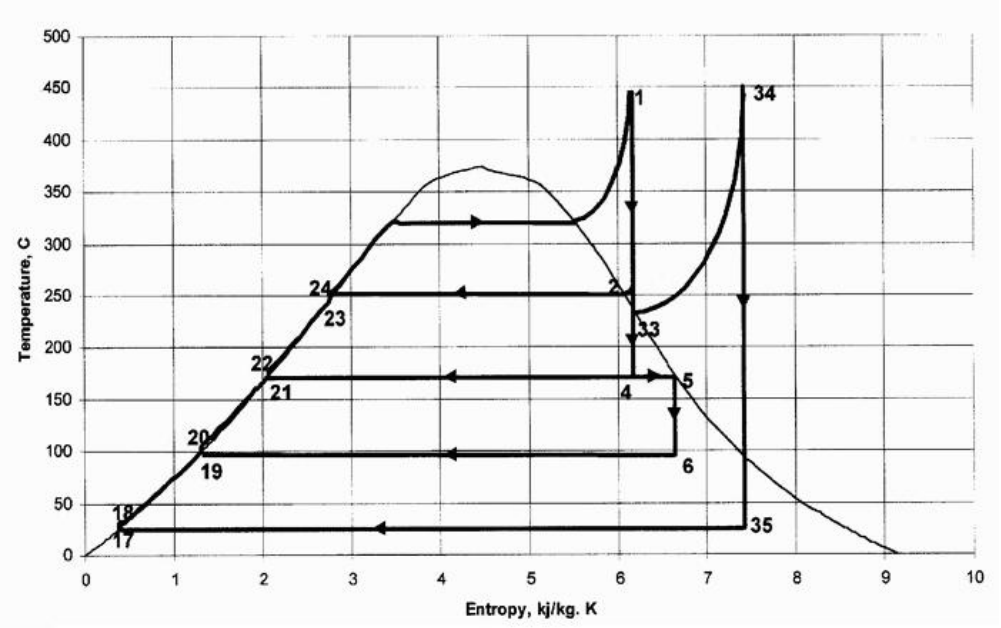

Figure 2.11: Regenerative and reheated Rankine cycle, [22]

where $\dot{m_{air}}$ and $\dot{m_w}$ are respectively the mass of air and water and the the subscripts "o" and "i" refers to the values at the condenser output and inlet.

The overall thermal transmittance (U) in a condenser is the amount of heat transmitted per unit of time, unit of surface and degree of temperature difference being the property which defines the behavior of the condenser. The thermal transmittance is written as in the equation (2.23):

$$U = \frac{\dot{m_w} C_{pw}}{A} Ln\left(\frac{\theta_1}{\theta_2}\right) \tag{2.23}$$

where θ_1 is the temperature difference between the steam and the cooling water entering the condenser, and θ_2 is the temperature difference between the the steam and the cooling water after passing through the condenser.

The most common types of condensers used in combined cycle power plants are the water-cooled condenser and the air-cooled condenser.

Water-cooled Condenser

In this type of condensers, the cooling water is the refrigerant fluid and it removes the heat from the steam flow condensing the steam to water. That condenser consists of a bunch of pipes through which the cooling water flows while the steam flows out of the pipes. The cooling water can be provided from a river or the sea, from where it is pumped to the condenser. Before returning to the river or sea the water is put in a holding pond. The water-cooled condenser can be either classified in shell-and-tube or in tube-and-tube type, Petchers [6].

Air-cooled Condenser

The Air-cooled condenser is used in places where it is difficult to find a source of cooling water. This is generally the most expensive type of condenser. When the ambient temperature is high the resulting operation temperature in the condenser can reduce significantly the efficiency of the refrigerator system. Air-cooled condensers do not need water treatment and have less problems of freezing up with cold temperatures. Air-cooled condenser require less maintenance than other types but the service life is shorter than water-cooled condensers due to the coil degradation.

In air-cooled condensers the steam flow is condensed into finned tubes by ambient air. The cooling air is moved by axial fans, which are moved by electric motors.

Cooling Tower

A cooling tower is a heat exchanger in which two fluids, water and cooling air, are put in direct contact to transfer heat. The process consists of a water flow which is sprayed into a rain-like pattern, through which the ambient air is induced by fans.

2.3 Heat Recovery Steam Generator

The heat recovery steam generator (HRSG) is an important subsystem of a combined power plant which uses the energy from the exhaust gases of the turbine for transferring heat to water and generating steam at high temperature and pressure.

The exhaust gases leave the gas turbine at approximately ambient pressure and at very high temperature (500°C to 600°C). This energy is used for the HRSG to produce steam. Although there are many configurations of HRSG, most of them are divided in the same number of sections as the steam turbine. There is one section for high pressure (HP), low pressure (LP) and sometimes for an intermediate pressure (IP). Each section of the HRSG has a evaporator or steam generator and depending on the section is possible to find an economizer or a superheater, Boyce [4].

A HRSG is composed basically of individual heat exchangers which exchange the energy from the exhaust gases of the turbine with the water/steam of the Rankine cycle.

The water enters first in the economizer for being pre-heated and then goes through the evaporator where the steam is generated at constant pressure and temperature. Finally the steam is superheated in the superheater. After that, the superheated steam enters the turbine where it is expanded and the power is generated.

The majority of the heat is transferred by convection and for increasing the heat surface finned tubes are used. As the heat transfer on the waterside is much higher than on the exhaust gas side, due to the bigger temperature difference between gas and water than between gas and steam, the fins are used on the gas side to rise the heat transfer.

2.3.1 Types of HRSGs

The selection of the HRSG depends of many factors but the most determinant are the initial cost and the global efficiency of the plant. A 1% of increase in efficiency leads to a 3-4% of increase in the costs, Boyce [3].

The most common units used in combined cycle power plants are the the drum type HRSG with natural circulation. The type shown in Figure 2.12 is formed by separate components: drums, economizers, superheaters, generating tubes and blowdown systems. The tubes are disposed vertically and the exhaust gas flow is horizontal. In HRSGs with forced circulation, the mixture of steam and water is pumped through the evaporator tubes. But the use of pumps brings to the cycle a parasitic load lowering the efficiency of the cycle. There are some vertical HRSGs with natural circulation or the other possibility are the Once Through Steam Generators, which do not have the defined sections as we can find in the drum HRSG. The OTSG is a pipe in which the water enters at one side and the steam leaves the pipe at the other side. There are no evaporators and no drums so there is no defined point where the evaporation takes place and the interface between water and steam changes its position depending on the heat supplied.

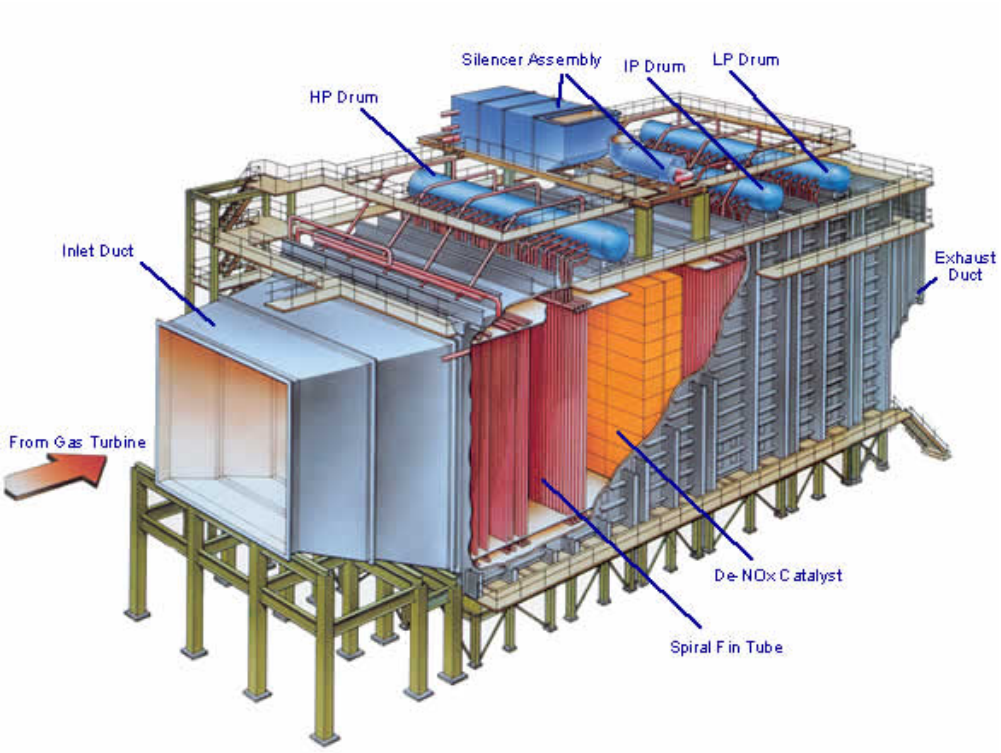

Figure 2.12: Section of an horizontal HRSG, [20]

The three different types of HRSGs are shown in Figure 2.13.

Water is being delivered to the drum with the help of the pumps. In the drum, the

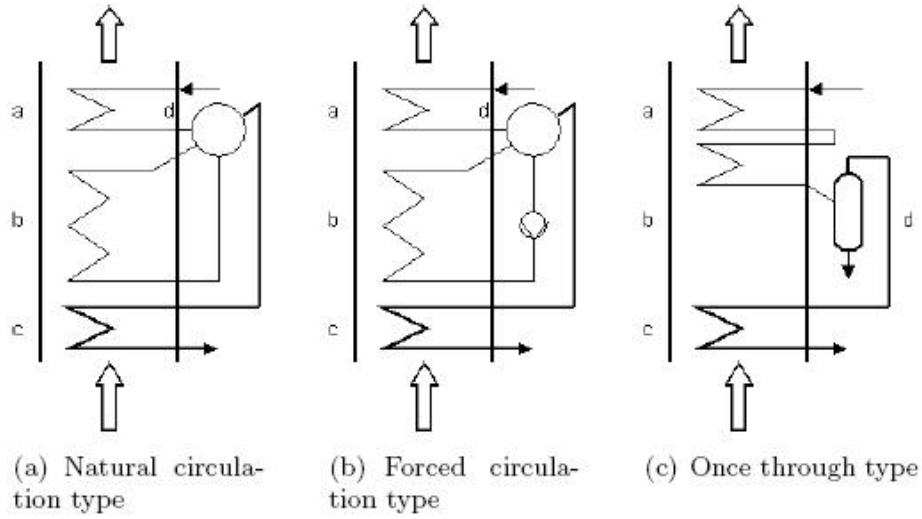

(a) Natural circulation type (b) Forced circulation type (c) Once through type

Figure 2.13: Types of HRSGs, [20]

feed water is mixed with the mixture of water/steam being the steam separated due to the higher density of the water.

The circulation ratio can be described as the ratio between the mass flow of water circulating into the evaporator and the mass flow of steam leaving the evaporator, Effenberger [21] .

$$U = \frac{m_{circ}}{m_s} \tag{2.24}$$

The circulation ratio depends on the pressure and normal values for natural circulation are from 5 to 50 and pressures around 160 bar, while for forced circulation normal values are between 3 to 10 and pressures around 180 bar.

Other possible classification for HRSG can be made depending on supplementary firing. There are unfired, supplementary fired and exhaust fired HRSGs. In unfired HRSGs, the energy supplied for the turbine is used without changes, while in the others the mass of gas from the turbine is mixed with additional fuel to increase the steam production, Boyce [3].

One of the advantages of the supplementary firing is that the system is able to follow the demand, providing more power at peak loads. In these systems the gas turbine is sized according to base load demand, but it has to deliver enough power for higher peaks loads.

2.3.2 Design considerations

Some other features should be taken into account in the design of HRSGs.

Pinch Point

The pinch point is the temperature difference between the gas at the evaporators exit and the steam saturation temperature. For lowers pinch points the transferred heat is higher. But the heating surfaces have to be bigger with the consequent increase of pressure drop and costs. Higher pinch points could mean a lower production of steam. The range for normal values of pinch points is between 8-22° C.

Approach Temperature

The approach temperature is defined as the temperature difference between water at the evaporator inlet and the steam saturation temperature. The production of steam is higher at small approach temperatures. Typically, approach temperatures are in the 5.5-11° C range.

The Figure 2.14 represents the q,T diagram for one section of the HRSG where we can see the evolution of the water and steam going through the HRSG:

Off-design performance

The gas turbine performance and in particular the exhaust energy determines the operation of the HRSG. The variation in the ambient conditions, the load or the own health of gas turbine change the output conditions of the gas flow, changing the behavior of the HRSG too.

Gas turbines without inlet air temperature cooling deliver at high ambient temperatures less power due to the higher air density, increasing the volume of the air and decreasing the mass flow of air which can be compressed at the same time. As Ganapathy [5] says, the power output could variate as much as 15-25% between the coldest and hottest temperatures. To avoid this change of performance the possibilities are use evaporative coolers, mechanical or absorbtion chillers or thermal storage can be used.

Temperature (° C)	-6.7	4.4	15.6	26.7	37.8	48.8
Power (kW)	38.15	38.6	35.02	30.82	27.36	24.04
Exhaust Temperature(° C)	390	415.6	425	437.8	450.6	465.6
Exhaust Flow (kg/s)	141.52	137.89	129.73	119.75	110.68	102.06

Table 1: GT Performance at different ambient temperatures. Data for LM 5000 gas turbine, [5]

In Table 1 and Figure 2.16 we can see that the power output in the gas turbine and the flows of gas and steam have a decreasing tendency when the ambient temperatures are hotter.

When the gas turbine load decreases, the exhaust temperature of the gas turbine goes down. As the mass flow of gas contains less energy the steaming potential in the HRSG decreases.

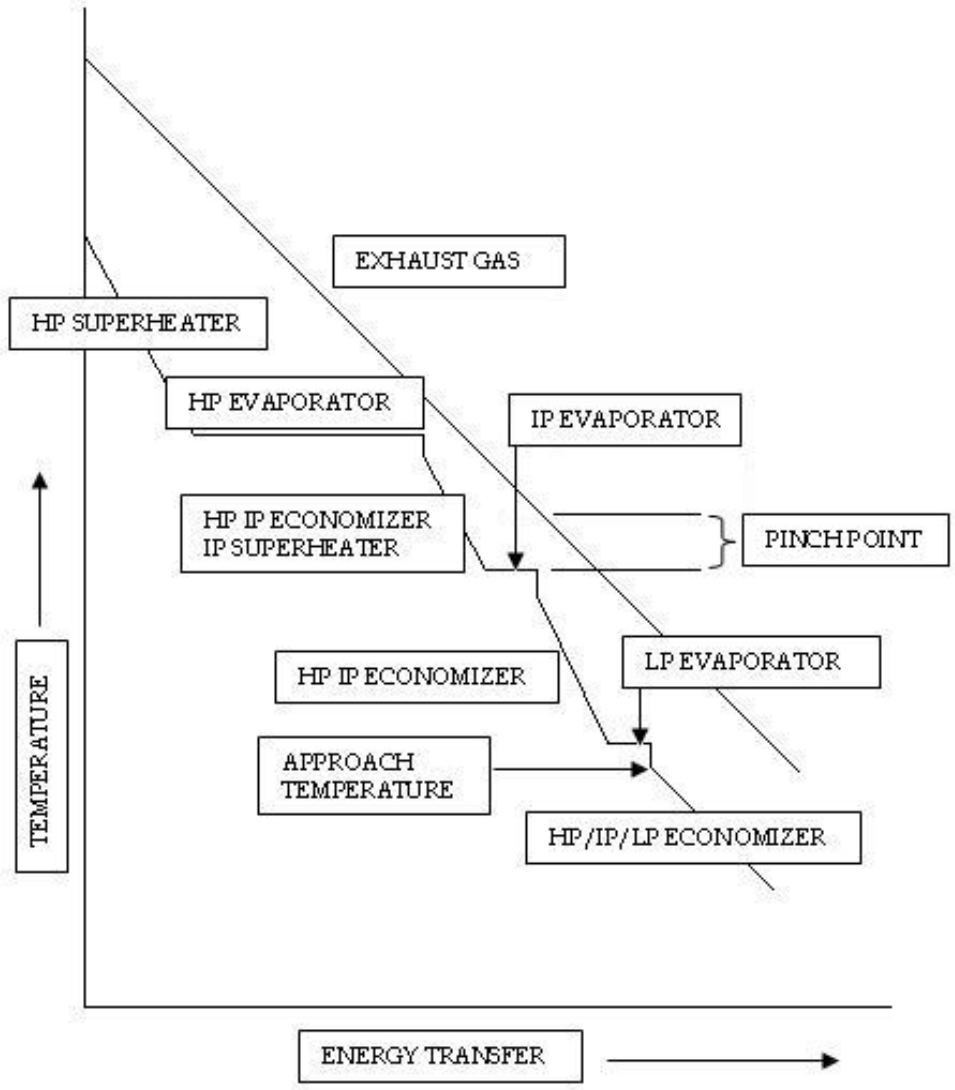

Figure 2.14: Energy transfer diagram in an HRSG of a combined cycle power plant, [4]

2.4 Combined Cycle Power Plants

A Combined Cycle Power Plant, CCPP, is the combination of two cycles: Brayton and Rankine. The Brayton cycle works as the topping cycle and the Rankine cycle as the bottoming, being the energy transferred from the gas cycle to the steam cycle. The HRSG is the component which transfers the energy from one to the other cycle. Thermal efficiencies of the combined cycles can reach as high as 60%, Boyce [3]. In the typical combination the gas turbine produces about 65% of the power and the steam turbine about 35%, while unit thermal efficiencies of the gas turbine and the steam turbine are between 30%-40%.

The condensate entering the HRSG goes through a deaerator where the gases from the

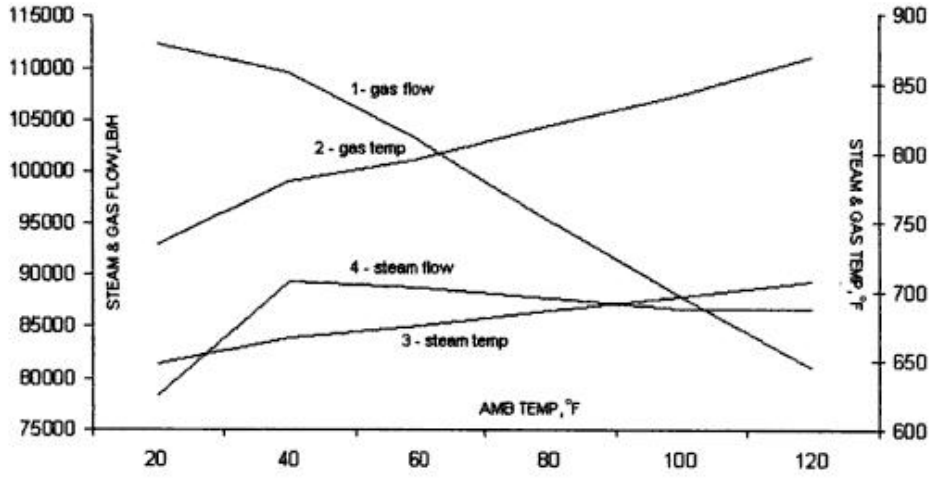

Figure 2.15: HRSG performance versus ambient temperature. Gas flow shown has a multiplication factor of 0.1, [5]

water or steam are removed. This is important because a high oxygen content can cause corrosion in the pipes and the rest of components in contact with the water/steam. The deaerator is normally placed on top of the feedwater tank and the process occurs when the water is sprayed and then heated, thus releasing the gases.

Deaeration also takes place in the condenser and sometimes this could lead to not utilizing a separate deaerator/feedwater tank, and the condensate being fed directly into the HRSG from the condenser.

The economizer is used to heat the water under its saturation temperature. The risk of generating steam in the economizer has to be taken into account because that can block the flow. To prevent the appearance of steam in the economizer a feedwater control valve can be installed for keeping the pressure high and avoiding the steaming.

The steam turbines in most of the large power plants are at minimum divided in two sections: the High Pressure Section (HP) and the Low Pressure Section (LP). In some plants, the HP section is as well divided into a High Pressure Section and an Intermediate Pressure Section (IP). The HRSG is divided in the same sections as the steam turbine. The LP steam turbine's performance is further dictated by the condenser backpressure, which is a function of the cooling and the fouling.

The efficiency of the steam section in many of these plants varies from 30%-40%. To ensure that the steam turbine is operating in an efficient mode, the gas turbine exhaust temperature is maintained over a wide range of operating conditions. This enables the HRSG to maintain a high degree of effectiveness over this wide range of operation.

In a combined cycle plant, high steam pressures do not necessarily imply a high thermal efficiency. Expanding the steam at higher pressure causes an increase in the moisture con-

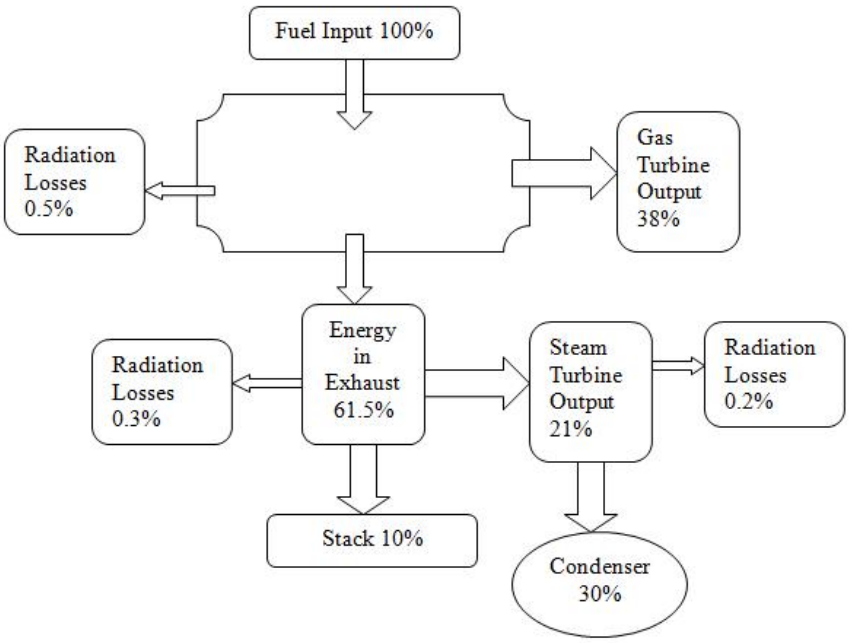

Figure 2.16: Energy Distribution in a Combined Cycle Power Plant, [3]

tent at the exit of the steam turbine. The increase in moisture content creates major erosion and corrosion problems in the later stages of the turbine. A limit is set at about 10% moisture content, Boyce [4].

One advantage of working with high steam pressures are that the volume flow of steam is reduced. That means that the sections of turbines, condenser, pipes and the rest of components can be smaller and the cost decreases.

However, increasing the steam temperature at a given pressure lower the steam output of the steam turbine slightly. This occurs because of two contradictory effects: first the increase in enthalpy drop, which increases the output; and second the decrease in flow, which causes a loss in steam turbine output. The second effect is more predominant, which imply the lower amount of steam. Besides, lowering the temperature of the steam also increases the moisture content.

Increasing the pressure of any section (LP, IP and HP turbines) will increase the work output of the section for the same mass flow. However, at higher pressure, the mass flow of the steam generated is reduced.

3 Concentrating Solar Power Plants

Solar energy is the energy generated by the sun which is converted in useful energy by the human being for heating or electricity generation. Every year the sun supplies 4 times more energy than we consume, so its potential is almost unlimited.

The technology used in thermal power plants is the same used in conventional power plants, except that the heating source is the Sun. The heat energy is used to drive a steam turbine and to produce electricity with generators coupled to the turbines. In the conventional power generation, the heat energy comes from combustion of fossil fuels or from nuclear fission. Unlike traditional power plants, concentrating solar power systems produce a source of energy without emissions and the only impact is the land use. Other benefits of concentrating solar power plants include low operating costs and an increase in energy independence from foreign oil imports.

Solar energy, in contrast with fossil fuels, is not available around the clock and the intensity of the available energy in a defined point of the Earth depends on the day of the year, the hour and the latitude. Besides, the quantity of energy that can be obtained depends on the orientation of the receiver mechanism. The gaps can be filled in two ways: switching to fossil fuel combustion or storing the colected heat energy for when the Sun is not available.

Concentrating solar power plants produce electric power by converting the energy of the sun into high-temperature heat using various mirror configurations which concentrate the rays of the Sun for obtaining a high temperature. At least 300°C are necessary in order to generate power effectively and economically. For reaching this is essential to have a high percentage of direct solar radiation. This is more the case in the Sun Belt between the 35^{th} northern and 35^{th} southern latitudes.

Concentrating solar power (CSP) plants consist of two parts: one that collects solar energy and converts it to heat (solar field), and another that converts heat energy to electricity (power island). The power gained from sunlight can be increased if the light is gathered and concentrated on a single point and the heat is then channeled through a conventional generator. For concentrating the Sun's rays there are two possibilities: concentrating the radiation in a fixed point (here the concentrators have to follow the Sun by moving along two axes) or using linear concentrators and only need to move along one axis in order to follow the Sun.

3.1 Solar Thermal Concentrating Collectors

In practice the most used concentrators are linear concentrators because they are more suitable for assembly on a large scale and less costly to construct. The different types of linear concentrators are explained in the following.

3.1.1 Parabolic-Trough Power Plants

The first commercial CSP were parabolic trough systems installed in the United States in the 1980's and are the most proven, developed and commercially-ready CSP technologies.

Parabolic trough technology is a clean and mature solar power solution with years of successful power generation behind it. The technology has been improving steadily for the last 30 years, and modern troughs operate more efficiently and at lower cost. Today, there is more than 700 MW of CSP trough power in operation around the world, with 400 MW under construction and around 20 GW in development.

The parabolic trough collector is a linear concentrator which is moved along one axis and focuses the Sun's energy to a fluid carrying receiver tube situated at the focal point where the mirror concentrates all the sunlight. The tube is filled with a thermo-oil as heat transfer medium and it is heated when it passes through the solar collector and then flows into a heat exchanger where the steam is generated. The latest parabolic trough collectors use synthetic oils and they can reach the temperature of 350°C. Due to the limited temperature in thermo-oil systems and also the high cost of the thermo-oil, next generation of CSP aims at using direct steam generation. We will use water in our study of a CCPP with Solar Boosting.

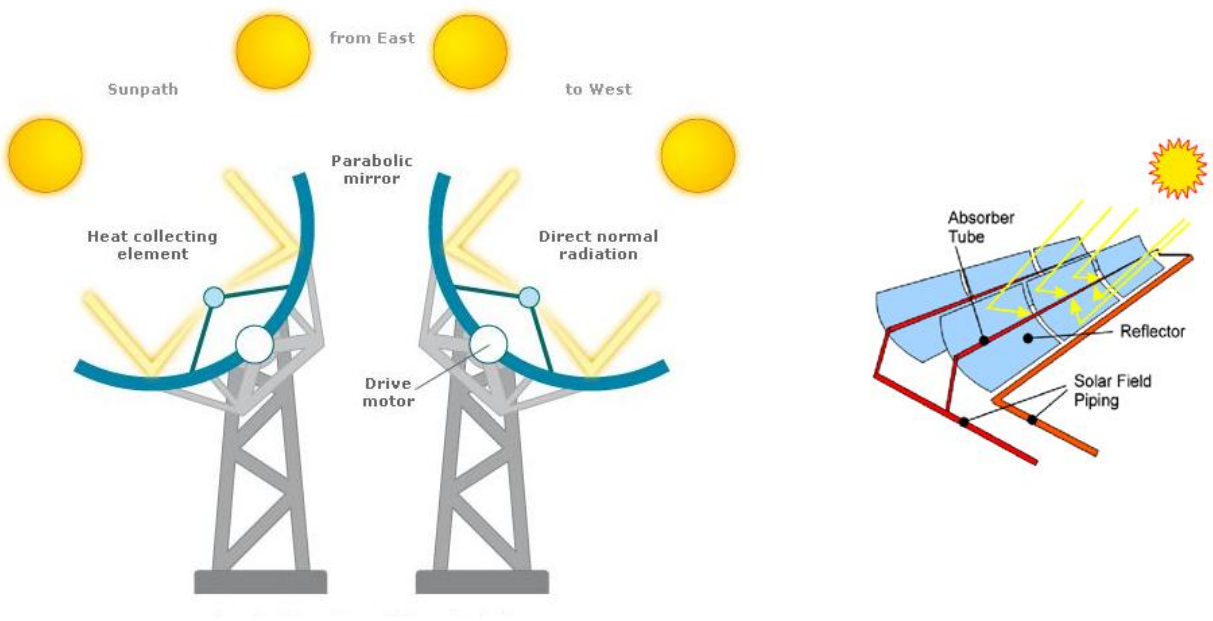

Figure 3.1: Operating Scheme for Parabolic Trough Technology, [9]

The troughs are placed in parallel rows to form a collector field. The rows lined-up along a north-south axis can track the sun's trajectory during the day, ensuring that the sunlight is always focused on the receiver tube. Some trough systems incorporate thermal storage to produce electricity even when the sun is not shinning.

The actual dimensions of the parabolic trough collectors are: the opening width have 5.71 m and the collector length have 99 m. The absorber pipe is made of steel, covered with an optically-selective surface coating and inserted in an evacuated glass tube. It absorbs the radiation from the solar spectrum effectively keeping the thermal losses to the ambient at minimum by re-radiating only a small amount of radiation energy. Thick glases with a

low content of iron are used to built the mirrors. German organizations have developed the Eurotrough collector, which is lighter and stiffer, and is less cost to produce, to assemble and to maintain.

Figure 3.2: Parabolic trough solar collectors at Kramer Junction in the Mojave desert in California, [19].

In Europe, two power plants called Andasol I and II and situated in Granada, Spain, are currently in operation using the parabolic trough technology and delivering to the electric grid 50 MW_e output power each. In California, the nine SEGS (Solar Electricity Generating System) have three generations of parabolic trough collectors in service, Wengenmayr [8].

Linear Fresnel Collectors are a similar design which uses a long, narrow, shallow-curvature or flat mirrors to focus the light onto a linear absorber positioned above the mirrors.

3.1.2 Dish Stirling Systems

The dish concentrator is a parabolic silvered dish, which by moving along two axes focuses the radiation of the Sun onto a single point. At the focus point the receiver is situated and there is as well a thermal engine directly connected to it. These systems work as an independent power generation, being unconnected to a power grid.

Their principal advantage is a very high efficiency over 30%, which is a result of the combination of a nearly paraboloid concentrator with an excellent thermal engine. When the Sun is not shining the dish stirling can be fed with fuel is satisfy the power demand. The maximum size of the dish stirling is limited by the wind forces, which deform the reflecting surface. The maximum surface is 100 m^2 and the maximum electric power output is 10kW.

Figure 3.3: Solar Power Group's Fresnel mirror test rig at the Plataforma Solar de Almeria in Spain,[19].

The costs of generating electricity are still above those of parabolic trough power plants. However, cost may decrease in the near future.

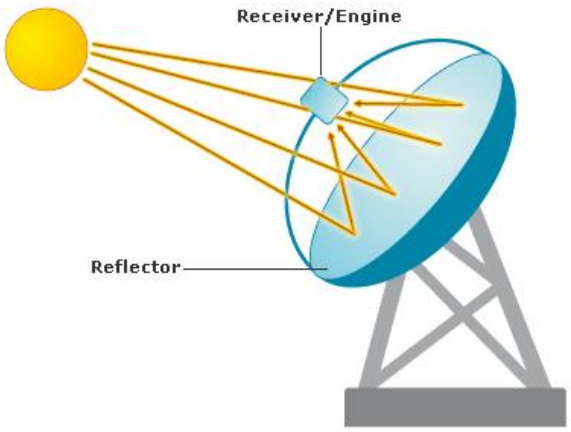

Figure 3.4: Dish Stirling Operating Scheme, [9]

3.1.3 Central Receiver System

The central receiver system divides the big surface of the dish stirling in smaller concentrator mirrors called heliostats. The heliostats focus the rays of the Sun onto a common point sit-

uated on a central tower, where the receiver collects the heat. The heliostats are flat mirrors and they can not concentrate as much as the ideal paraboloid does.

Large central receiver systems with thousands of heliostats, each with 100 m^2 of reflecting surface, require towers of 100-200 m high and they can collect several hundred MW of solar radiation power.

The first plant with central receiver system called PS10 is situated in Solúcar Platform in Sevilla, Spain. Its started operation in 2007 with 11 MW of output power. The second and biggest in the world, PS20, is since 2009 in operation with 20 MW of power output.

Figure 3.5: Aerial Photography of Solúcar Platform with the PS10 and PS20 Receiver Tower Systems

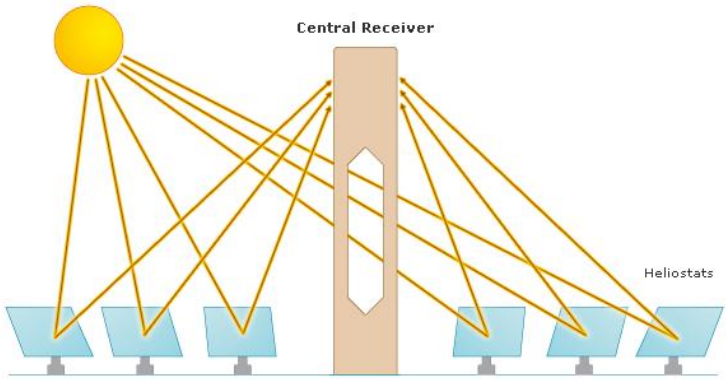

Figure 3.6: Tower Receiver Operating Scheme, [9]

In the first test of this technology the doubt was the heat transfer medium to use. It first appeared attractive to use the superheated steam itself which avoids the intermediate heat exchangers and enables a direct connection to the steam turbines. However, the problem

was how to control the generation of superheated steam with changing radiation conditions. Besides, storing the heat energy was almost impossible without having a big amount of heat losses. Therefore, the PS10 Solar Power Plant is based on saturated steam at moderate temperature and pressures to avoid these problems.

Other possibility is the use of alkali-metal salts as heat medium transfer. They have two advantages: the good heat transfer properties and the possibility of storage at low pressures in tanks. However, the high melting point makes necessary electrical heating the pipes to avoid freezing out of the salts with the pipe blockage as result.

3.2 Parabolic Trough Power Plant Configurations

3.2.1 Solar Mode

In these systems the only heat source which moves the steam turbine is the Sun. As the Sun does not radiate continuously the heat source is not stable and systems for thermal storage are necessary. In summer, the average operating hours are 10-12 hours, which means the remaining time the plant can only be operated using the stored energy.

Since the Sun rises in the morning the solar field starts delivering heat to the thermal cycle. During the radiation peak, the excess heat is stored in the thermal storage system which will be in charge of delivering the necessary heat during the period when the Sun's radiation is not enough.

The differences between the available thermal storage systems are basically the storage medium used. In the following we will describe the most common storage mediums:

- **Salt:** Sodium-nitrate salts and Potasium-nitrate salts are cheap materials for storage systems. They have a high transmission coefficient and can be stored in big salt tanks. The problem is their high melting point which needs electrical heating of the piping for avoiding the blockage for example during system start up.

3.2.2 Direct Steam Generation

In a parabolic trough collector, the oil as a heat transfer fluid is heated by concentrated solar radiation. The thermal energy contained in the oil is transferred to the Rankine cycle where the power is generated. One of the limitations is the chemical stability of the synthetic oil when it is heated at high temperatures, being the limit about 395°C. That limits the maximum temperature of the steam in the Rankine cycle being not possible to reach higher efficiencies.

One of the possible alternatives is Direct Steam Generation (DSG)in the collector field. This configuration consists of evaporating and superheating the water directly in the solar field which makes the oil-water heat exchangers unnecessary. With the DSG the steam can reach temperatures from 400°C to 550°C increasing the thermal efficiency of the Rankine cycle. The optimization and demonstration of these technology components has been done in the a 700 m collector loop in the Plataforma Solar de Almería, [10].

Three different regimes of operation are possible:

- **Once Trough System:** preheates, evaporates and superheates the feed water. This system is the simplest and cheapest but the control of the temperature in the receiver tube is complex due to the inhomogeneous distribution of temperature on the tube circumference.
- **Injection System:** the water is injected in several points of the receiver tube. This system presents the problem of a complex measurement and control operation.
- **Recirculation System:** in this system the collector tube is divided in two sections. In the first section the water is preheated and evaporated, while in the second the water is superheated. In between the two sections there is a water-steam separator, where the water content in the mixture is separated and sent back to the solar collector inlet.

3.2.3 Integrated Solar Combined Cycle (ISCC)

The Integrated Solar Combined Cycle (ISCC) consists of a conventional Combined Cycle Power Plant (CCPP) which is combined with a parabolic trough solar field. The solar field produces superheated steam which is fed into the heat recovery steam generator (HRSG) of the combined cycle allowing the increase of the themal efficiency of the steam cycle in the CCPP.

The benefits of employing this technology are to overcome some problems related with

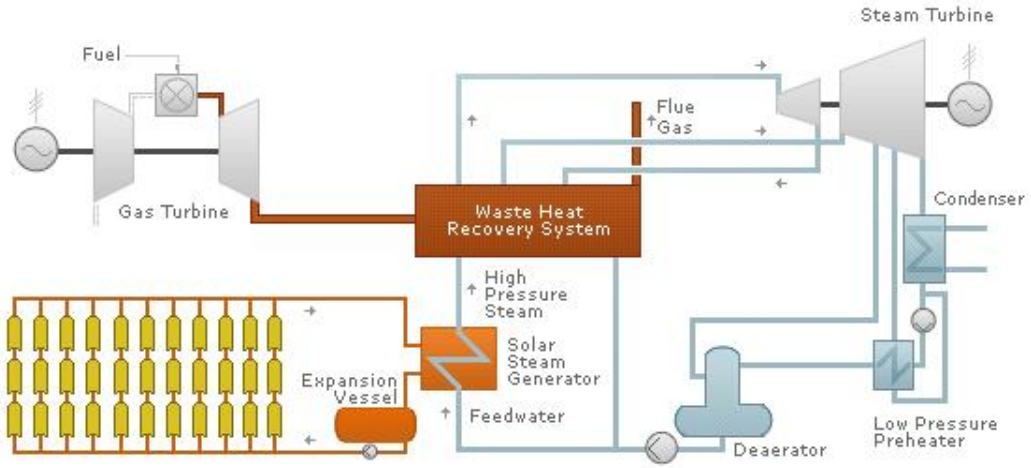

Figure 3.7: ISCC Operating Scheme

the start up and shut down in solar power plants, reduce the capital costs and improve the solar-to-electricity efficiency.

4 Modeling and Simulation with EBSILON® Professional

In this chapter several modeling processes of a Combined Cycle Power Plant will be described. The software used for modeling is EBSILON® Professional 8.0, which we will call Ebsilon. Ebsilon is a mass and energy balance calculation program for thermodynamical cycles. With Ebsilon we will be able to simulate the performance of a combined cycle power plant in design and partload conditions, which is adequate for analyzing its performance under several loading conditions.

In the following, we will shortly describe the features and tools available in Ebsilon.

4.1 Basics of the Ebsilon Software

EBSILON is the abbreviation for "Energy balance and simulation of the load response of power generating or process controlling network structures" and is suitable for nearly all stationary thermodynamic model request coming out of energy cycles or plant schemes.

Ebsilon permits the balancing of components, individually or in groups, as well as subsystems integrated in bigger systems, without taking into account whether these components or systems form a closed or an open cycle. The model structure of Ebsilon is based on:

- standard components, which are used for modeling common power plants,
- programmable components for modeling complex power plants processes with user-defined behaviour.

The data basis of Ebsilon is made up of:

- IAPWS-IF97 or the IFC67 steam table,
- cp-polinomial for air/fuel gas.

Ebsilon is a variable program system, by means of which you can balance all occurring power plant circuits using a closed solution based on a sequential solution method.

The cycles are constructed from objects. The object types can be:

- Components
- Pipes
- Macros (such as the gas turbines from the library)
- Value Crosses
- Text Fields
- Graphical elements

- OLE Objects

Components and pipes form cycles, while value crosses, text fields, graphical elements and OLE objects are used for displaying the results, such as comments and explanations.

In a short description, the basic control elements and tool bars are:

- Standard toolbar,
- Component bar, for selecting a component from a category,
- Component wizard bar, for accessing components classified by numbers,
- Ebsilon bar, for starting simulations,
- Zoom bar, for zooming in the model and finding objects.

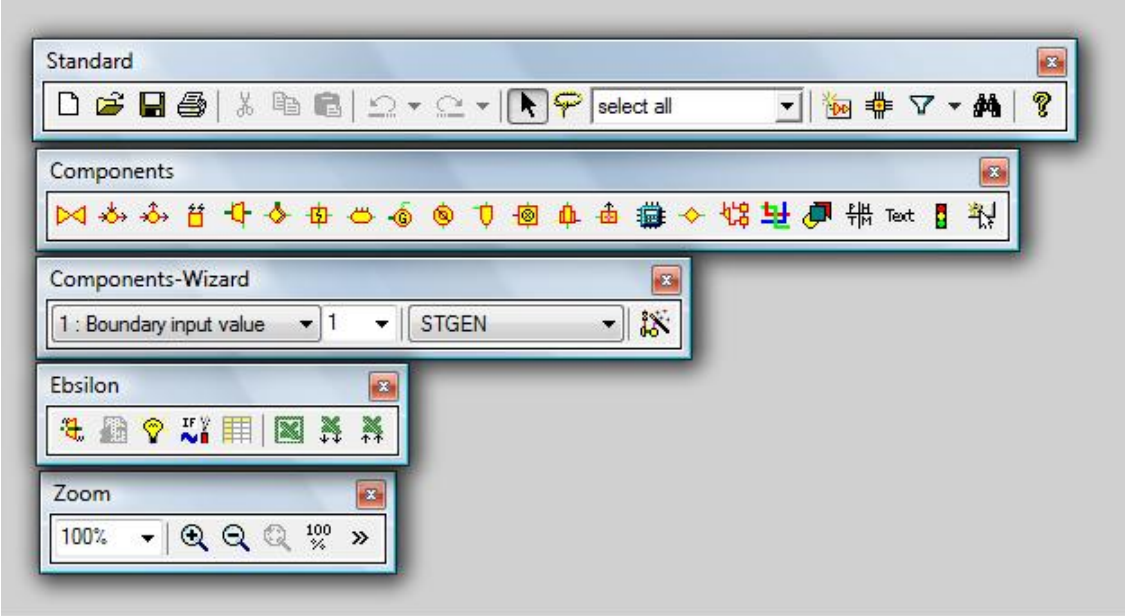

4.1.1 Data introduction

After defining the topology of the cycle, it is time to define the values that characterize it. There are two ways of doing that:

1. Some components can define or calculate values in affiliated pipes, like e.g. the steam generator, as shown in Figure 4.1.
2. The other possibility is to set the value directly on the pipe using the ”Measured/General value input”, as shown in Figure 4.2.

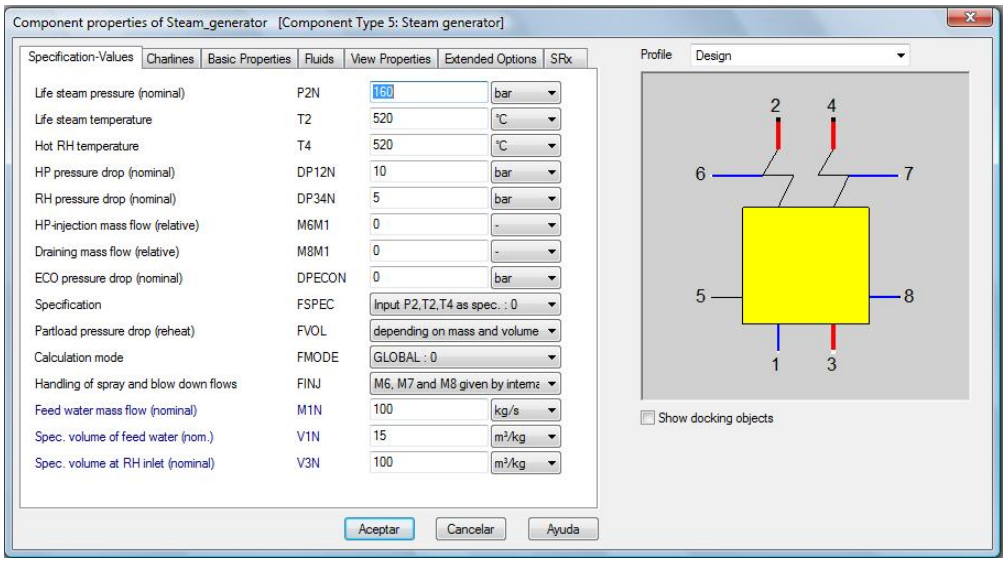

Figure 4.1: Defining data on component's pipes

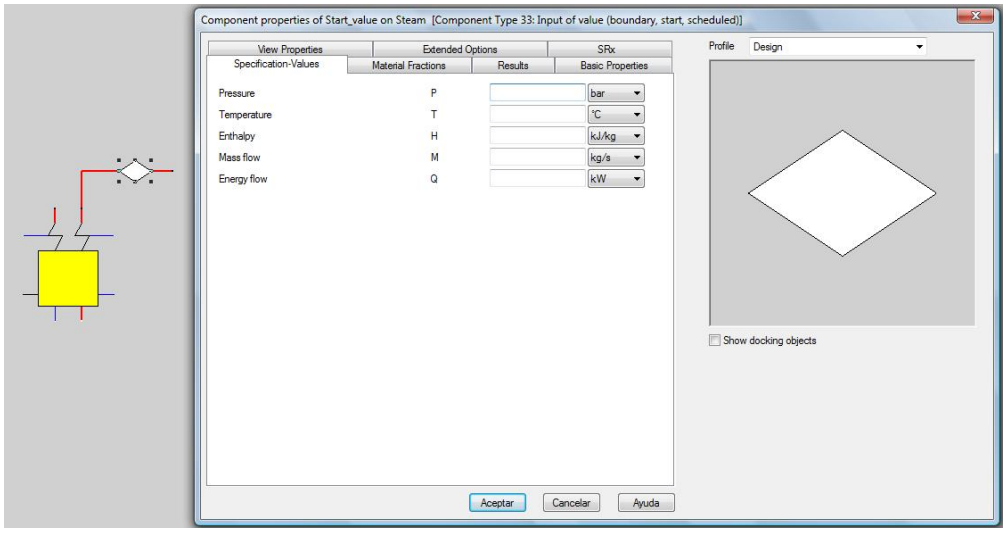

Figure 4.2: Defining data on the pipe

4.1.2 Calculation Modes

After building the cycle we set the design reference by defining the nominal conditions. Once the calculation in nominal conditions is done, the calculated parameters are memorized and we can start analyzing the cycle in different conditions. In the following we present a shortly description of the different available modes for working in Ebsilon.

- **Design Model:** in this model the power plant is built taking into account the design conditions. After defining the features of the plant, it is simulated and the parameters are calculated automatically. Some fixed parameters, as the surfaces of the heat exchangers, will be memorized.

- **Partload Model:** Ebsilon provides the possibility to create different profiles from one model, each one has the same topology but its own parameters and results. The partload operation is used when we want to simulate the performance of the plant working

under different load situations. The new profile Partload has the same parameters as the root profile (Design) but calculates in off-Design mode. All the input values are inherited from the parent profile.

- **Validation Model:** that model is used for controlling the performance of existing plants. Weak points can be detected and from that derives that quality statements about power plants can be derived.
- **Optimization Model:** the optimization model is used for the variation of power plant parameter and what-if calculations. Different strategies of optimization can be applied as well as a combination with the validation model.

In our analysis of Solar Retrofit in Combined Cycle Power Plants. We will use the Design and Partload models in studying the impact caused for feeding the plant with energy coming from a solar field.

5 Model of the Gas Turbine GE 9FA

5.1 Gas Turbine GE 9FA in Design Conditions

The chosen turbine for the design of our combined cycle power plant is the General Electric's GE 9FA. The nominal conditions for the gas turbine are presented in the next Figure 5.1:

Simple Cycle Performance	50Hz
Output	255.6 MW
Heat Rate	9250 Btu/kWh (9757 kJ/kWh)
Pressure Ratio	17.0:1
Mass Flow	1,413 lb/sec (641 kg/sec)
Turbine Speed	3000 rpm
Exhaust Temperature	1,116°F (602°C)
Model Designation	PG9351FA

Combined Cycle Performance	50Hz (S109FA)	50Hz (S209FA)
Net Plant Output	390.8 MW	786.9 MW
Heat Rate	6020 Btu/kWh (6350 kJ/kWh)	5980 Btu/kWh (6305 kJ/kWh)
Net Plant Efficiency	56.7%	57.1%
GT Number & Type	1 x MS9001FA	2 x MS9001FA

Figure 5.1: Nominal conditions of the GE 9FA in a simple cycle or in a CCPP, [13]

In the construction of the cycle of the GE 9FA Turbine, the selected components are a compressor, a combustion chamber and a turbine. The conditions established during the design

process are the ISO conditions: 1.013 bar and 15°C for ambient air.

In nominal conditions, the turbine has a pressure ratio of 17 and is crossed by a mass flow of 641 kg/s. The temperature of the gas flow after the expansion is 602°C at the outlet. Using a "general input value" we set the nominal exhaust temperature and the mass flow, while the pressure is sett in the turbine component. The general input value has to be situated after the turbine, because we only know the exhaust temperature. After writing all data and simulating the performance of the turbine, we obtain that 627.04 kg/s of air are necessary for reaching the nominal conditions in the gas turbine.

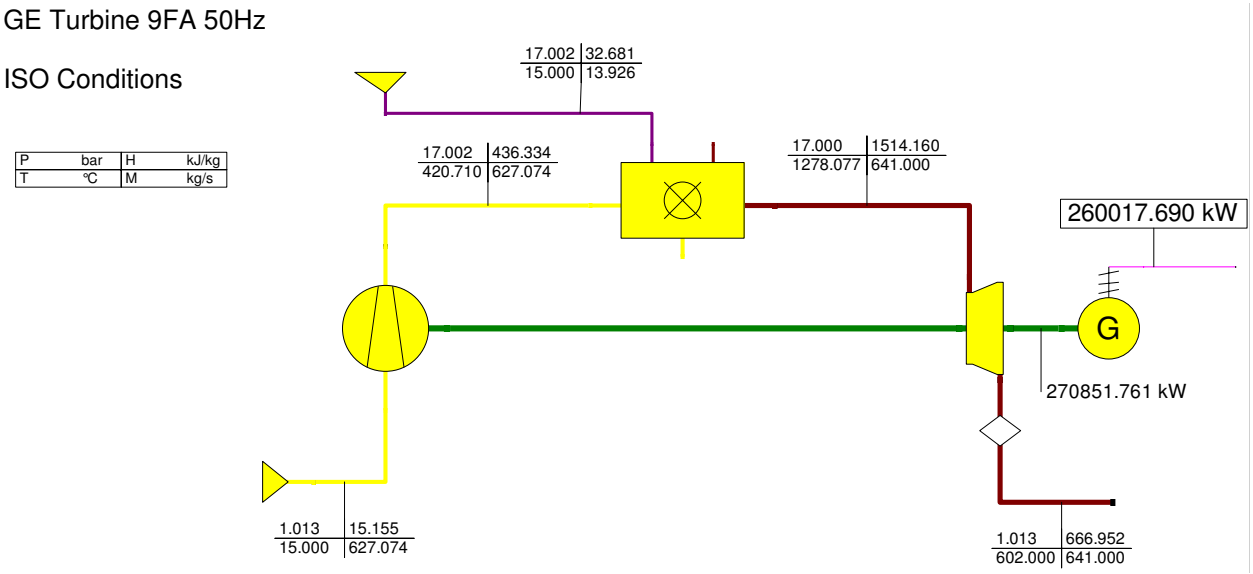

Figure 5.2: Model of GE 9FA in Design Conditions

Once we know that information we are able to set the air conditions at the entrance of the gas turbine. Using a "boundary value input" we set the conditions of the air (1.013 bar, 15°C and 627.04 kg/s) and simulate the performance again. The results are the same that in the step before, we are reaching again the nominal conditions for the gas turbine. The reason of doing this last step is because we will control the turbine performance in partload by means of the amount of air which enters the compressor and the mass of fuel burnt in the combustion chamber. Now, it is possible to set the new parameters of the air in partload by introducing the values in the "boundary value input" at the entrance of the gas turbine.

Comparing the data of the Figure 5.2 and Figure 5.1 we can conclude that the performance of model of the GE 9FA Turbine represents approximately the performance of the turbine in reality. Both the exhaust temperature and the gas flow coincide with the data given for General Electric and the only difference is the power output, which is higher in our model. That could be a consequence of a different air ratio which could result as a different turbine inlet temperature, different isentropic efficiencies in turbine and compressor or the electrical efficiency of the generator.

The previous results show the gas turbine behaviour in nominal conditions. In the following

we will discuss the behaviour of the same turbine when the conditions of the surroundings change and when the net needs less power than the delivered power in nominal conditions.

5.2 Gas Turbine GE 9FA in Off-design

The gas turbine working in nominal conditions means that the turbine works in the same conditions for which it was designed. Partload conditions are the conditions in which the turbine works under different specifications. Partload can be reached when the ambient conditions changes, the temperature, or when the turbine is delivering less power than the nominal power. The objective of this study is to establish the performance of the gas turbine in the first case, when the air temperature differs from the ISO temperature, although we will also briefly describe the performance when less than nominal power is enough.

5.2.1 Variation of Ambient Temperature

The variation of ambient temperature produces a change in the turbine behaviour because the air entering the turbine changes its properties, such as temperature and humidity.

For our study we will suppose a variation of 5% in humidity (ϕ) when the temperature changes 15°C. Besides, the density (ρ) changes when the temperature does in a way that, the density is inversely proportional to the temperature.

This has to be taken into account because in the different seasons of the year, the ambient temperature raises, being higher than 15°C, or decreases and the air density is different as well. That means that the same turbine working at a fixed place will deliver more or less power depending on the season of the year.

In Europe, in summer normally the ambient temperature is higher than 15°C and that means the air density is lower. As we know, the air density is inversely proportional to its volume, so the volume occupied for the same amount of air will be bigger. Thus, the amount of air entering the compressor will be lower, due to the fact that compressor has a fixed volume capacity, and the gas flow passing through the turbine is lower too. That means that the same turbine working in summer has lower power output, because the expanded mass flow is smaller. If we think that in summer the demand of electricity is not lower than in winter, although no energy for heating is required, the same turbine working in summer conditions will not be enough for satisfying the energy demanded. For this reason, it is necessary to analyze how much can vary the turbine efficiency depending on the ambient temperature.

In winter, for colder temperatures than 15°C, the opposite occurs. The density will decrease and the compressed mass of air will be bigger. That changes the performance of the turbine in a way that in winter delivers more power, if there is no limit for the turbine inlet temperature.

In the following we will analyze three representative cases for the partload behaviour, 30°C, 45°C and 0°C.

First of all, we have to calculate the variation of density and air flow for each case. Knowing

the decrease percentage in the humidity when the temperature rises, we can calculate the resulting density at the required temperature which let us calculate the mass flow of air entering the compressor of the gas turbine.

As example, the calculations for the case at 30°C are described in the following:

$$\rho_{30} = \rho_N \frac{T_N}{T_{30}} = 1.147 kg/m^3 \tag{5.1}$$

$$\dot{m_{30}} = \dot{m_N} \frac{\rho_{30}}{\rho_N} = 596.03 kg/s \tag{5.2}$$

The density values obtained in each case are showed in the Table 5.2.1:

T_{amb} (°C)	ρ (kg/m^3)	ϕ (%)
0	1.273	105
15	1.207	100
30	1.147	95
45	1.11	90

At 30°C, we get a mass of air of 596.03 kg/s, which is smaller than in nominal conditions as we said. The new air flow has to be set at the compressor entrance using the "boundary value input" as we explained before. The temperature has to be changed too.

In every case of partload we will have now new conditions of temperature and mass flow. Ebsilon calculates by itself the amount of fuel which has to be burnt in the combustion chamber. The parameter which determines the amount of fuel is the air ratio.

The air ratio (called ALAM in Ebsilon and represented in tables as λ) is a parameter in the combustion chamber which enables the regulation of the maximum temperature of the cycle. The air ratio is defined as the ratio between the mass of air and the stoichiometric mass of air for a known fuel flow.

By changing the air ratio, we give the order to the combustion chamber to accept more or less fuel. That means that the maximum temperature of the cycle, after the combustion chamber, is changing. This is interesting because in our case that we are studying we want either higher or lower temperatures. That can be regulated by varying the air ratio. If we increase the air ratio we accept more air in reference to the stoichiometric air and the maximum temperature of the cycle decreases. The exhaust temperature of the turbine decreases as well. If the air ratio decreases, the temperatures increase.

For determining the exhaust temperature of the turbine, we have followed the next criteria described:

1. When the ambient temperature is hotter than in nominal conditions (30°C and 45°C), the temperature in the exhaust of the turbine remains constant.

2. At colder temperatures than in nominal conditions (0°C) that the maximum temperature in the cycle remains constant. The temperature before entering the turbine does not vary.

Figure 5.3 shows the evolution of the exhaust and inlet temperature of the gas turbine according to the criteria followed for establishing the temperatures in partload.

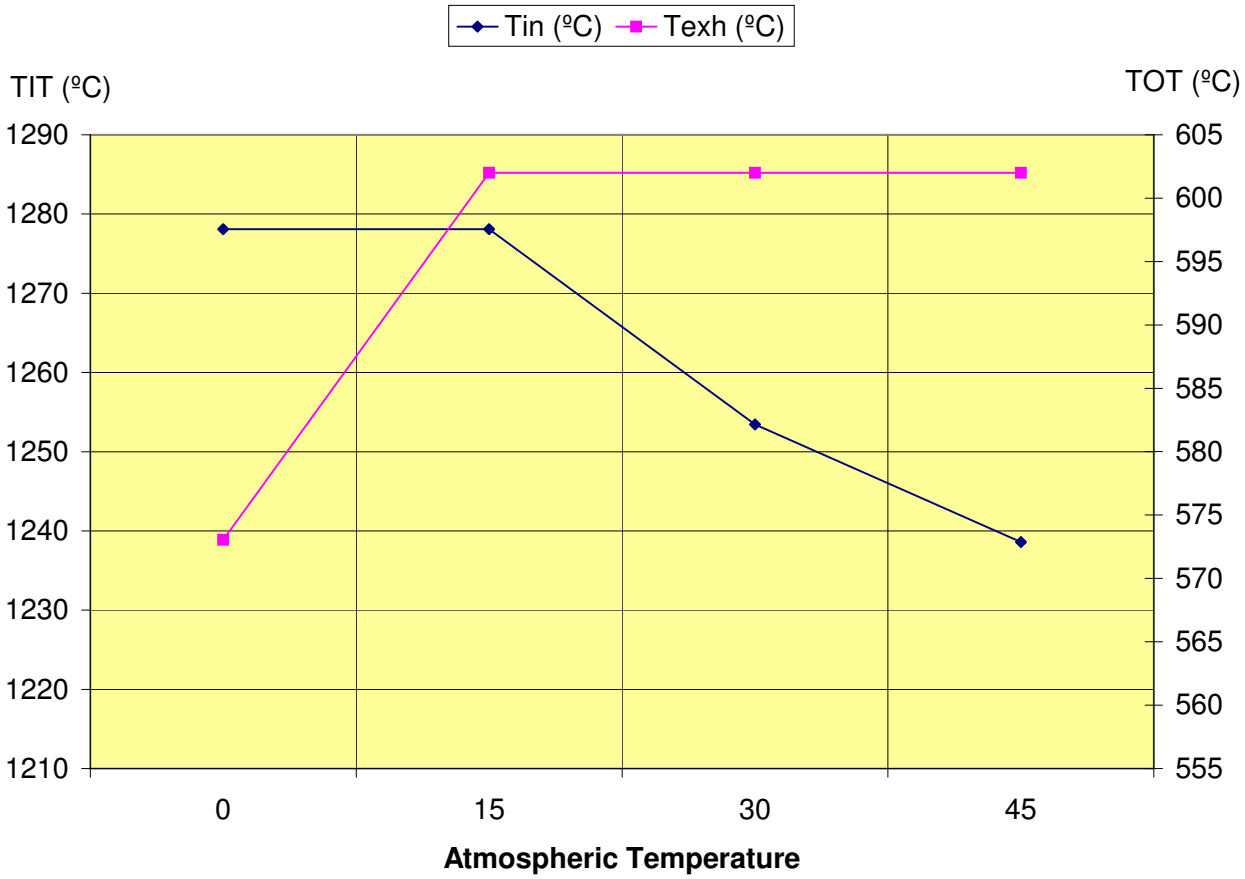

Figure 5.3: Temperature Evolution in Off-design

We already know that in a combined cycle power plant, the energy in the exhaust gases of the gas turbine is transferred to the steam cycle by using a HRSG. The exhaust gases of the gas turbine have a big amount of energy when they are leaving the turbine with a temperature over 600°C. The parameters which define the HRSG are set for the design case, that means that the surfaces of the heat exchangers are designed according to these conditions. At other conditions they are of course constant. For adequate performance of the combined cycle power plant the conditions of the steam cycle should remain constant. In consequence the outlet temperature (TOT) of the gas turbine should be as constant as possible independent from the ambient temperature.

In the Table 2 and the Table 3 the different values of mass flows, temperatures and air ratios obtained in each case are shown:

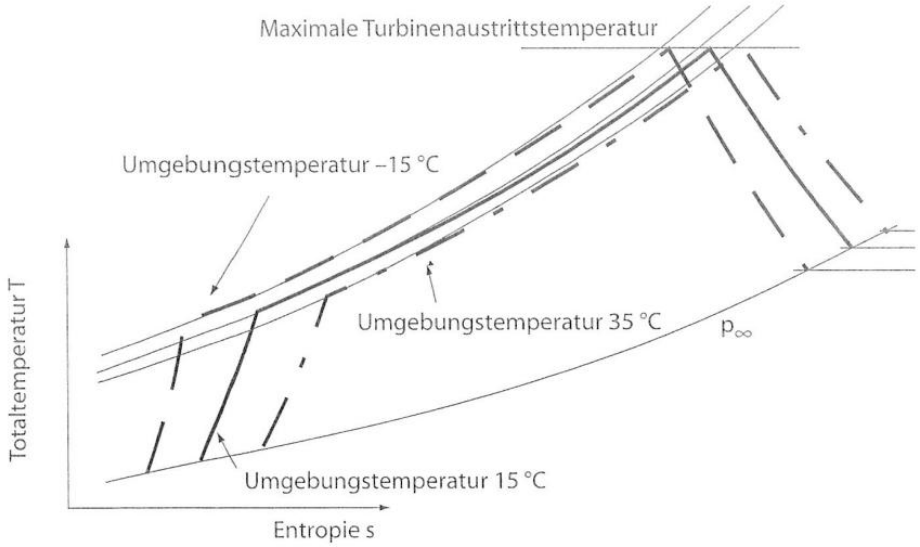

Figure 5.4: Variation of gas turbine performance in T-s diagram depending on the ambient temperature, [7]

T_{amb} (°C)	$\dot{m}_{air}$ (kg/s)	$\dot{m}_{fuel}$ (kg/s)	$\dot{m}_{gas}$ (kg/s)
0	661.5	15.9	677.0
ISO	627.1	13.9	641.0
30	596.0	12.4	608.5
45	576.0	11.4	588.4

Table 2: Mass flows in Off-design

As we can see, the power of the gas turbine is higher when the ambient conditions are colder due to the fact that a bigger amount of gas is expanded in the turbine and the pressure ratio is higher than in nominal conditions. That makes the gas turbine power output higher in winter, while in summer it decreases.

5.2.2 Variation of fuel and air flows

When an amount of power smaller than in nominal conditions is enough for satisfying the demand, the gas turbine can works in partload as well.

In first place, the pursued objective is to determine how much power we need. As we said, we want to obtain the variation in power but always taking into account that after the gas turbine there is a heat recovery steam generator and the exhaust temperature in the gas turbine has to remain constant. For adjusting the exhaust temperature we will vary again the air ratio.

In this case the criteria followed establishes a constant exhaust temperature while the range of power is between the 50% of the load and nominal conditions. For obtaining a constant exhaust temperature, the air ratio has to be changed in the same way that we have already explained when the gas turbine works in an ambient with changing temperatures. For obtaining the required power, the mass of air has to be changed as well, taking into account

T_{amb} (°C)	p_{in} (bar)	λ	Power (MW_e)	TIT (°C)	TOT (°C)
0	18.0	2.462	318.63	1278.0	573.0
ISO	17.0	2.595	260.02	1278.1	602.0
30	16.0	2.762	213.53	1253.4	602.0
45	15.4	2.916	183.85	1238.6	602.0

Table 3: Parameters in Off-design

that the smaller amount of air the less power is delivered. Depending on the required power, Ebsilon calculates by itself the amount of fuel necessary for doing that the gas turbine delivers exactly that amount.

The Figure 5.5 shows the evolution of the gas flow and exhaust temperature when the performance of the gas turbine varies from 30% to 110% of the nominal power.

- The ratio M_{gas}/M_{gas0} represents the decrease of the gas flow with regard to the nominal gas flow.
- The ratio T_{exh}/T_{exh0} represents the variation of temperature with regard to the exhaust temperature in design conditions.

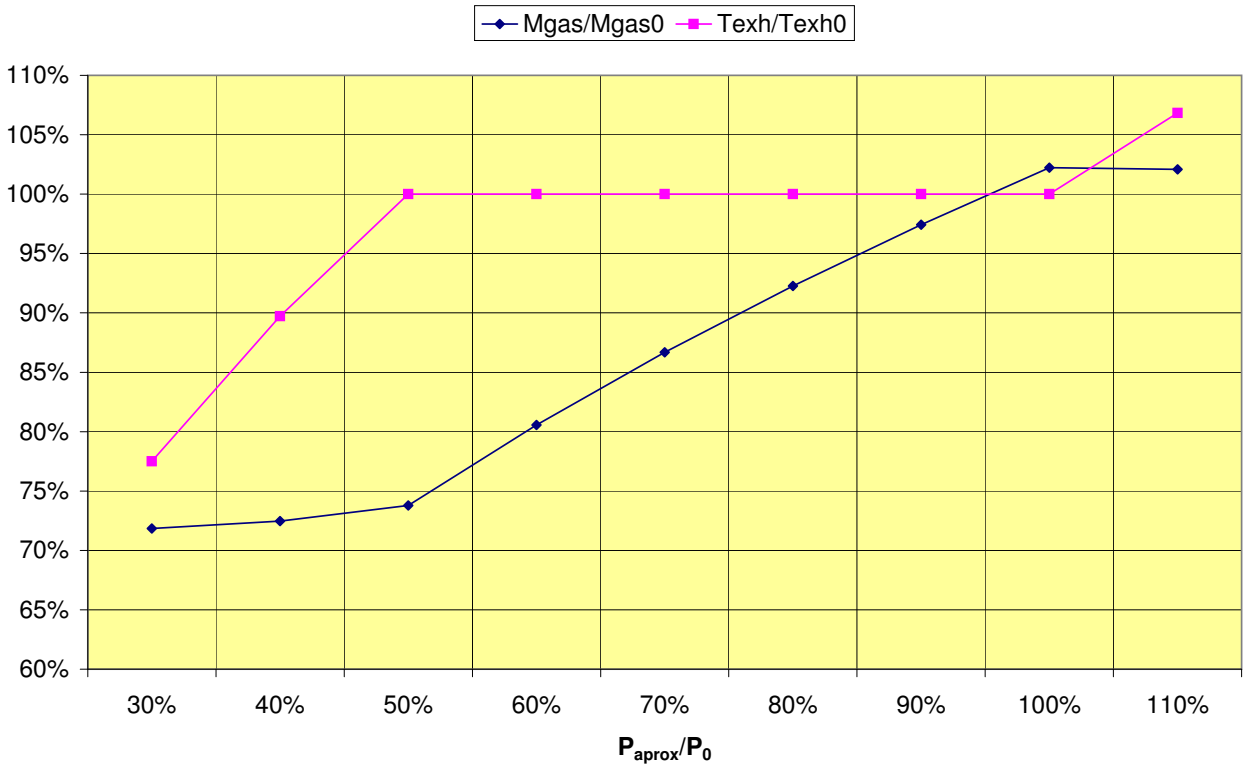

Figure 5.5: Temperature and Mass flow Behaviours in Off-desing for a specific power

As we can see in the Figure 5.5 less mass goes through the turbine when we move into partload operation. That means that the air flow and the fuel flow decrease.

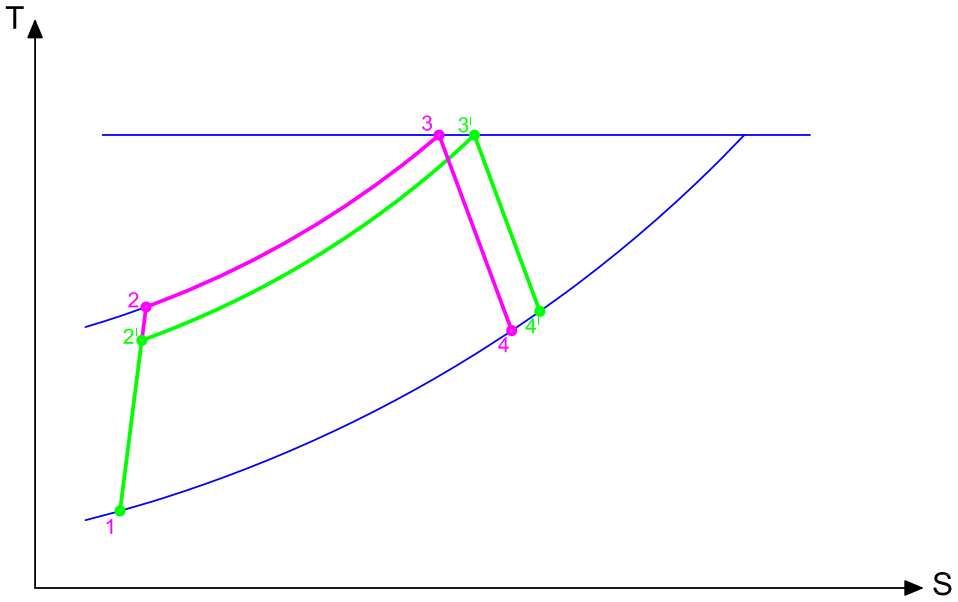

Figure 5.6: Comparison between the T,s diagrams for the gas turbine accepting less air

In the Figure 5.6 the cycle 1-2'-3'-4' represents the gas turbine working with less air. In the graphic, we can see that when the air flow is small the compression process is shorter and the combustion is longer until reaching the maximum temperature in the cycle. This new "longer" combustion in process 2'-3' means that the amount of fuel burnt is bigger than in process 2-3. In a real gas turbine the mass of air entering the compressor is controlled by changing the orientation of the blades at the entrance (inlet guides vanes).

Although in Table 4 the amount of fuel is decreasing at the same time as the amount of air, the fuel decreases slower compared with the variation of air flow. The decrease of the amount of air entering the compressor leads to a constant outlet turbine temperature, as we can see in Figure 5.5.

In Table 4 the different values obtained for every parameter are shown in each case of off-design:

- The parameter Partload represents the ratio between the necessary power and the nominal power.
- The parameter P_{aprox} is the power that in reality is obtained in the turbine in each case.
- The ratio P_{aprox}/P_0 represents how close we are of obtaining the partload percentage necessary.

As an example we will explain the case of 80%:

The amount of power obtained in nominal conditions is 270852 kW. In this case we need the

80% of the nominal power, which is $0,8 \cdot 270852 = 216682,21$ kW. For reaching that amount, we will vary the air ratio and the mass of air entering the compresor. That also produces that the mass of fuel changes. At the end we obtain a value similar to the power needed, 216683 kW. This value is called P_{aprox} and the ratio P_{aprox}/P_0 represents the exactitud with which the delivered power is obtained. If the P_{aprox}/P_0 coincides with the Partload needed, then the deliverd power is exactly the required amount. In that case of 80% the ratio P_{aprox}/P_0 is exactly 80%, which means that the numbers obtained are correct.

In Figure 5.7 the model of the gas turbine working at the conditions of the case described is showed.

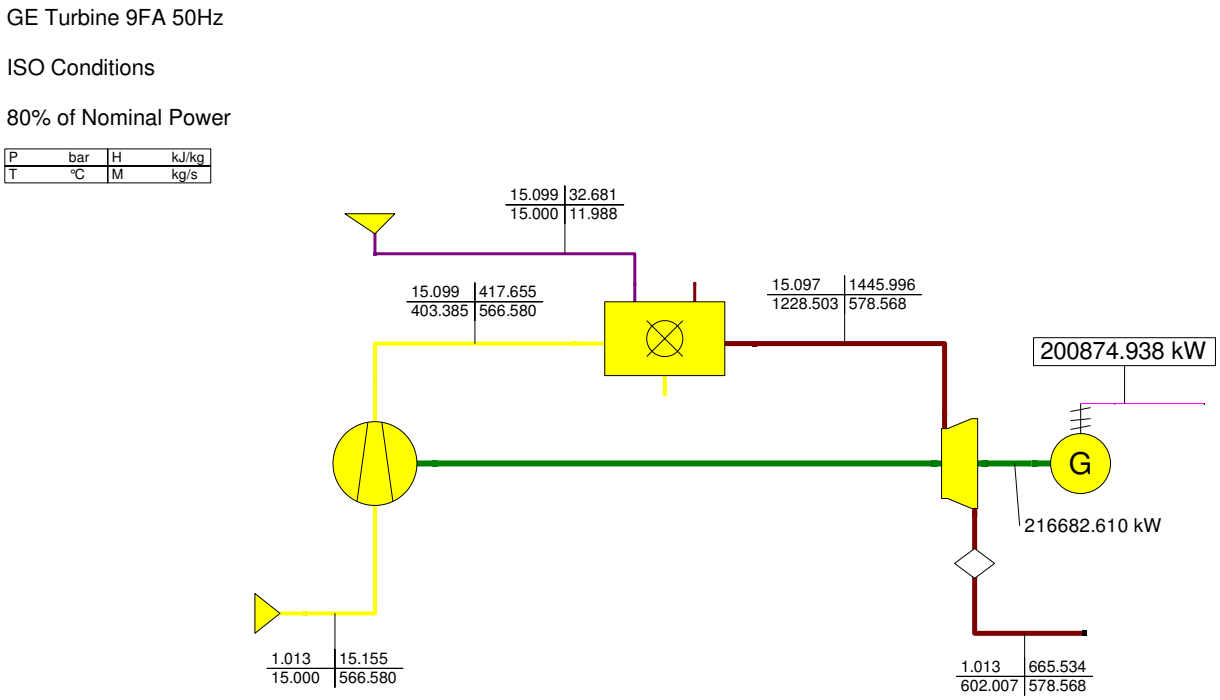

Figure 5.7: Gas Turbine working at 80% of nominal power

Although in Table 4 the amount of fuel is decreasing at the same time as the amount of air, the fuel decreases slower compared to the variation of air flow.

5.2.3 Variation of Efficiency in Components

As we explained before, the gas turbine efficiency depends only on the pressure ratio and the nature of the working fluid. Working in partload conditions means changes in the pressure ratio of the gas turbine and in its power output. But also the other components of the gas turbine working in part load suffer a change in their performance which has to be taken into account in the overall efficiency of the gas turbine.

Partload	P_0 (kW)	P_{aprox} (kW)	$\dot{m}_{air}$ (kg/s)	$\dot{m}_{fuel}$ (kg/s)	$\dot{m}_{gas}$ (kg/s)	λ	T_{exh} (°C)
110.00%	297937	297932	625.0	15.1	640.1	2.380	643.1
100.00%	270852	270852	627.1	13.9	641.0	2.595	602.0
90.00%	243767	243768	597.9	13.0	610.9	2.657	602.0
80.00%	216682	216683	566.6	12.0	578.6	2.724	602.0
70.00%	189597	189597	532.6	11.0	543.6	2.798	602.0
60.00%	162512	162512	495.3	9.9	505.2	2.881	602.0
50.00%	135426	135426	453.9	8.8	462.7	2.976	602.0
40.00%	108341	108342	447.0	7.4	454.4	3.459	540.1
30.00%	81256	81304	444.5	6.1	450.6	4.220	466.6

Table 4: Variation of Parameters in Off-design when the power is specified

P_{aprox}/P_0	M_{gas}/M_{gas0}	T_{exh}/T_{exh0}
110.0%	99.7%	106.8%
100.0%	100.0%	100.0%
90.0%	95.4%	100.0%
80.0%	90.4%	100.0%
70.0%	84.9%	100.0%
60.0%	79.0%	100.0%
50.0%	72.4%	100.0%
40.0%	71.3%	89.7%
30.0%	70.9%	77.5%

Table 5: Relative Parameters in Off-design

In Ebsilon compressors and turbines have an established default value of isentropic efficiency. The isentropic efficiency in a compressor or a turbine is a comparison between the real power obtained or consumed and the isentropic case. The default isentropic efficiency for turbines is 0.9 and for compressors is 0.85 and in partload that value is defined by some correction curves. The variation of isentropic efficiency is directly proportional to the change of mass flow which is going through the compressor or turbine.

The Tables 6 and 7 show the respective correction curves:

$\dot{m}/\dot{m}_N$	$ETAI/ETAI_N$
0	0.85
0.4	0.9
0.7	0.95
1	1
1.2	1.1

Table 6: Variation of Efficiency in the Turbine with the mass flow

The value of the isentropic efficiency is represented in Tables 6 and 7 by the name of *ETAI*.

$\dot{m}_1/\dot{m}_{1N}$	$ETAI/ETAI_N$
0	0
0.4	0,9
1	1
1.2	1.1

Table 7: Variation of Efficiency in the Compresor with the mass flow

5.3 Off-load Model of HRSG, Steam Turbine and Condenser

In this chapter we pretend to analyze how the parameters in every component variate when the operation of the steam cycle is not in design conditions.

Heat Exchangers

The heat transfer capacity of a heat exchanger variates with the change in mass flow trough the heat exchanger. The transfer surfaces in the heat exchanger are defined in design conditions and remain constant in every mode of operation. The variation of the product of the heat transfer capacity and the transfer surface is defined by some default correction curves implemented in Ebsilon.

A heat exchanger is a component where two fluids transfer heat between them. The Figure 5.8 shows a section of a heat exchanger in Ebsilon software. Independent of water or steam (1-2) the variation of the heat transfer capacity of the heat exchanger for each fluid is represented in Table 8. In Table 9 the gas side (3-4) is represented. As we can see, it is assumed that the heat transfer capacity remains constant in the gas pipe of the heat exchanger when the mode of operation is off-load.

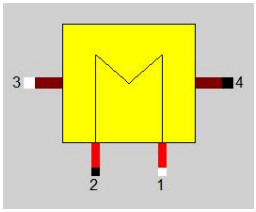

Figure 5.8: Section of a heat exchanger in Ebsilon

Condenser

The heat transferred in the condenser also variates with the mode of operation. Although the condenser is also a heat exchanger we only study the pipe in which the steam is condensed to water, the other pipe is not interesting because it is suppose that the condenser can use as much as it needs for condesing the steam. The Table 10 shows the variation of heat transfer capacity with the mass of steam condensed in off-load.

Steam Turbine

In steam turbine, the pressure variates in accordance with the Stodola's law which defines a variation in pressure proportional to the variation of mass flow expanded through the steam

M_1/M_{1N}	kA_1/kA_N
0	0.5
0.4	0.6
0.5	0.7
0.6	0.8
0.7	0.85
0.8	0.9
0.9	0.95
1	1
1.1	1.04
1.2	1.07

Table 8: Variation of Heat Transfer Capacity with the mass flow on the steam/water pipe.

M_3/M_{3N}	kA_2/kA_N
0	1
0.4	1
0.5	1
0.6	1
0.7	1
0.8	1
0.9	1
1	1
1.1	1
10	1

Table 9: Variation of Heat Transfer Capacity with the mass flow in the gas side

M_1/M_{1N}	kA_1/kA_N
0	0.5
0.4	0.6
0.5	0.7
0.6	0.8
0.7	0.85
0.8	0.9
0.9	0.95
1	1
1.1	1.04
1.2	1.07

Table 10: Variation of heat transfer capacity with the condensed mass flow.

turbine . The correction curve defines in this case a correction factor, with which the pressure calculated according to the Stodola's expansion law is multiplied. This simplifies the pressure adaptation to the real plant states. The correction curve is shown in Table 11.

M_1/M_{1N}	$P1/P1_{St}$
0	1
0.2	1
0.4	1
0.5	1
0.6	1
0.7	1
0.8	1
0.9	1
1	1
1.1	1
1.2	1

Table 11: Stodola Correction for the Steam Turbine

6 Modeling a Single Pressure CCPP

The simplest steam cycle consists of a steam turbine, a condenser, the heat exchangers of the one level pressure heat recovery steam generator and the pumps. This is the single pressure cycle (1P) and the heat recovery steam generator consists of two economizers, the evaporator, two superheaters and one reheater.

The performances of the steam turbine and the condenser have been explained in the chapters "Steam Cycle" and "Types of Condensers", but it is important to notice that in our CCPP the steam turbine will have always three stages of expansion although the HRSG has only a single pressure level. The reason of three stages in the steam turbine is because we have reheat and a deaerator and we need some opening point for taking the steam. In the reheat the steam goes again through a heat exchanger where it is heated and recovers its energy and the deaerator needs to extract some steam from the steam turbine at low pressure.

By superheating the steam leaving the evaporator we ensure that the saturated steam converts into dry steam and there is no water droplets in the steam flow. The superheater also rises the steam temperature at the inlet of the steam turbine which allow us to obtain more power output.

The reason of having two superheaters in the HRGS is because we need to control the temperature. Feed water is injected for controlling the superheat temperature. Although the pipe connection is made in the cycle, we will not use the feed water injection for controlling the superheater temperature in the modeling of the one pressure CCPP. This temperature will be controlled in our model by using the settings in the components.

The reheat process has been explained in the chapter "Improvements for increasing the work output" of the gas turbine. The pipe which enters the reheater is called the cold reheat pipe. In this pipe there is another connection for injecting feed water in case we want to control the reheat temperature. As in the case of superheaters we will not use it, being the mass flow through the pipe 0 kg/s. The reheat temperature will be controlled by using the setting in the reheater pipes.

The performance of the evaporator has also been explained in the chapter "Types of HRSGs". As a shortly description we should say that the single pressure cycle has only one evaporator which defines the one level pressure HRSG. In the evaporator the water is converted into saturated steam at constant pressure and temperature. The evaporator has a drum where the water is separated from the steam and recirculated for being evaporated, while the steam is leaving the evaporator for entering the superheaters.

The economizer consists of a heat exchanger where the water is heated before entering the evaporator. The purpose of this component is to save energy by preheating the water before the evaporator. In the single pressure cycle we have two economizers. That is because we can extract water between the economizers and inject it as in the cold reheat pipe.

The steam cycle also has a deaerator. The deaerator is the component which guarantees that there is no air and other dissolved gases going from the feed water to the HRSG. Dissolved oxygen in boilers can cause corrosion damage in the steam systems and forming oxides in metal piping. The water which enters the deaerator comes from a preheater where its temperature is raised being the elimination of the air easier at higher temperatures.

The preheater situated at the end of the gas stream has the purpose of lowering the temperature of the gas leaving the HRSG. If the gases leave the HRSG at a high temperature we are wasting energy. Instead of wasting this energy, we can use it for heating the feed water and helping the deaerator in eliminating the gases contained in the water. In the preheater there is a recirculation circuit for rising the water temperature. That is because the water entering the heat exchanger can be at low temperature (around $30°C$) which would lead to condensation of the flue gas and dew point corrosion.

The Figure 6.1 describes the combined cycle power plant with the single pressure heat recovery steam generator. The values of the heat transfer capacity (kA) are written on top of every heat exchanger. The Pinch Point in the evaporator is 8°C and the Approach Temperature is 10°C. The Figure 6.2 shows the q, T diagram of the HRSG. We have to remark that normally the reheat would be split.

The condenser is water cooled and it works at 0.04 bar of pressure and 15°C (temperature of the water). The steam turbine delivers 117.5 MW which by taking into account the electric efficiency of the generator are equivalent to 112.8 MW_e. These data are presented in Table 12.

CCPP Single Pressure	
Gas Turbine Power (MW_e)	260
Steam Turbine Power (MW_e)	117.5
High Pressure (bar)	120
Reheat Pressure (bar)	20
Low Pressure (bar)	4.2

Table 12: Powers and Pressures for the CCPP Single Pressure

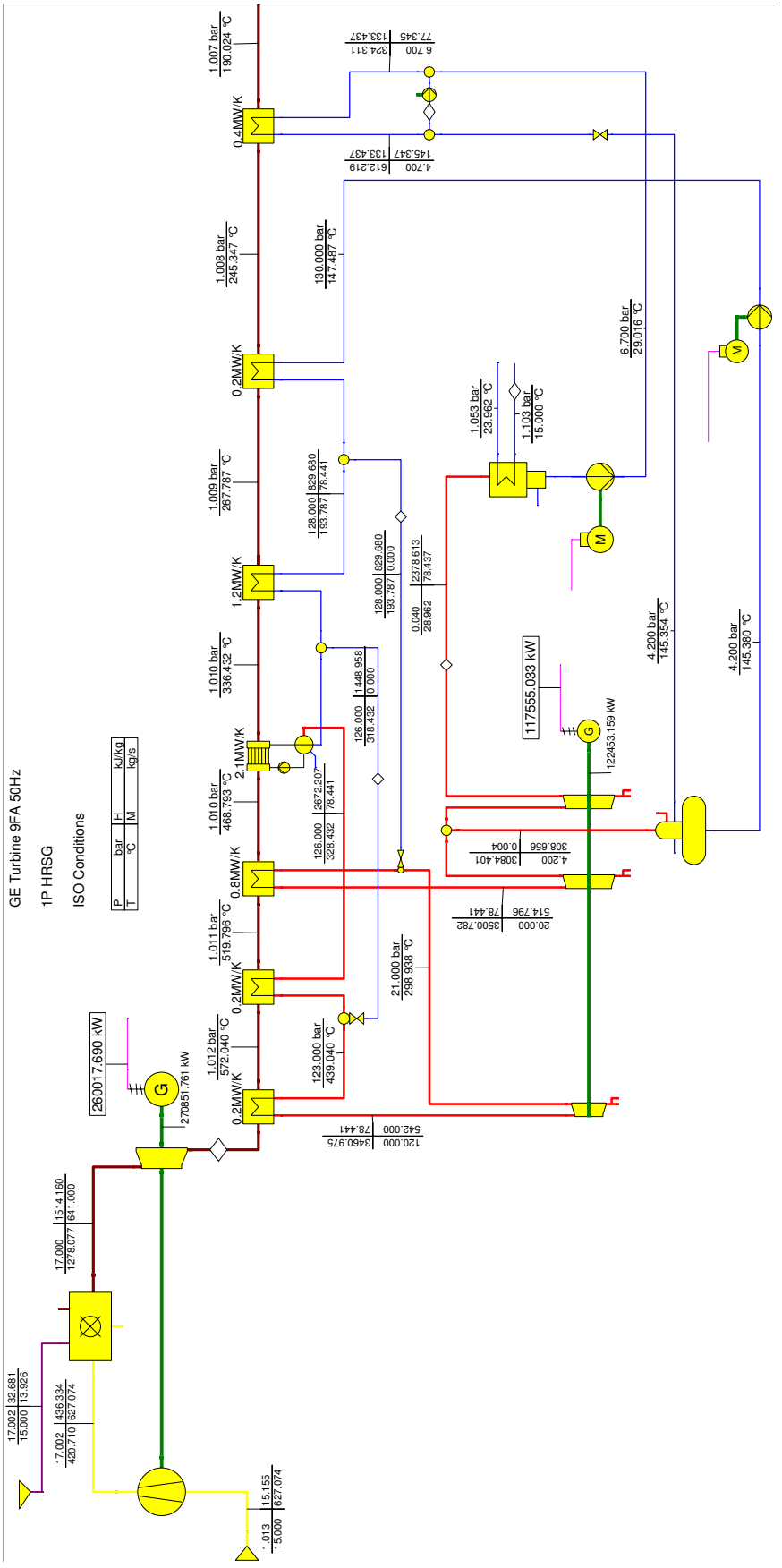

Figure 6.1: CCPP with a Single Pressure HRSG

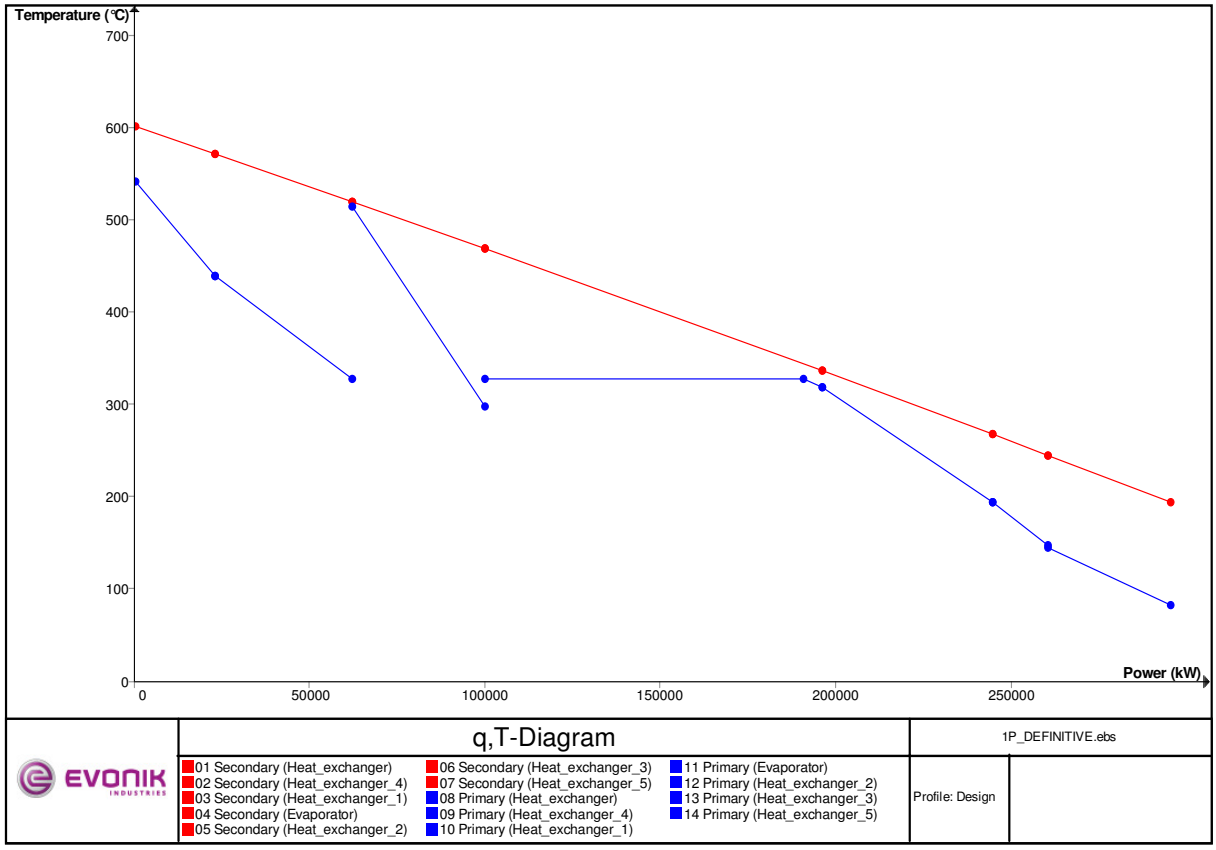

Figure 6.2: Heat transfer in the HRSG in a Single Pressure CCPP

All the generators in the cycles have the same electrical efficiency, 96% in nominal conditions. For pumps the isentropic efficiency is 80% in nominal conditions and it will change in partload operation, while the mechanical efficiency is 99.8% and it will be constant in all the modes of operation. The variation of efficiencies in partload for generators and pumps is showed in Table 13 and Table 14.

Q_1/Q_{1N}	$ETAG/ETAG_N$
0	0.9
0.4	0.92
0.5	0.94
0.6	0.96
0.7	0.97
0.8	0.98
0.9	0,9
1	1
1.1	1
1.2	1

Table 13: Variation of Electrical Efficiency in Generators in Partload

M_1/M_{1N}	$ETAI/ETAI_N$
0	0.92
0.6	0.94
0.7	0.96
0.8	0.98
1	1
1.1	0.98

Table 14: Variation of Isentropic Efficiency in Pumps in Partload

7 Modeling a Two Pressure CCPP

By dividing the heat transfer process in the heat recovery steam generator in two stages, we have now two evaporators, one for high pressure and other for the low pressure. The new HRSG is composed of two superheaters at high pressure and one superheater at low pressure, two reheaters at the reheat pressure and two evaporators. The low pressure evaporator has one economizer, while the high pressure evaporator has two. We also have in this cycle the preheater at the end of the gas flow and the steam turbine is divided in three stages.

The feed water, after being preheated and leaving the deaerator, is divided in two pipes and pumped to the different pressure levels. Approximately, the 13% of the water goes to one economizer and then to the low pressure evaporator. After being evaporated and converted in saturated steam is injected in the cold reheat pipe acting as cooling steam in the reheat process. The 87% of the water goes first through two economizers and then is evaporated in the high pressure evaporator. This process needs two economizers before reaching an adequate temperature for entering the evaporator.

In the new HRSG we have the two superheaters with the water injection between them, as in the case of a single pressure CCPP. The reheat process is divided in two stages with the water injection in between. In the cold reheat pipe saturated steam at low pressure is added for cooling and between the two reheaters water is injected. As in the single pressure process we are not injecting spray water.

CCPP Two Pressures	
Gas Turbine Power (MW_e)	260
Steam Turbine Power (MW_e)	124.4
High Pressure (bar)	120
Reheat Pressure (bar)	32
Low Pressure (bar)	5.1

Table 15: Power and Pressures for the CCPP Two Pressures

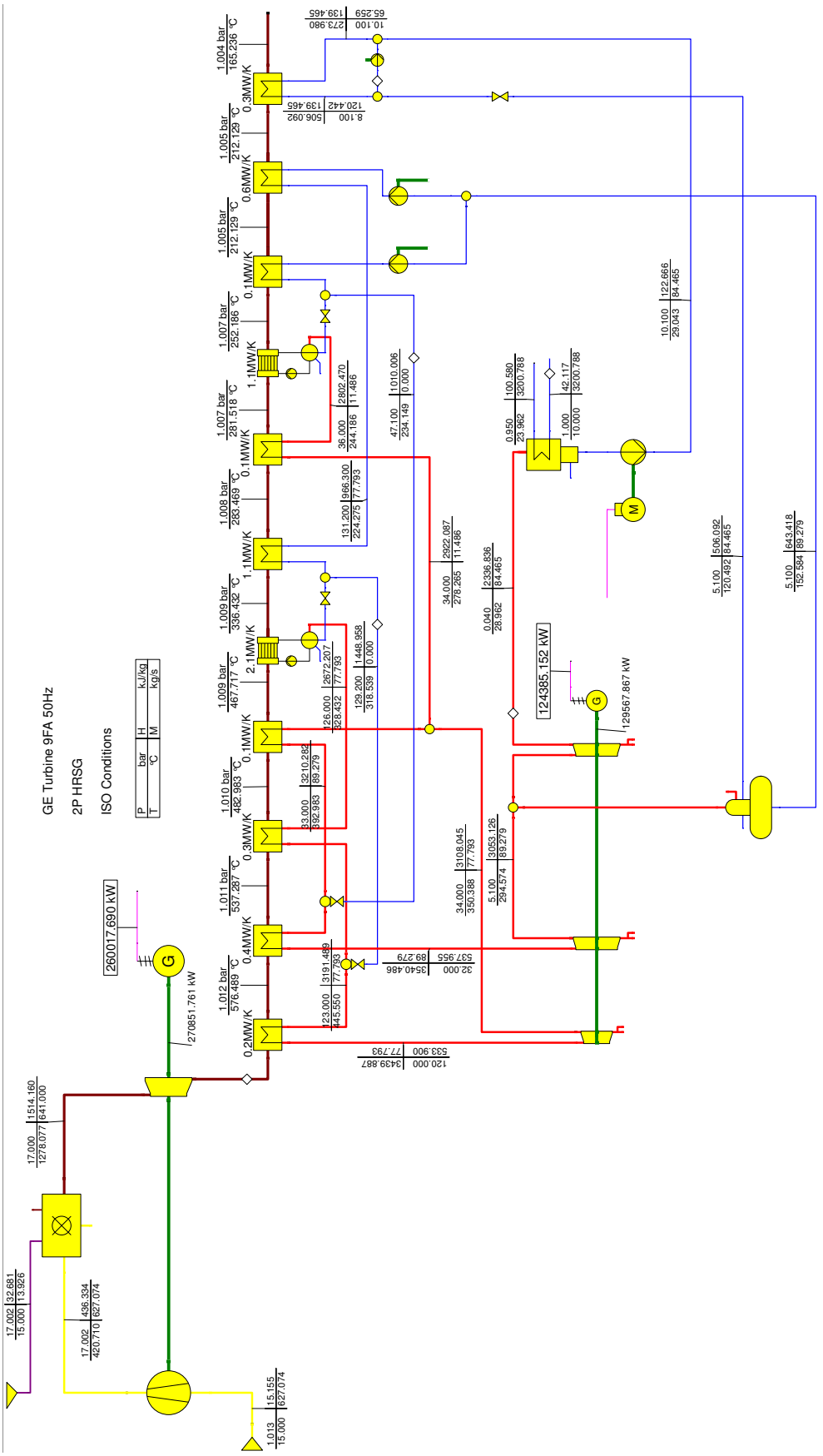

Figure 7.1: CCPP with a Two Pressure HRSG

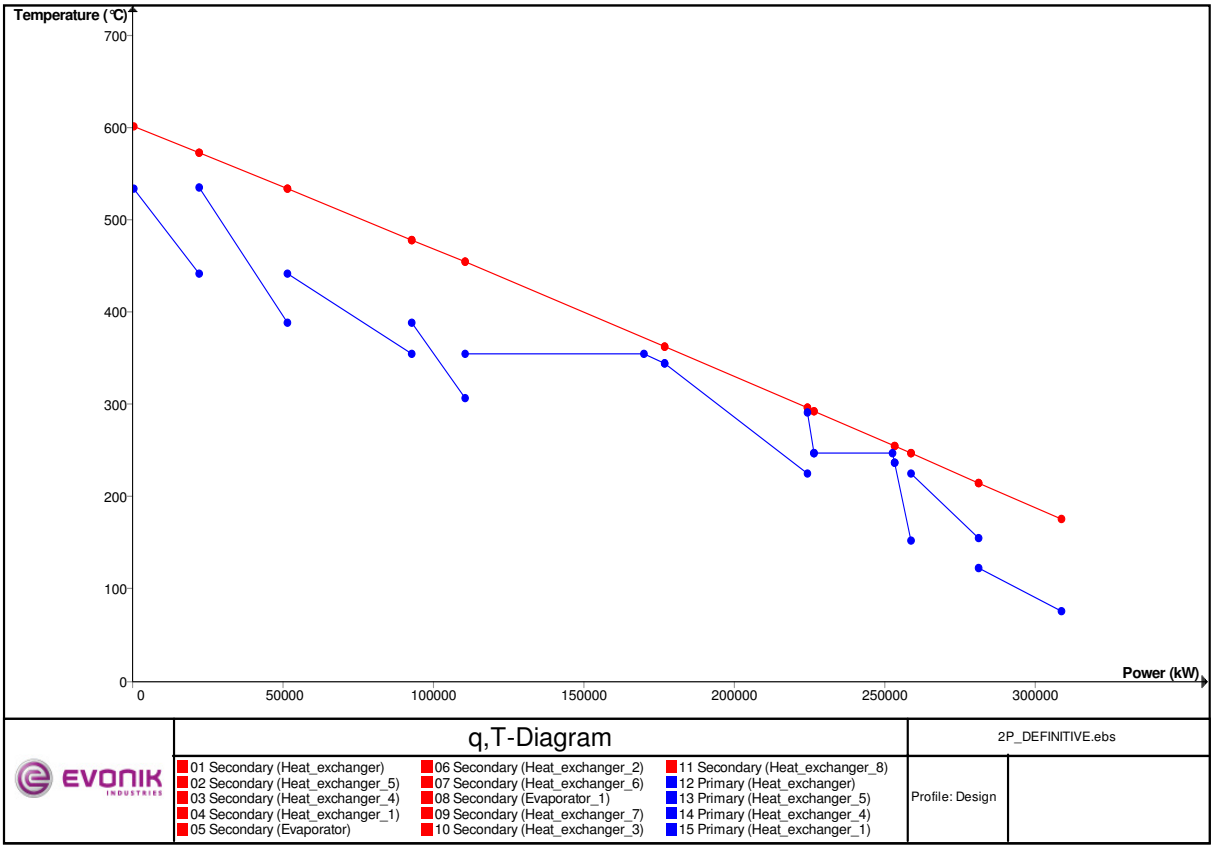

Figure 7.2: Heat transfer in the HRSG with Two Pressure CCPP

8 Modeling a Three Pressure CCPP

If we add a third evaporator, the HRSG is divided now in three stages and the steam is produced now at three different levels of pressure. The HRSG includes two superheaters at high pressure and one at the reheat pressure which superheats the steam produced in the intermediate evaporator. The high pressure evporator has two economizers, the intermediate pressure evaporator has only one while the low pressure does not have any. The steam after the low pressure evaporator is sent to the deaerator.

In the three pressure model, the water after leaving the deaerator is divided into three pipes. One part of the water (about the 15%) is evaporated at low pressure and comes back to the deaerator. Its energy is helping to heat the water in the evaporator and to remove the air contained. Other part of the water (about the 18%) goes to the intermediate pressure evaporator and is finally injected as saturated steam in the cold reheat pipe. The biggest part of the water (the left 67%) is heated first in the econmizers and evaporated in the high pressure evaporator.

As in the two pressures cycle, we have here two superheaters with spray water injection and two reheaters with spray water injection and saturated steam injected in the cold reheat pipe.

In our three pressures model appears as well an extra circuit designed for injecting solar boosting in the CCPP. This circuit is not in operation in this model and its performance will be explained later.

8.1 Performance of Three Pressure CCPP in ISO Conditions

Table 16 presents the results obtained for the Three Pressure CCPP working at the conditions for which it was designed.

CCPP Three Pressures	
Gas Turbine Power (MW_e)	260
Steam Turbine Power (MW_e)	138.5
High Pressure (bar)	155
Reheat Pressure (bar)	32
Low Pressure (bar)	4.7

Table 16: Power and Pressures for the CCPP Three Pressures

Comparing the results for the final electric power delivered to the net, the three pressure cycle produces more power than the other two cycles. This is a consequence of having a bigger HRSG which transfers more power to the steam cycle generating more steam and increasing the efficiency of the cycle.

8.2 Performance of Three Pressure CCPP with Changing Ambient Temperature

As we have explained for the gas turbine, its offload performance changes when the ambient temperature changes. The steam-water cycle depends on the exhaust gases of the gas turbine so its performance will change as well.

We will study the same cases studied for the gas turbine, at three different temperatures: 0°C, 30°C and 45°C.

Working in an ambient temperature lower than the design temperature causes an increment of efficiency of the gas turbine due to the higher density of the air which enables accepting more air into the compressor. However, the exhaust temperature of the gases is lower and with it the energy available in the gas stream for heating the water/steam in the HRSG. That means that although the gas turbine power output increases, the steam turbine power output decreases.

All the settings of the components in the steam/water cycle remain constant except in

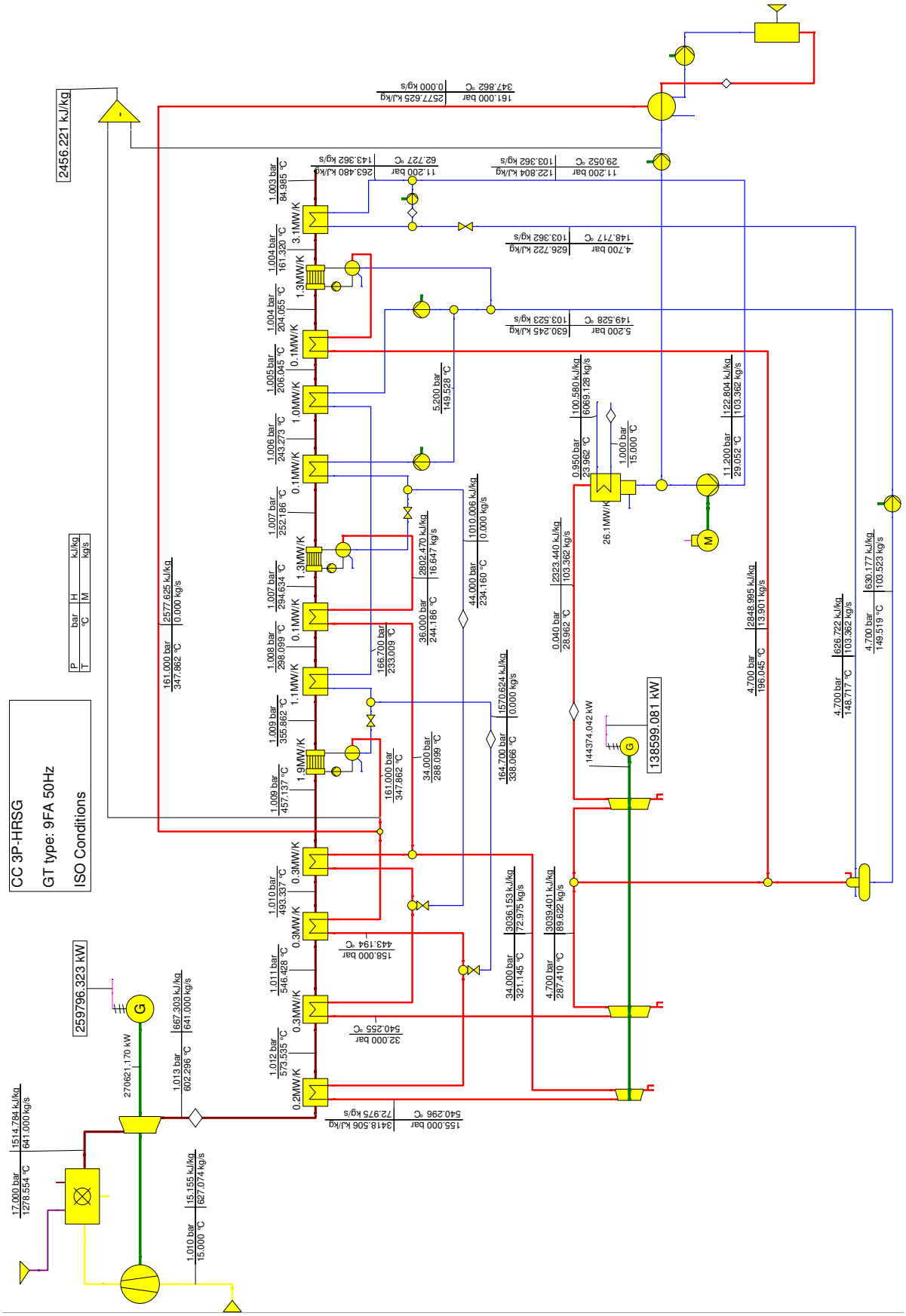

Figure 8.1: CCPP with Three Pressure HRSG at ISO Conditions

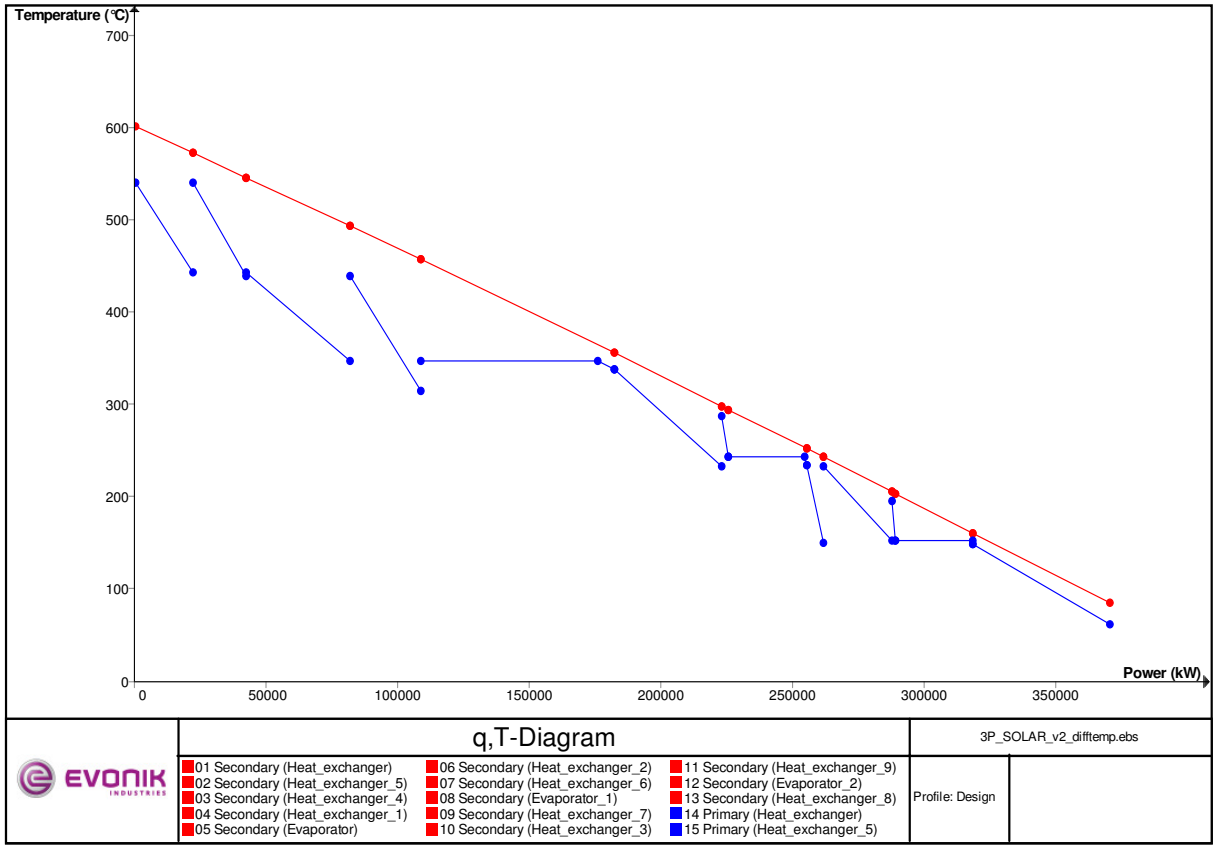

Figure 8.2: Heat transfer in the HRSG with Three Pressure CCPP at ISO Conditions

the condenser, where the cooling water suffers a variation in temperature at the same time that the ambient temperature changes. In this case, when the ambient temperature is 0°C, we suppose the sea water has a temperature of 10°C.

Cases	Gas Turbine Power	Steam Turbine Power	$\dot{m}_{steam}$ (kg/s)	$\dot{m}_{gas}$ (kg/s)
ISO	260 MW_e	138.5 MW_e	72.9	641
0 °C	318.6 MW_e	134.6 MW_e	70.4	677
30 °C	213.3 MW_e	122.5 MW_e	69.2	608.5
45 °C	183.6 MW_e	115.4 MW_e	66.9	588.4

Table 17: Comparison between the Partload Performance and Design Performance

The Table 17 shows the power and mass fluctuation when the ambient temperature changes. As we can see, although the gas turbine delivers more power when the ambient temperature is lower, the steam turbine always has its maximum power at design conditions. The closer to ISO conditions the higher power delivered.

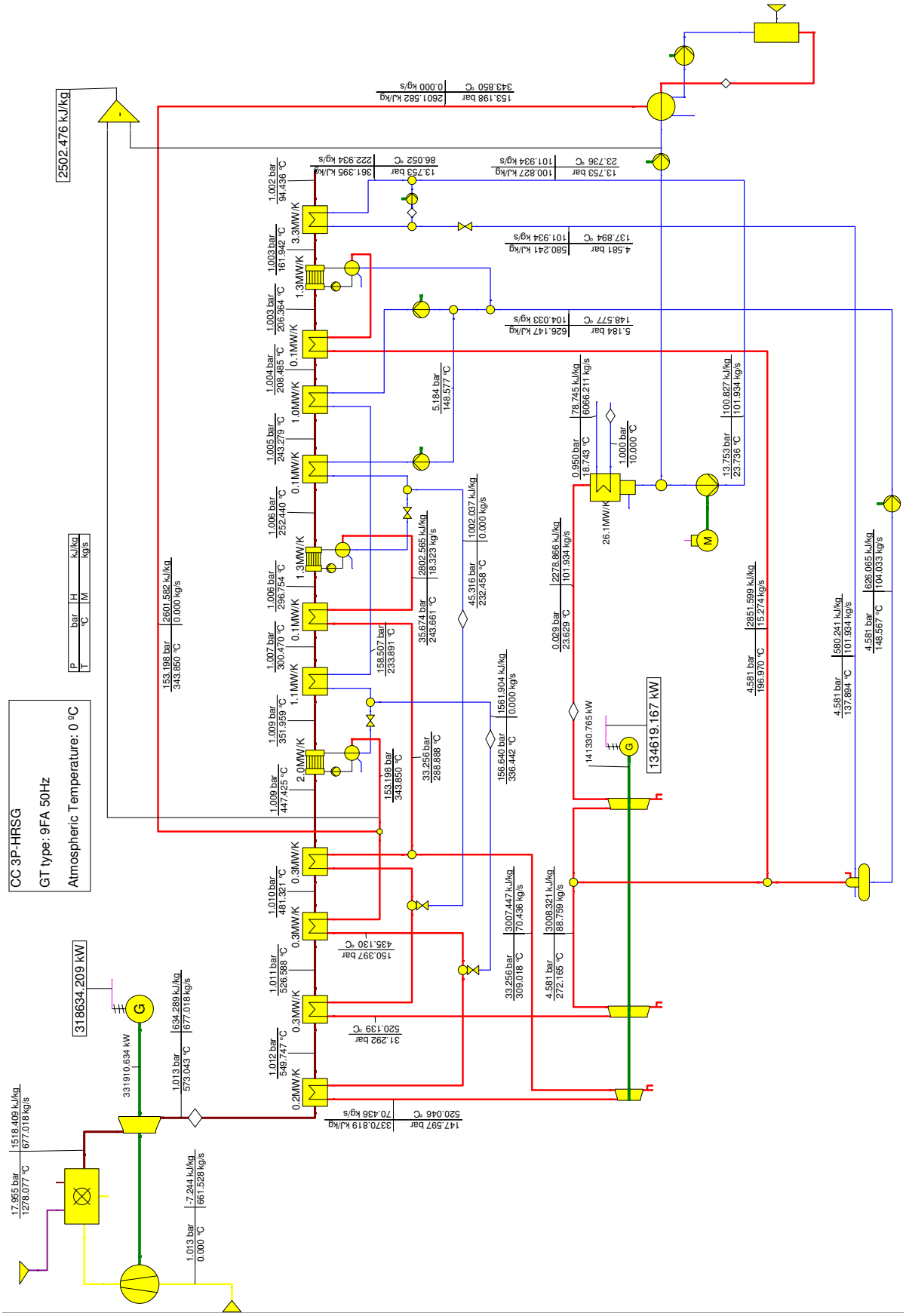

Figure 8.3: Three Pressure CCPP at 0°C

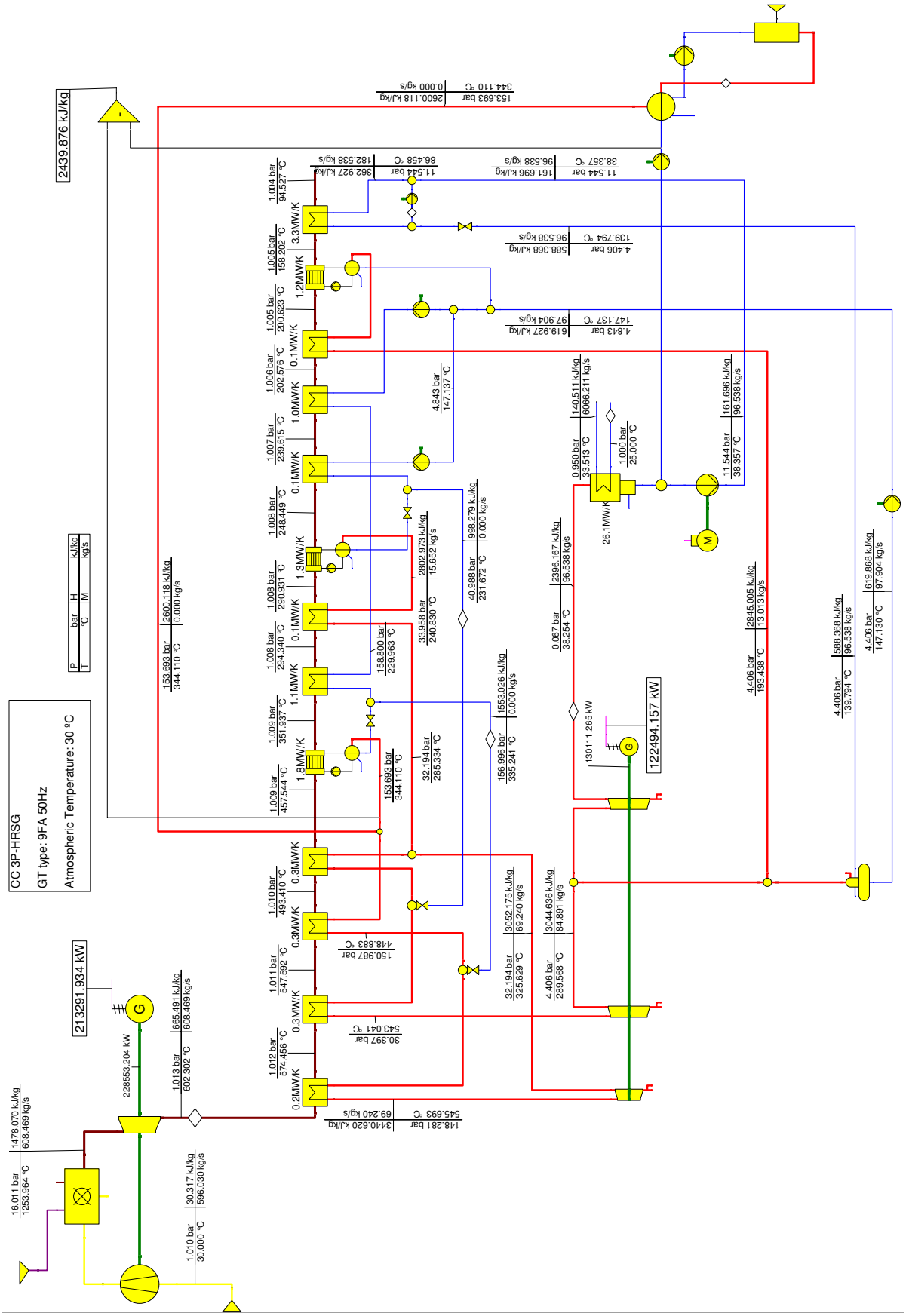

Figure 8.4: Three Pressure CCPP at 30°C

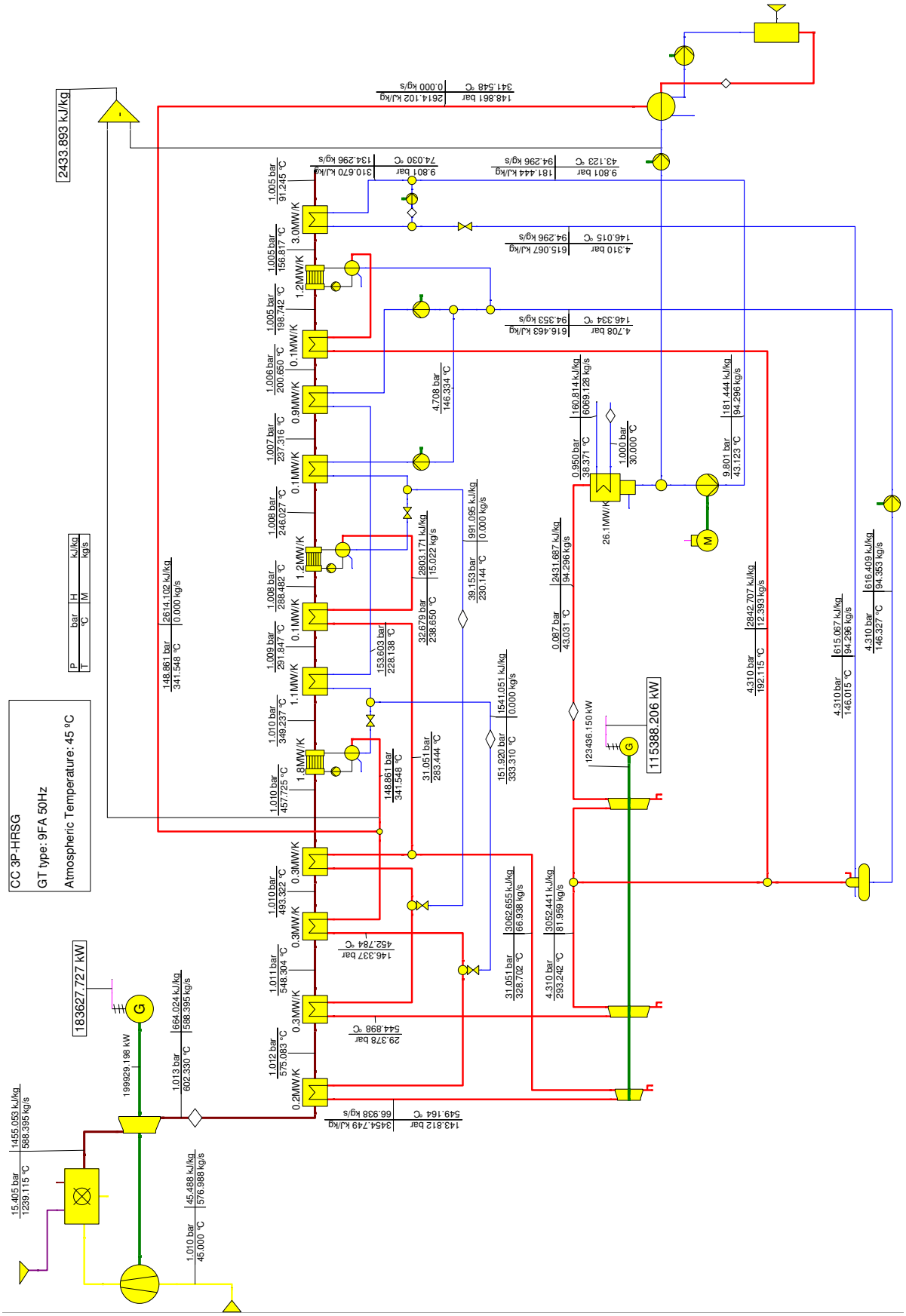

Figure 8.5: Three Pressure CCPP at 45°C

9 Standard Three Pressure CCPP with Solar Boosting

The efficiency of the Rankine cycle increases with the steam pressure and the amount of steam expanding through the turbine. When the ambient temperature rises the mass flow expanded through the gas turbine decreases and the energy available in the gas stream decreases as well. For this reason the heat transferred in the HRSG is smaller. That generates a smaller amount of steam in the HRSG and the power output of the steam turbine decreases due to the less mass of steam expanded.

At hot temperature conditions the overall efficiency of the CCPP decreases. Usually hot temperatures and sunny sky come together so if the location of our CCPP is in a place where the incident radiation of the Sun is enough for running a solar field, the energy which that field provides can help the electricity production in the CCPP. With a parabolic trough system installed next to the combined cycle plant, the incident radiation can be used as heat energy into the Rankine cycle of the CCPP. With this energy the lack of input energy in the Rankine cycle is compensated and the power output of the steam cycle increases.

That configuration, called Solar Boosting, is only possible when the Sun is shining and the mass flow of steam going through the steam turbine is smaller than in design conditions. We consider a parabolic trough solar field next to the CCPP in which the steam is generated directly using a once through system. In the solar field the water is converted into saturated steam and injected in the Rankine cycle. In state of art technology the solar field would be cooled by synthetic oil and the steam would be generated in an additional evaporator, see Figure 3.7. In this work we analyze an advanced system based on direct steam generation.

For modeling the solar boosting we have designed an extra circuit, shown in Figure 9.1. The water, after leaving the condenser, is pumped to the drum of the forced circulation solar steam generator. The water evaporates into saturated steam and goes through the steam drum. There, water in the mixture it is separated from the steam and recirculated in the solar boosting cycle. The concentrator heat exchangers of the solar field are not simulated in Ebsilon. Instead we use a "boundary value component" for setting the solar heat added in each case. We set a recirculation mass flow in the solar boosting circuit always higher than ten times the mass of saturated steam generated.

The amount of heat added is calculated as the heat necessary to heat the water from the conditions after leaving the condenser until saturated steam at high pressure. This specific heat is the difference between the enthalpy of the condensed water at high pressure and the enthalpy of the steam generated in the high pressure evaporator. The specific heat is multiplied by the mass flow added in each case getting the final value of heat added to the cycle.

There are four different possibilities for injecting the steam into the Rankine cycle depending on the point of injection and the properties of the injected steam:

- **Cold Reheated Steam:** the steam is injected after the first expansion in the turbine before the reheat exchanger.
- **Hot Reheated Steam:** the steam is injected after the reheat, just before entering in the second stage of the turbine.

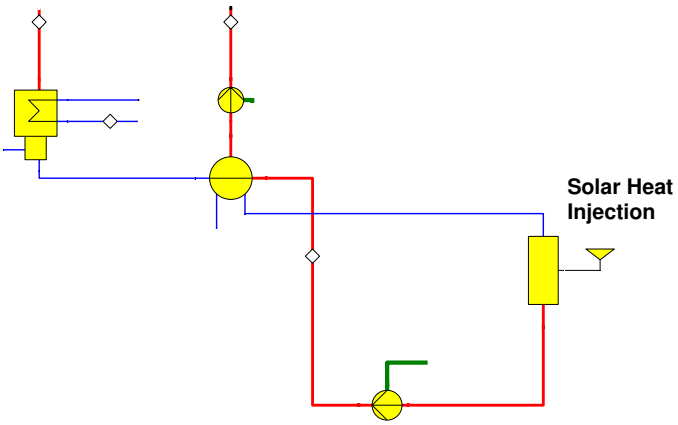

Figure 9.1: Solar Boosting Components

- **Saturated High Pressure Steam:** the solar field generates saturated steam at high pressure which is injected after the high pressure evaporator.
- **Hot High Pressure Steam:** in this configuration the steam is injected at high pressure in the hottest point of the circuit, after the superheaters.

The Figures 9.2 and 9.3 illustrate these definitions.

In this work we only discuss the Cold Reheated (CRH) and the Saturated High Pressure (SHP) steam configuration because they are the robust configurations. Systems with Hot Reheated (HRH) steam or Hot High Pressure (HHP) steam may have problems of thermal stress due to the temperature difference of the fluids in the injection point. In addition, solar absorbers for 540°C steam temperature are not yet available and the number of solar boosting hours at high pressure is expected to be lower.

9.1 Standard Three Pressure CCPP with Solar Boosting and Saturated High Pressure Steam (SHP)

In the Standard Study of Solar Boosting, saturated steam at high pressure will be injected in the HRSG in a point of the pipe which connects the HP evaporator with the superheater. The properties of the injected steam depend on the case of study.

The case of study is that in which the temperature is warmer than in design conditions. It is assumed that the incident radiation is able to heat the receiver fluid in the parabolic trough. Although at ISO conditions (15°C) it is possible to obtain heat energy from the collector field we suppose at these conditions the CCPP is working at full operation and the solar heat is not necessary. We suppose that at 0°C, in winter, the Sun hardly shines and it is not possible to obtain energy from the solar field. The only considered cases will be 30°C and 45°C.

APPROACH "A"

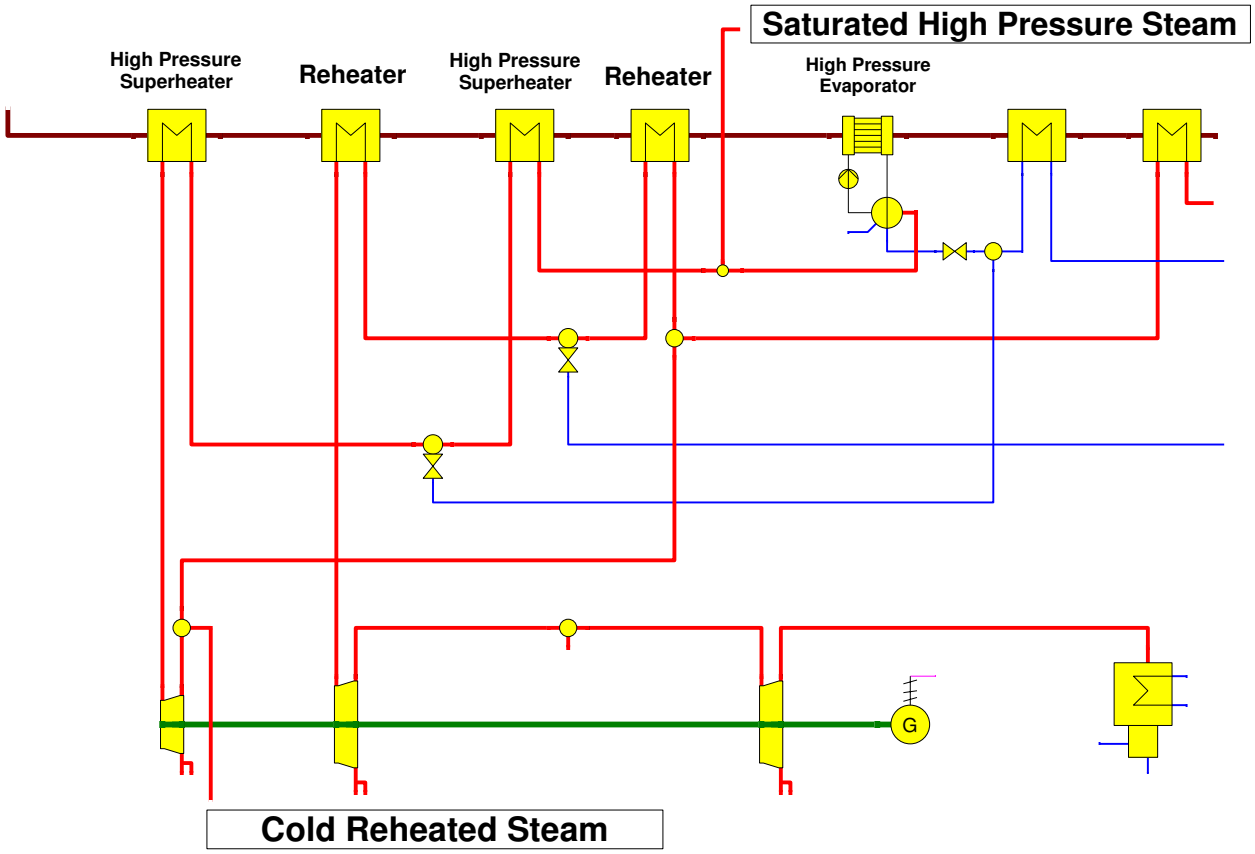

Figure 9.2: Diagram of Cold Reheated Steam and Saturated High Pressure Steam injection points.

With the Solar Boosting study we pretend to find out the maximum solar heat which can be injected into an existing Rankine cycle. That means that the design parameters must remain unalterable:

- the pressure in the steam drum can not exceed the design pressure in nominal conditions.
- the HRSG shall not be modified.
- the high pressure and reheat temperatures must remain constant.
- the amount of solar heat added is as big as possible but the combination of solar steam and the HRSG steam is never bigger than the HRSG steam in design conditions.

In every case we considered different amounts of solar heat added. The three chosen loading cases are: adding a 5%, 10% or 12% of the nominal steam flow. It is not possible to add more than 12% of nominal steam because the section of the steam turbine does not accept more flow.

The steam mass flow at ISO conditions are 72.9 kg/s and the corresponding masses added in each case are presented in Table 18.

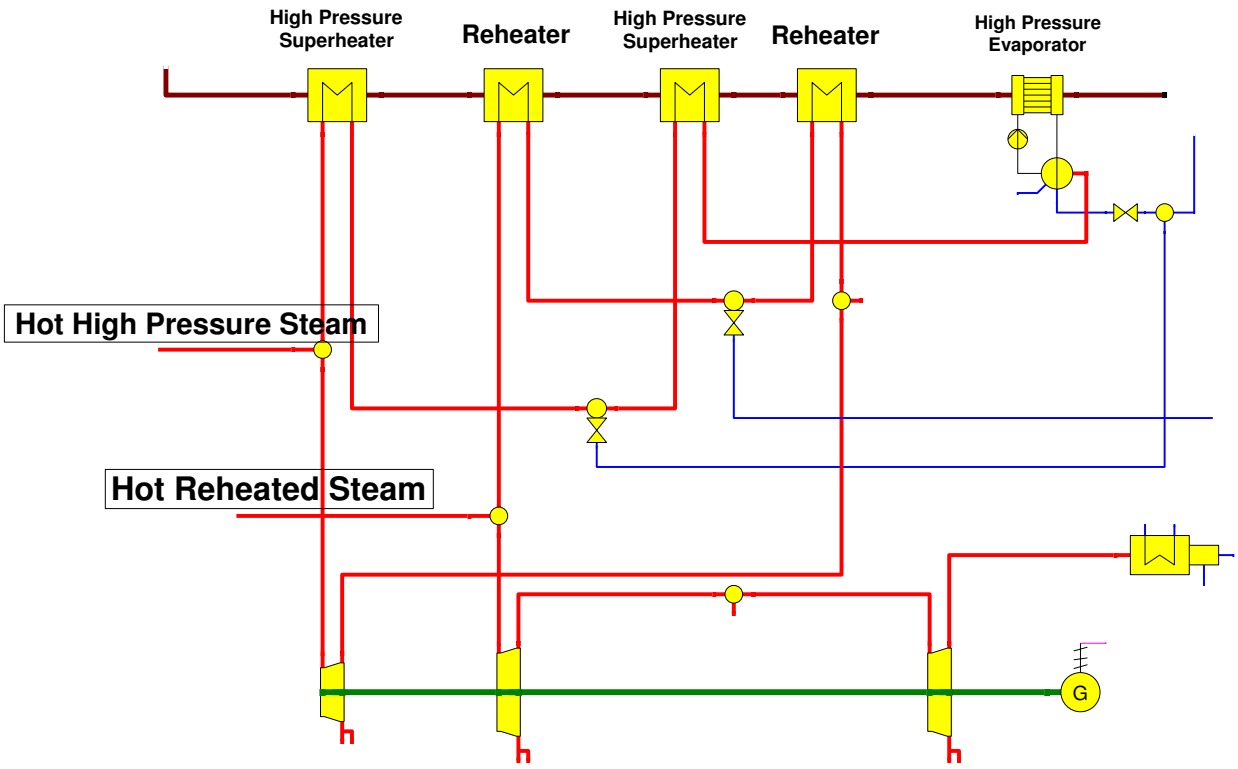

Figure 9.3: Diagram of Hot Reheated Steam and Hot High Pressure Steam injection points.

	$\dot{m}_{solar}$ (kg/s)
5%	3.6
10%	7.3
12%	8.7

Table 18: Mass flow of Steam added in each case.

Looking at the results shown in the Table 19 we can conclude that the addition of steam coming from the solar field always increases the steam cycle power output because more steam is being expanded in the steam turbine.

The table 19 also compares the results obtained for each cycle when solar heat is added. As we can see in the table the bigger amount of solar heat added the bigger output power of the steam turbine. Besides, by adding the same percentage of steam heated by solar energy, the output power is bigger at lower temperatures. That is because the fluegas mass flow of the gas turbine is higher at lower temperatures, so the result is a higher heat input to the steam cycle because more energy is being transferred in the HRSG. The maximum power that we can obtain in our study is at 30°C by adding the 12% of steam in design case.

The models of the three cases at 30°C are shown in Figures 9.4, 9.5 and **??**nd at 45°C in the Figures 9.7, 9.8 and 9.9.

	Cases	$P_{steamturbine}$ (MW_e)	$\dot{m}_{HPEVAP}$ (kg/s)	Q_{solar}(MW)
NO SOLAR	ISO	138.48	72.9	
	0°C	134.62	70.4	
	30°C	122.49	69.2	
	45°C	115.4	66.9	
SOLAR, 5% of nominal steam flow (3.6 kg/s)	30°C	125.84	67.43	8.85
	45°C	118.58	65.12	8.83
SOLAR, 10% of nominal steam flow (7.3 kg/s)	30°C	129.16	65.6	17.61
	45°C	121,8	63.3	17.57
SOLAR, 12% of nominal steam flow (8.7 kg/s)	30°C	130.36	64.9	21.09
	45°C	123.03	62.57	21.04

Table 19: Comparison between Three Pressure Cycles when Solar Heat is added.

Looking at Figure 9.6 we can see that compared to the operation without solar boosting, see Figure 8.4, the high pressure rises by 7 *bar* and the high pressure and reheat temperatures drop by 7-9 °C.
After seeing the results of this study two interesting questions have to be solved:

1. Is the solar field construction profitable?
2. It is economic to built the CCPP in a way to use solar steam at nominal conditions?

The discussion of these two question will be done in the consecutive studies in chapters 9 and 10.

9.2 Standard Three Pressure CCPP with Solar Boosting and Cold Reheated Steam (CRH)

Other possibility for injecting the steam is the Cold Reheated (CRH) steam injection. As we explain before, with this configuration the steam heated with solar energy is added to the cycle after the first expansion stage in the steam turbine.

We will divide this study in two parts:

- In the first part, the amount of energy injected in the cycle will be exactly the same than in the case of injecting saturated high pressure (SHP) steam. With this we want to compare the two methods.
- In the second part, the amount of energy injected is the energy needed for increasing the temperature of the feed water to the cold reheat temperature after the first expansion stage in the steam turbine. The amount of energy is calculated by multiplying the enthalpy difference between the point of injection and the water after the condenser and the mass of steam heated.

The results of the first part are shown in the Table 20. Comparing the output power of the steam turbine in the cases of CRH and SHP we can conclude that by adding the same

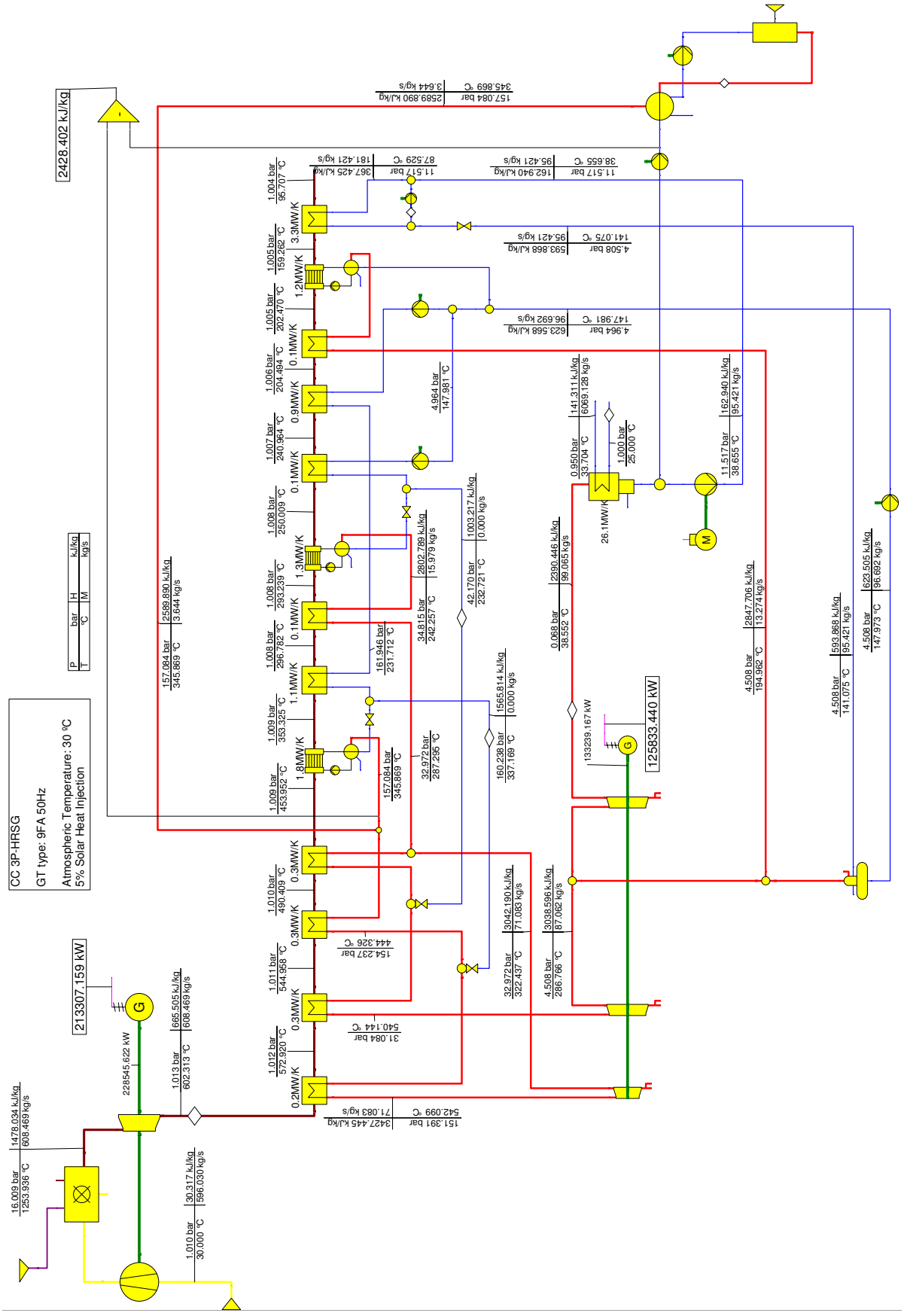

Figure 9.4: Three Pressure CCPP at 30°C with a 5% of high pressure steam added as Solar Heat

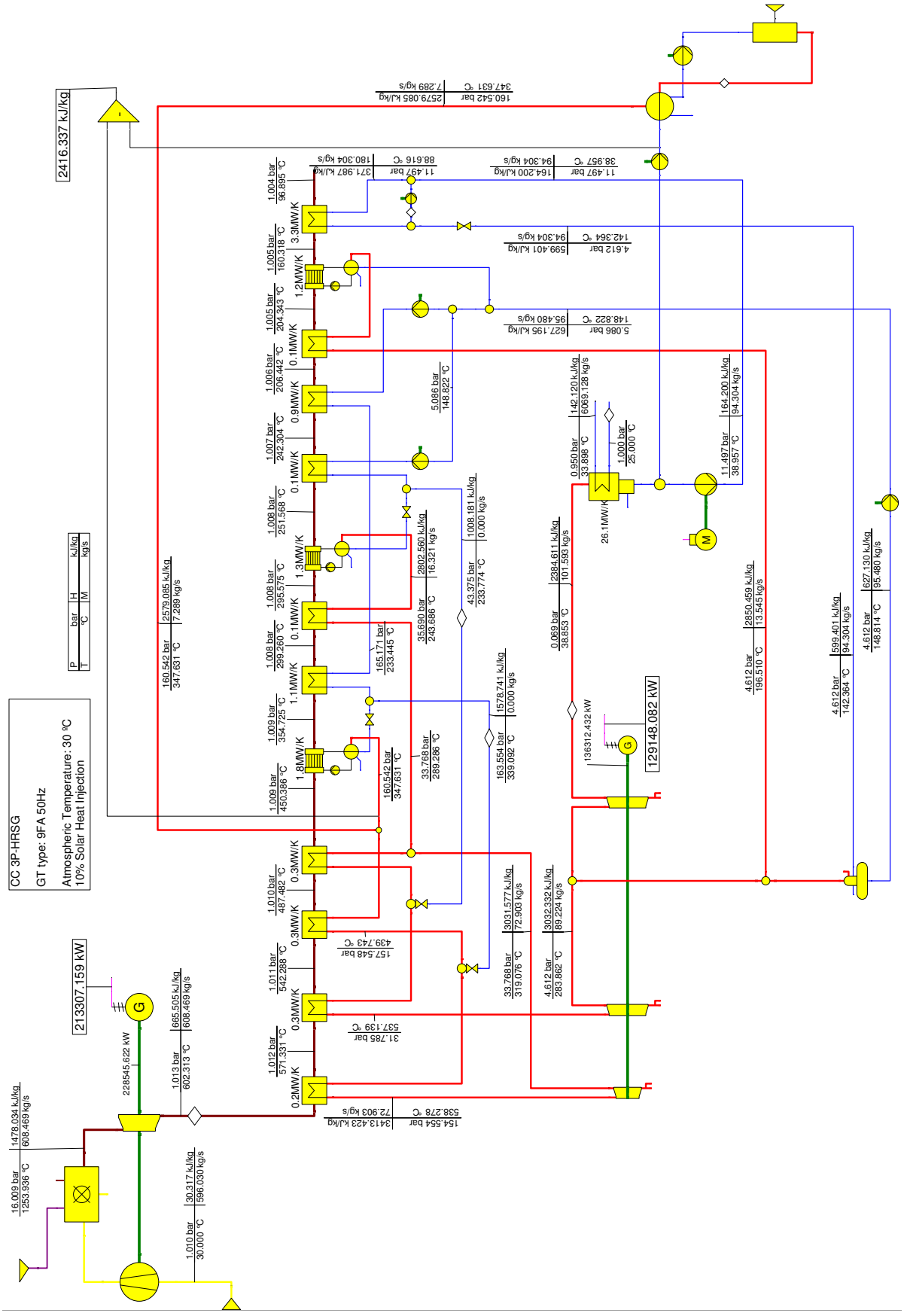

Figure 9.5: Three Pressure CCPP at 30°C with a 10% of high pressure steam added as Solar Heat

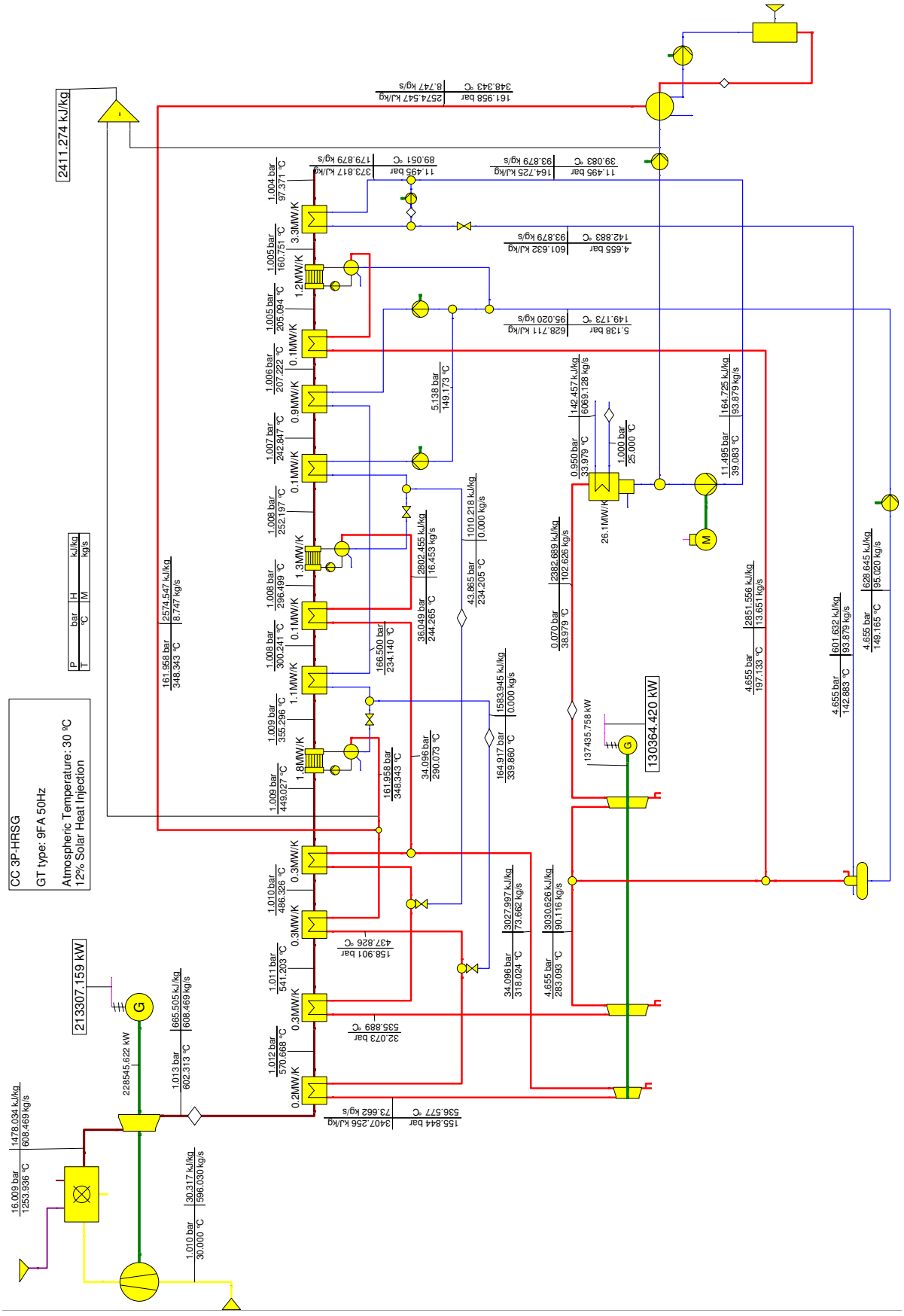

Figure 9.6: Three Pressure CCPP at 30°C with a 12% of high pressure steam added as Solar Heat

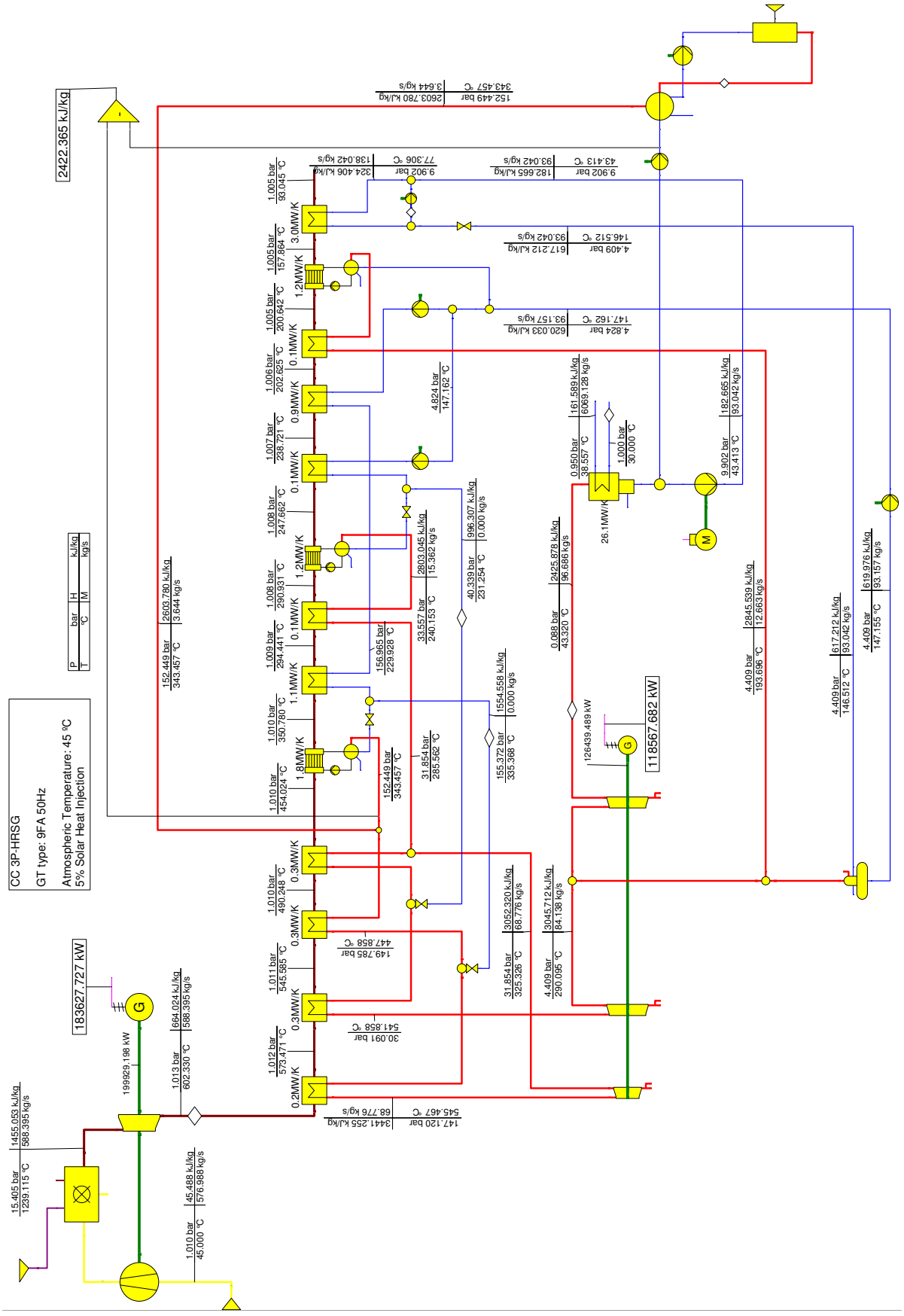

Figure 9.7: Three Pressure CCPP at 45°C with a 5% of high pressure steam added as Solar Heat

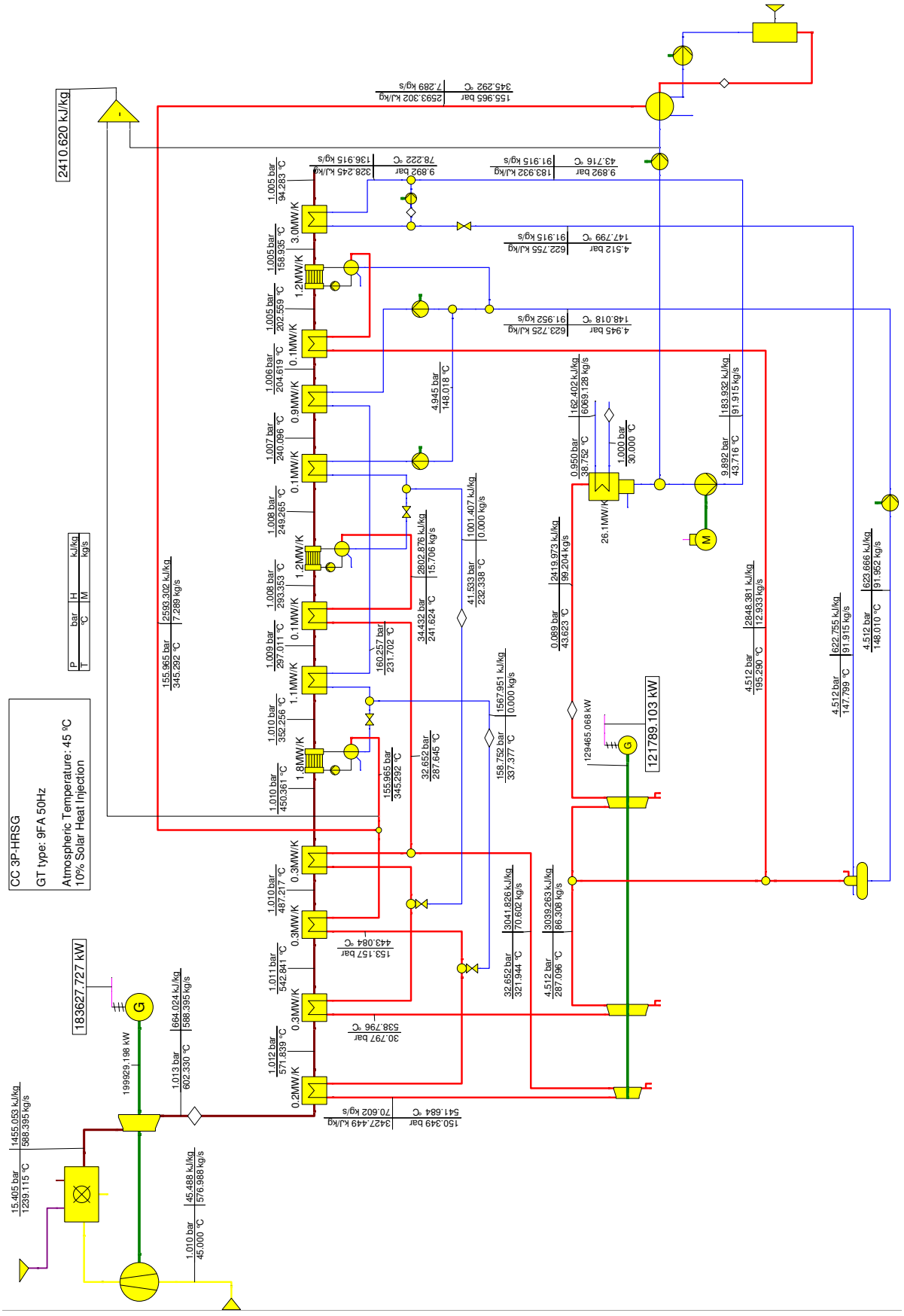

Figure 9.8: Three Pressure CCPP at 45°C with a 10% of high pressure steam added as Solar Heat

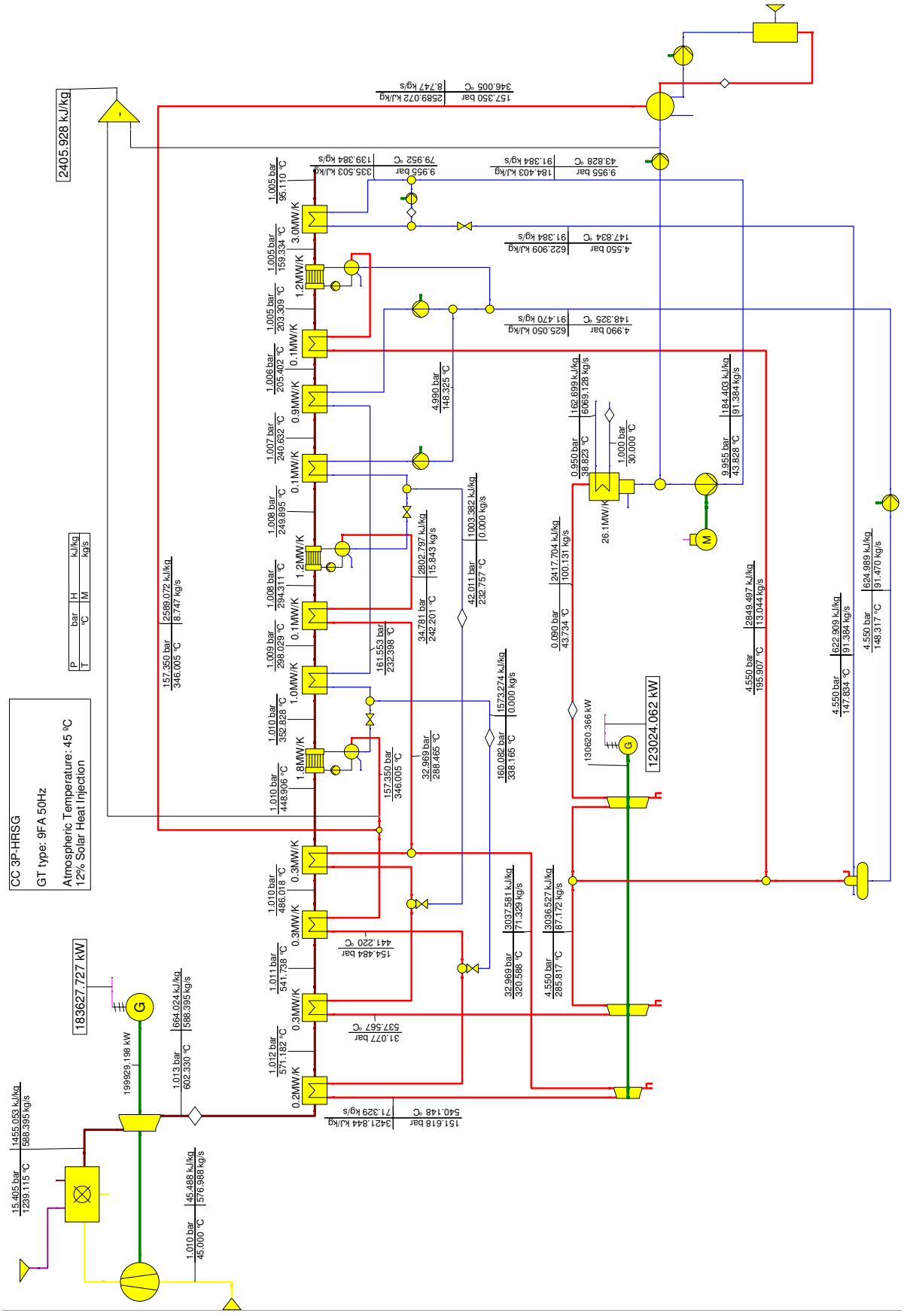

Figure 9.9: Three Pressure CCPP at 45°C with a 12% of high pressure steam added as Solar Heat

T (°C)	Q_{solar}(MW)	$p_{steamturbine}$ (MW_e)	$\dot{m}_{HPEVAP}$ (kg/s)	$\dot{m}_{solar}$ (kg/s)
30	8.85	125.27	68.7	3.4
45	8.83	117.98	66.4	3.4
30	17.61	128.02	68.6	6.7
45	17.57	120.65	65.8	6.7
30	21.09	129.03	67.9	8
45	21.04	121.68	65.6	8

Table 20: Three Pressure CCPP with Solar Boosting: solar steam added as CRH.

Percentage of nominal steam flow	Temperature °C	$p_{steamturbine}$ (MW_e)	$\dot{m}_{HPEVAP}$ (kg/s)	$\dot{m}_{solar}$ (kg/s)	Q_{solar} (MW)
5 %	30	125.83	68.6	4	10.59
	45	118.5	66.3	4	10.55
10 %	30	129.07	67.9	8.1	21.61
	45	121.77	65.6	8.1	21.18
12 %	30	130.05	67.7	9.7	25.53
	45	123.05	65.4	9.7	25.46

Table 21: Three Pressure CCPP with Solar Boosting injected as CRH.

amount of solar heat the SHP injection improves the steam turbine power output.

For calculating the amount of solar heat needed for heating the condensed water at high pressure until superheated steam at high pressure we use the same procedure than in the case of adding saturated steam. We calculate the enthalpy difference between both points of measure and multiply it for the mass flow added. The Table 21 shows the results obtained for the second part of the study.

Comparing the Tables 20 and 21 we can conclude that:

- By adding the same amount of solar heat, with the SHP technology the steam turbine delivers more output power than with the CRH technology. That proves that adding steam at high pressure is always better so the efficiency of the SHP technology is higher than the CRH efficiency.
- By adding the energy needed for increasing the temperature of the feed water to the steam temperature in the point of injection in each case, the SHP technology allows to obtain more output power (130.36 MW_e with SHP, while with CRH 130.05 MW_e) with the addition of a lower amount of solar heat (21.09 MW_{th} in the case of SHP, while 25.53MW_{th} with the CRH technology). That means that for obtaining the same power output the addition of solar heat in the case of CRH has to be bigger. The consequence of that is the need of more efficient parabolic troughs or a bigger covered collector surface in the solar field with the CRH technology.

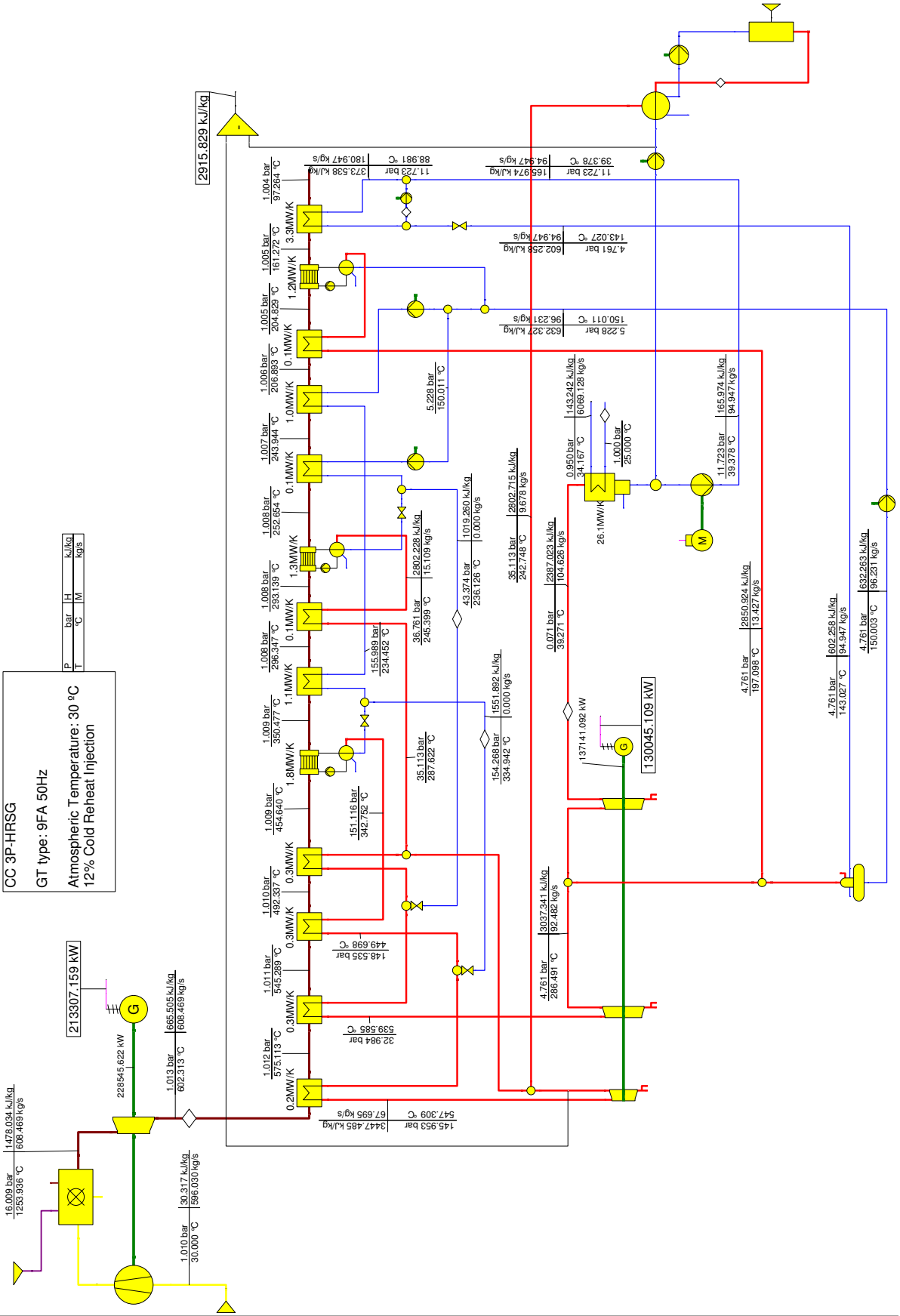

Figure 9.10: Three Pressure CCPP at 30°C with a 12% of high pressure steam added as Solar Heat with CRH Injection

10 Conversion Efficiency of Solar Boosting

The energy conversion efficiency is an useful ratio for comparing the impact of introducing solar heat. We will define it as the ratio between the additional electric power when we inject the CCPP with solar steam and the amount of solar heat that we are injecting.

$$\eta_{solar} = \frac{P_{el,solar} - P_{el}}{Q_{th,solar}} \tag{10.1}$$

We will compare the conversion efficiencies for both SHP and CRH technologies at 30°C.

10.1 Conversion Efficiency of Saturated High Pressure Steam

For the case of injection with saturated high pressure steam, the conversion efficiency is calculated as:

$$\eta_{solar,30°C} = \frac{P_{el,30°C,solar} - P_{el,30°C}}{Q_{th,30°C,solar}} = \frac{130.36MW_e - 122.49MW_e}{21.09MW_e} = 0.373 \tag{10.2}$$

The SHP technology has a nominal gross efficiency which is only 1% lower than the efficiencies published in literature for PTC systems (38.5% gross efficiency in [14]).

10.2 Conversion Efficiency of Cold Reheated Steam

When the injection of solar heat is made in the cold reheat pipe:

$$\eta_{solar,30°C} = \frac{P_{el,30°C,solar} - P_{el,30°C}}{Q_{th,30°C,solar}} = \frac{130.05MW_e - 122.49MW_e}{25.53MW_e} = 0.296 \tag{10.3}$$

Comparing the results for SHP and CRH we can conclude that the SHP is a more efficient technology. With SHP we obtain 130.36 MW_e by injecting only 21.09 MW_{th} of solar heat, while with CRH we need more thermal heat for reaching lower power output. Although the SHP technology is more expensive than CRH in terms of installation in the CCPP, because the injection is done around 155 bar, due to its high efficiency we need a smaller solar field than with the CRH technology being cheaper in terms of construction of the solar field.

11 Impact of Solar Steam Injection on Temperatures and Pressures

11.1 Impact of Saturated High Pressure Steam Injection

In this chapter we will discuss briefly the impact of injecting saturated steam at high pressure as solar heat on the temperature of the superheated steam and its pressure. The Table 22 shows the values of pressures and temperatures in each case:

In the Table 22 the $p_{HP,SH,INLET}$ represents the high pressure value of the saturated steam in the point of injection. The $T_{HP,ST}$ represents the temperature of the superheated steam before entering the steam turbine.

Saturated Steam			
Percentage of solar steam added	T_{AMB}	$p_{HP,SH,INLET}$ (bar)	$T_{HP,ST}$ (°C)
0%	ISO	161	540
0%	30 °C	153.7	545.7
5%		157.2	541.9
10%		160.5	538.3
12%		162	536.6
0%	45 °C	149	549
5%		152.6	545.3
10%		156	541.7
12%		157.3	540.2

Table 22: Variation of temperature and pressure with the injection of saturated steam at high pressure.

Taking a look at the results we see that the partload operation of the CCPP causes a decrease in pressure. However, the injection of saturated steam at high pressure makes the pressure rise. With the temperatures occurs the opposite, the partload operation leads to a increase in temperatures while the injection of saturated steam results in a decrease. That occurs because when we work in partload at 30°C for example, the gas turbine is delivering a fixed energy to the HRSG. If we inject new mass flow from the solar the heat exchangers have to heat more mass flow now and the temperature is lower. With the pressure occurs the opposite, with the injection of solar steam the pressure has to increase because of the bigger mass flow in the cycle.

11.2 Impact of Solar Heat Injection as Cold Reheated Steam

The Table 23 presents the results for the injection of cold reheated steam at intermediate pressure. T_{HRH} represents the temperature in the cold reheat pipe and p_{RH} represents the pressure of reheat, before entering the second stage of the steam turbine.

Saturated Steam			
Percentage of solar steam added	T_{AMB}	p_{RH} (bar)	T_{HRH} (°C)
0%	ISO	32	540
0%	30 °C	30.4	543
5%		31.5	541.8
10%		32.5	540.2
12%		33	539.6
0%	45 °C	29.4	544.8
5%		30.5	543.5
10%		31.6	542
12%		32	541.4

Table 23: Variation of temperatures and pressures when solar heat is added as cold reheated steam.

With the injection of cold reheated steam the variation of pressures and temperatures is exactly in the same way than with saturated high pressure steam. But with CRH the variation in both pressure and temperature is smaller compared with SHP as we can see in the Table 24.

Technology	ΔP (bar)	ΔT (°C)
SHP	8.3	9
CRH	2.6	3.4

Table 24: Variation of temperatures and pressures with solar steam injection

It is worthwhile to mention that the limit of HP value is not attained. The pressure is lower than in the ISO case (155 bar), see Figure 9.10.

12 Thermal Efficiency of the CCPP

The thermal efficiency of the CCPP is defined as the ratio between the output power obtained from the whole power plant and the energy given to the gas turbine. The energy given to the gas turbine is the amount of fuel burnt in the combustion chamber multiplied by its lower heating value. For the case of an ambient temperature of 30°C:

$$\eta_{30°C} = \frac{P_{GT} + P_{ST}}{\dot{m}_{fuel} \cdot Hu} = \frac{213.3MW + 122.5MW}{12.4kg/s \cdot 50.015MJ/kg} = 0.541 \tag{12.1}$$

12.1 Thermal Efficiency of the CCPP with Solar Boosting

If we assume that the solar energy is for free, we can calculate the thermal efficiency of the CCPP when solar heat is injected:

$$\eta_{30°C,SHP} = \frac{P_{GT} + P_{ST}}{\dot{m}_{fuel} \cdot Hu} = \frac{213.3MW + 130.4MW}{12.4kg/s \cdot 50.015MJ/kg} = 0.554 \tag{12.2}$$

$$\eta_{30°C,CRH} = \frac{P_{GT} + P_{ST}}{\dot{m}_{fuel} \cdot Hu} = \frac{213.3MW + 130.1MW}{12.4kg/s \cdot 50.015MJ/kg} = 0.553 \tag{12.3}$$

The thermal efficiency of the CCPP increases with the addition of solar heat and is higher in the case of the SHP technology.

13 Standard Three Pressure CCPP with Increased Solar Boosting

Until now we have studied the introduction of solar energy in a CCPP for improving the overall efficiency. We only considered the cases with warmer temperatures and partload performance in the gas turbine.

The steam turbine is designed for given conditions (ISO Conditions) and the design calculations correspond to these conditions. That means that, for example the cross section

of the steam turbine is fixed in design conditions and it defines the limit of the steam flow through the turbine. If we want to inject more steam in the cycle the total mass never can be bigger than in the design conditions.

Even in ISO conditions (15°C) it is possible to obtain solar energy with the parabolic trough technology. That means, that at ISO conditions we are wasting the energy obtained in the solar field because the limited cross section does not allow to inject more steam in the Rankine cycle. Wasting this solar energy makes the solar field less economic.

We can consider the injection of solar energy in design conditions by making the cross section of the steam turbine bigger. How big? We have to design a new steam turbine whose mass flow in design conditions is the sum of the solar steam and the steam flow that we had in the previous steam turbine in ISO conditions.

APPROACH "B"

For modeling this concept in Ebsilon we will use the three pressure cycle with solar boosting. But the difference now is that we will also introduce steam heated with solar energy in design conditions.

The Table 26 shows the results obtained for the three pressures CCPP when in design conditions we add a 12% of solar heat. We have to notice that the HRSGs in both cycles (with solar or no solar in design conditions) are not exactly the same. In the cycle with solar injection in design conditions, the gas temperature in the economizer at the end of the gas stream is not so low as in the cycle without solar injection. This is because the mass of water through it is bigger and the temperature of the water is higher as well. That makes impossible to reach the temperature of 85°C at the end of the gas steam. Instead we reach a temperature of 86.7°C and despite of this small difference we can consider that both HRSGs work in a similar way.

By comparing the results for ISO conditions, with or without solar heat injection, we can conclude that the addition of solar heat to the CCPP in design conditions allows reaching higher output power. If the hours of operation of the solar field are bigger we will obtain more energy for a defined investment costs and the energy will be cheaper in a long-term.

Conditions	$\dot{m}_{HPEVAP}$ (kg/s)	$\dot{m}_{solar}$ (kg/s)	$p_{steamturbine}$ (MW_e)	Q_{solar}(MW)
ISO	72.9		138.5	
ISO with Solar Inject.	67.7	8.7	145.96	21.48

Table 25: Comparison between the CCPP working in ISO conditions with and without solar injection.

For all the cases in a range between 10°C and 45°C the mass of solar heat injected is the same. When the temperature rises and the gas turbine starts working in off-design conditions, the production of steam in the high pressure evaporator decreases. The solar heat needed for heating the mass flow decreases with higher temperatures and the result is a lower output power in the steam turbine.

12% of solar injection					
CASES	$\dot{m}_{solar}$ (kg/s)	$\dot{m}_{HPEVAP}$ (kg/s)	$\dot{m}_{total}$ (kg/s)	Q_{solar}(MW)	$p_{steamturbine}$ (MW_e)
design	8.7	67.7	76.5	21.48	145.96
10°C	8.7	67.8	76.5	21.57	142.90
30°C	8.7	64.1	72.9	21.32	130.24
45°C	8.7	61.9	70.7	21.26	122.24

Table 26: Results for a Three Pressure CCPP with 12% of Solar Injection in a range of 10°C to 45°C

APPROACH "C"

Other possibility is the addition of solar heat until reaching the maximum limit of mass flow going through the steam turbine in every case. As we said, when the temperature increases the mass of high pressure steam evaporated is smaller and the mass of solar heat which can be introduced in the cycle until reaching the limit is bigger. The mass flow going through the turbine is in all the cases constant and the solar heat increases with the temperatures. The result is a higher power output at warmer temperatures.

The last configuration makes sense because with warmer temperatures the amount of solar heat available is higher. The reasonable is to add more solar heat at higher temperatures and to improve the overall power output.

CASES	$\dot{m}_{solar}$ (kg/s)	$\dot{m}_{HPEVAP}$ (kg/s)	$\dot{m}_{total}$ (kg/s)	Q_{solar}(MW)	$p_{steamturbine}$ (MW_e)
design	8.7	67.7	76.5	21.48	145.96
10°C	8.7	67.8	76.5	21.57	142.90
30°C	16.1	60.4	76.5	38.80	136.69
45°C	20.6	55.9	76.5	49.35	132.39

Table 27: Results for a Three Pressures CCPP with Maximum Solar Heat Injection in a range of 10°C to 45°C

14 Economic Analysis of the Three Pressure CCPP with Solar Boosting

In this chapter a rough economic analysis of the costs for electricity production will be done. We will know if the price of producing electricity in our CCPP with solar boosting is economically competitive between others technologies. The comparison with the expected price and the real price allows us to determine if the project is feasible or not.

For doing the economic study we will assume that the CCPP is already built and currently in operation and due to the development of the solar technologies we want to equip

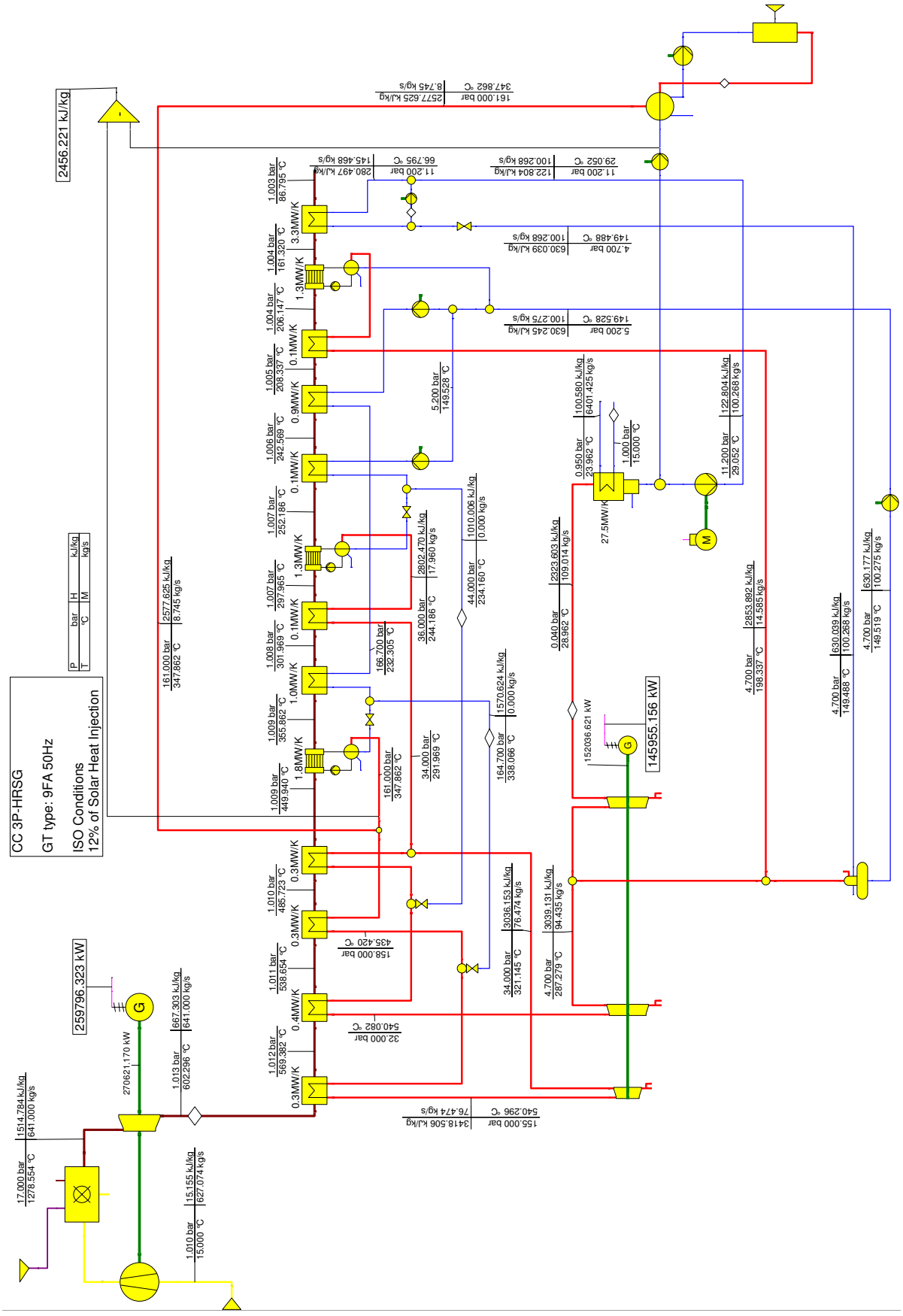

Figure 13.1: Three Pressure CCPP at ISO Conditions with a 12% of high pressure steam added as Solar Heat.

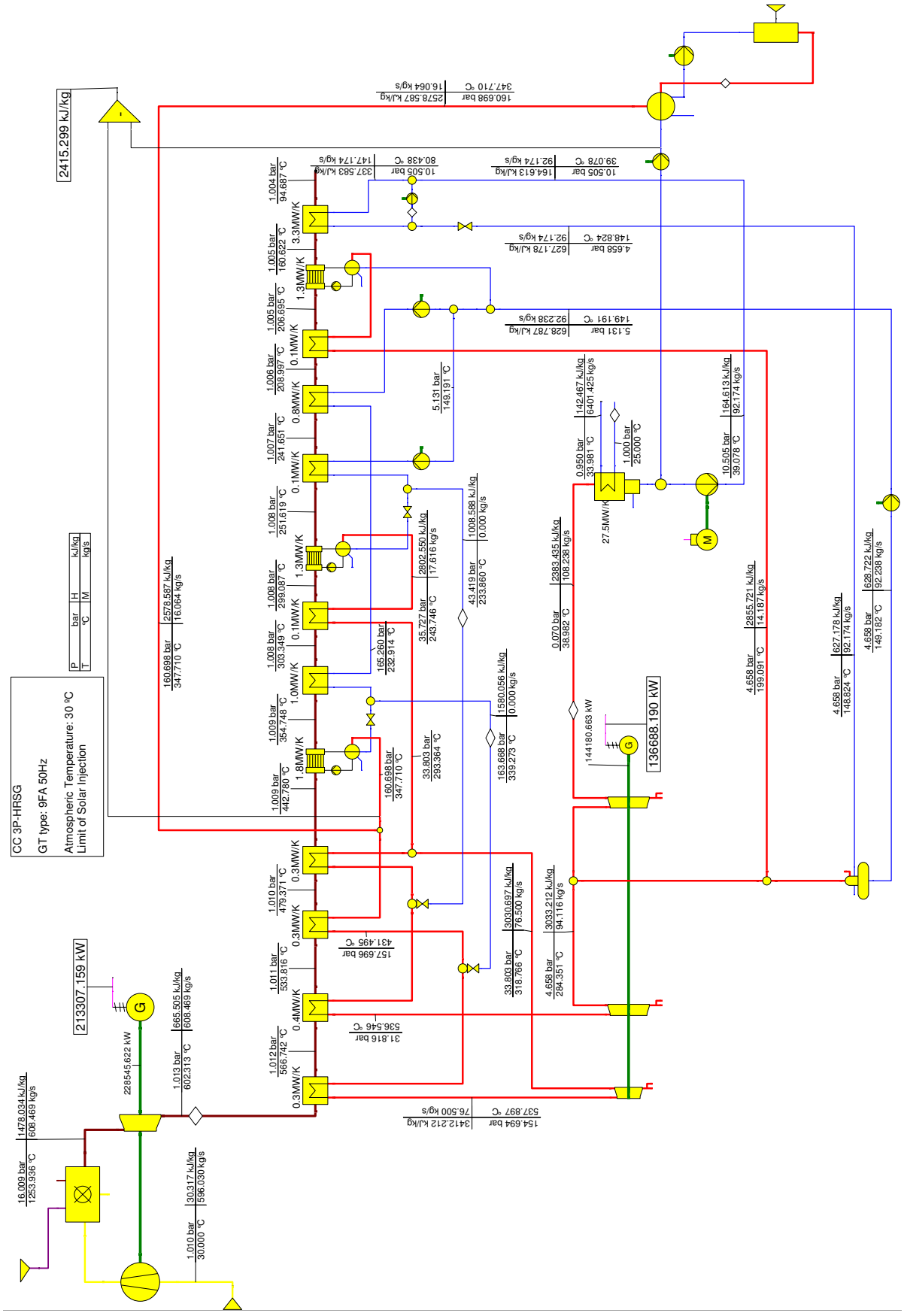

Figure 13.2: Three Pressure CCPP at 30°C with high pressure steam added as Solar Heat until reaching the mass flow limit in the steam turbine.

the present installations with a solar field for improving the electricity production with high ambient temperatures and sunny weather.

For designing the collector surface of the solar heat, we will consider two different technologies for the solar field: Parabolic Trough Concentrators (PTC) and Pneumatic Pre-Stressed Concentrators (PPC).

14.1 Pneumatic Pre-Stressed Concentrators (PPC)

The PPC system is currently developed by HELIOVIS AG and Vienna University of Technology and it is still in a prototype phase. The PPC technology consists of two pressurized air chambers separated by a membrane with mirror-coating, [14]. The curvature of the mirror is produced by a higher pressure in the upper air chamber. A picture of the PPC system is shown in the Figure 14.1

The solar field will be designed for injecting the CCPP with 12% of mass of steam in

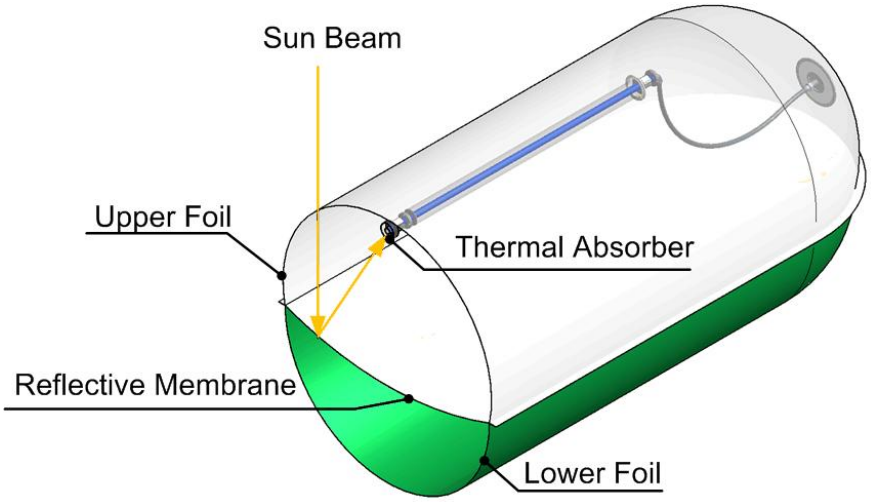

Figure 14.1: Sketch of pneumatic prestressed concentrator, [14]

nominal conditions as solar heat. At 30°C the heat needed for injecting that mass are 21.09 MW of thermal heat (Q_{th}).

Taking into account that the maximum optical efficiency of the PPC is $\eta_{opt} = 0.734$ the radiation needed in out solar field is:

$$Q_{rad} = \frac{Q_{th}}{\eta_{opt}} = \frac{21.09}{0.734} = 28.73MW \tag{14.1}$$

Besides, the specific power absorbed by the collectors in the solar field has a value of 800 W/m^2, being the necessary heat absorbed:

$$A_{collector} = \frac{Q_{rad}}{800W/m^2} = \frac{21.09 \cdot 10^6}{800 \cdot 0.734} = 35916.2m^2 \tag{14.2}$$

The collector surface needed for reaching the amount of solar heat required are 35916.2 m^2. The collector surface is the mirrored surface needed for absorbing the radiation, which is

different from the total surface of the solar field. The rows of collector have to keep a distance between them because of the shading effects for low incident angles. This distance is approximated as three times the diameter of the collectors and it allows us to determine the land surface necessary for installing the solar field.

Assuming that the land use factor is 3.5, the total surface required for installing the solar field is:

$$A_{solarfield} = A_{collector} \cdot 3.5 = 125706.7m^2 \tag{14.3}$$

For the study we assume estimated specific costs for the PPC technology of around 60 €/m^2. By multiplying the collector price per square meter and the square meters of collector surface we can calculate the capital expenditure (CAPEX):

$$CAPEX = 35916,2m^2 \cdot 60€/m^2 = 2154972€ \tag{14.4}$$

That is the required initial investment for building the solar field at the beginning of the construction. But for paying the construction during the period of operation of the solar field we have to calculate the annuity. The annuities are the fixed payments which have to be done every year during the predicted life of operation of the solar field for pay off the initial investment. The annuity includes the price of the construction and the increase of interest rate every year.

Considering a period of operation of 15 years (T) and an interest rate of 8% (r), the annuity is calculated as:

$$a = \frac{(1+r)^T \cdot r}{(1+r)^T - 1} = 0.1168year^{-1} \tag{14.5}$$

And the yearly payment is:

$$CAPEX \cdot a = 2154972€ \cdot 0.1168year^{-1} = 251700.7€/year \tag{14.6}$$

which in 15 years add makes a total of:

$$251700,7€/year \cdot 15years = 3775510.94€ \tag{14.7}$$

The difference of power that we could obtain by boosting the CCPP with the solar field is:

$$\Delta P_{30°C} = P_{solar30°C} - P_{30°C} = 130.36 - 122.49 = 7.87MW \tag{14.8}$$

$$\Delta P_{45°C} = P_{solar45°C} - P_{45°C} = 123.03 - 115.39 = 7.64MW \tag{14.9}$$

The assumption is that the CCPP is currently in operation and it is situated in Almería, in the south of Spain. Taking a look at the weather conditions from *TRANSYS-Database MEteotest* we can know how many days with enough radiation we can expect for running the solar field. The minimum incident radiation is assumed to be 600 MW/m^2. The number of hours with at least this minimum radiation are shown in Table 28.

By multiplying the number of hours of supposed operation of the solar field per year and the energy that we can obtain from it, we know the MWh that the solar field delivers per year:

$$7.87MW \cdot 689hours = 5422.43MWh_{30°C} \tag{14.10}$$

Temperature	$N°$ hours	$N°$ hours with $Q_{rad} \geq 600 W/m^2$
$20 \leq T < 30$	3184	689
$T > 30$	191	88

Table 28: $N°$hours with enough radiation energy for operating the solar field

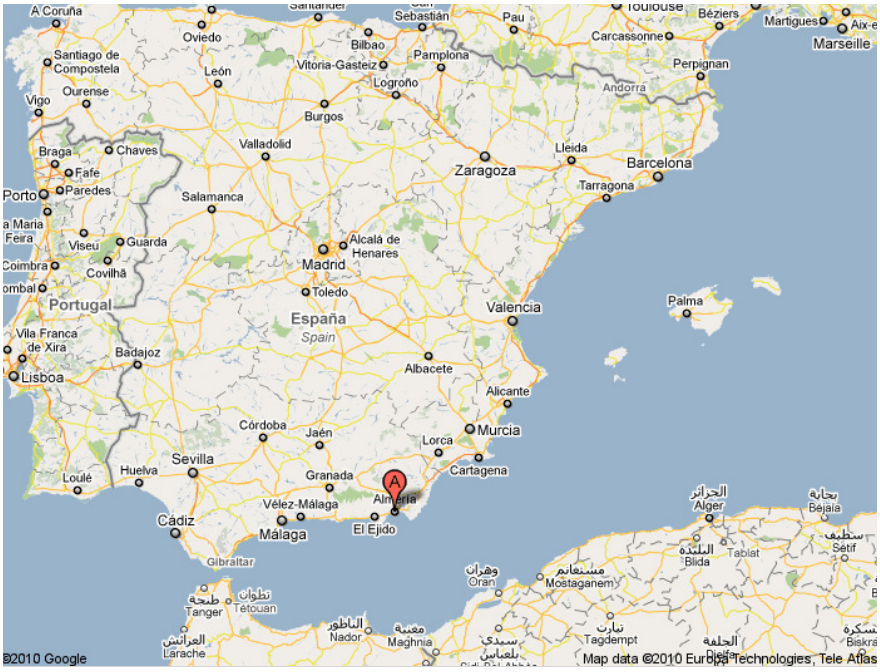

Figure 14.2: Location of the CCPP, www.Google.com

$$7.64MW \cdot 88hours = 672.32MWh_{45°C} \tag{14.11}$$

$$Total = 6094.75MWh \tag{14.12}$$

To calculate the cost of electricity (CoE) we assume the operating cost (OPEX) to be equivalent to the 2% of the specific capital expenditure,

$$CoE = \frac{CAPEX \cdot a}{\sum MWh} + \frac{OPEX}{\sum MWh} \tag{14.13}$$

$$CoE = \frac{CAPEX \cdot a}{\sum MWh} + \frac{0.02 \cdot CAPEX}{\sum MWh} = 48.36€/MWh \tag{14.14}$$

Producing one MWh of electricity with the CCPP and the solar field using PPC technology cost 4.836 $c€/kWh$.

14.2 Parabolic Trough Concentrators (PTC)

In this chapter the same economic evaluation will be done but now the technology used in the solar field are the parabolic trough concentrators (PTC). The CCPP and its location are exactly the same so the calculations for the weather conditions done for PPC are also valid for PTC.

The maximum optical efficiency for the PTC is η_{opt}=0.75 and the necessary radiation absorbed by the solar field has to be:

$$Q_{rad} = \frac{Q_{th}}{\eta_{opt}} = \frac{21.09}{0.5} = 28.12MW \tag{14.15}$$

The specific power absorbed by the collectors coincides with the case of PPC, 800 W/m^2, being the necessary heat absorbed:

$$A_{collector} = \frac{Q_{rad}}{800W/m^2} = \frac{21.09 \cdot 10^6}{800 \cdot 0.75} = 35150m^2 \tag{14.16}$$

And the necessary land extension considering a land use factor of 3.5 are:

$$A_{solarfield} = A_{collector} \cdot 3.5 = 123025m^2 \tag{14.17}$$

For PTC technology the cost of the collector is assumed to be around 280€/m^2, [14] and the initial investment required for the construction of the solar field:

$$CAPEX = 35150m^2 \cdot 280€/m^2 = 9842000€ \tag{14.18}$$

For the same expected period of operation the annual payments are equivalent to:

$$CAPEX \cdot a = 9842000€ \cdot 0.1168year^{-1} = 1149545.6€/year \tag{14.19}$$

which at the end makes a total of:

$$251700,7€/year \cdot 15years = 17243184€ \tag{14.20}$$

And the CoE:

$$CoE = \frac{CAPEX \cdot a}{\sum MWh} + \frac{OPEX}{\sum MWh} = 220.91€/MWh \tag{14.21}$$

The cost of producing one MWh of electricity with the PTC technology is 22.091 c€/kWh, which is more expensive than with conventional technologies or the PPC and for that reason less attractive.

15 Economic Analysis of the Three Pressure CCPP with Increased Solar Boosting

Until now we have done the calculations for knowing the costs of producing one MWh of electricity but we have only considered a range of temperatures between 20° C and 45° C. That was because we had a built CCPP with a steam turbine and the injection of solar steam was only possible when the mass of the steam turbine was smaller than in nominal conditions. Now, we will consider a built CCPP but our steam turbine is big enough and the injection of solar steam is possible in all the range of temperatures. Even in ISO conditions there are no additional costs of injecting solar steam because all the components of the CCPP can afford an increment of mass flow in the circuit.

The mass of steam injected in the new design case will be 12% of the nominal steam in

ISO conditions for the case without solar boosting, which are 8.75 kg/s. The total heat needed for injecting that mass in ISO conditions are 21.48 MW of thermal heat.

The difference of power that we could obtain in ISO conditions:

$$\Delta P_{ISO} = P_{solarISO} - P_{ISO} = 145.96 - 138.5 = 7.46MW \tag{15.1}$$

and taking into account that the number of hours with enough radiation for running the solar system are shown in Table 29:

Temperature	$N°$ hours	$N°$ hours with $Q_{rad} \geq 600W/m^2$
$0 \leq$ T < 20	5386	526
$20 \leq$ T < 30	3184	689
T > 30	191	88

Table 29: $N°$hours with enough radiation energy for operating the solar field

By multiplying the new number of hours of operation of the solar field and the power that we could obtain by using it, we know the MWh that the solar field produces:

$$7.87MW \cdot 689hours = 5422.43MWh_{30°C} \tag{15.2}$$

$$7.64MW \cdot 88hours = 672.32MWh_{45°C} \tag{15.3}$$

$$7.46MW \cdot 526hours = 3923.96MWh_{ISO} \tag{15.4}$$

$$Total = 10018.71MWh \tag{15.5}$$

By taking advantage of the radiation even in ISO conditions we can produce about 3900 MWh more that in the case before by not increasing too much the costs. As we said, the CCPP will be the same and the only thing which increases the investment in the installation is a bigger solar field because now it has to absorb more radiation.

15.1 Pneumatic Pre-Stressed Concentrators (PPC)

The calculations for the new solar field with PPC technology are presented in the following. The values of optical efficiencies and land use factors are the same that in the chapter before.

The collector surface needed for absorbing 21.48 MW of thermal heat are:

$$A_{collector} = \frac{Q_{rad}}{800W/m^2} = \frac{21.48 \cdot 10^6}{800 \cdot 0.734} = 36580.4m^2 \tag{15.6}$$

and taking into account the land use factor:

$$A_{solarfield} = A_{collector} \cdot 3.5 = 128031.33m^2 \tag{15.7}$$

The necessary initial investment for performing the construction of the solar field:

$$CAPEX = 36580.4m^2 \cdot 60€/m^2 = 2194822.89€ \tag{15.8}$$

Finally, the cost of the electricity using the bigger solar field:

$$CoE = \frac{CAPEX \cdot a}{\sum MWh} + \frac{OPEX}{\sum MWh} = 29.97€/MWh \tag{15.9}$$

With PPC technology and running the solar field joined the CCPP at all operation temperatures the cost of electricity decreases and it is even more competitive. With this configuration we will obtain benefits from the first day of operation.

15.2 Parabolic Trough Concentrators (PTC)

For the PTC technology, the collector surface and the surface needed for building the solar field are:

$$A_{collector} = \frac{Q_{rad}}{800W/m^2} = \frac{21.48 \cdot 10^6}{800 \cdot 0.75} = 35800m^2 \tag{15.10}$$

$$A_{solarfield} = A_{collector} \cdot 3.5 = 125300m^2 \tag{15.11}$$

The initial investmet:

$$CAPEX = 35800m^2 \cdot 280€/m^2 = 10024000€ \tag{15.12}$$

And the cost of producing one MWh of electricity:

$$CoE = \frac{CAPEX \cdot a}{\sum MWh} + \frac{OPEX}{\sum MWh} = 136.87€/MWh \tag{15.13}$$

With PTC technology this cost is higher, because although is a mature and proven technology its specific cost is still high and compared with PPC technology is not a competitive technology.

16 Conclusion and Summary

As a conclusion of our study, we will discuss the results obtained in the technical and economic analysis for the different cases and technologies used. Table 30 shows the comparison between the two proposed technologies.

The main results of the technical analysis were:

- For a 9FA Three Pressure CCPP designed and strictly limited by the ISO case, approximately 7 additional MW_e (2% of the installed CCPP power) can be obtained at 30°C, at a gross thermal efficiency of 37% by injecting to the steam cycle 21 MW_{th} of solar heat with the saturated high pressure method.
- In the case of the cold reheat steam injected to the cycle, also approximately 7 MW_e can be obtained at 3030°C of ambient temperature, at a gross thermal efficiency of almost 30%.

Comparing these results we can conclude that for obtaining the same amount of power output the size of the solar field whit the SHP is smaller. We will use the SHP in the construction of the solar field project.

Cases	Power	Techn.	CAPEX (€)	Land surface (m^2)	CoE($c€/kWh$)
Solar Boosting	6094.75	PPC	2154972	125706.7	4.836
20° C<T<45° C	MWh	PTC	9842000	123025	22.091
Increased S. Boosting	10018.71	PPC	2194823	128031.3	2.997
0° C<T<45° C	MWh	PTC	10024000	125300	13.687

Table 30: Comparison betwen different technologies and configuration for producing electricity

As the PTC technology has a better optical efficiency the amount of radiation absorbed per unit of surface is bigger than with PPC technology. That means that the land surface needed for the PTC technology is smaller than for the PPC technology. But the fact that the cost of the PPC technology is much smaller than the PTC technology, makes PPC a more attractive technology due to its higher profitability.

Taking into account that producing one kWh of electricity with conventional technologies costs about 5-6 $c€/kWh$ we can conclude that the PPC allows us to obtain a competitive price of electricity by using a cleaner technology. That means that the construction of the solar field for helping the CCPP is a feasible project and the initial investment will be recovered plus benefits.

Besides, running the solar field for a range of temperatures between 0° C to 45° C, allows us to obtain higher radiation with approximately the same costs. The difference between solar boosting and the increased solar boosting is the more expensive solar field due to its wider extension, but with the benefits of producing more solar energy and reducing the costs of electricity production.

References

[1] Saravanamuttoo,H.I.H., Rogers, G.F.C., Cohen H., Gas Turbine Theory, Pearson Education, Cornwall, 2001.

[2] Fundamentals of Gas Turbines, William B., John Wiley and Sons, Inc., United States of America, 1996.

[3] Boyce, M., Handbook for Cogeneration and Combined Cycle Power Plants, Asme Press, New York, 2002.

[4] Boyce, M., Ph.D and P.E., Gas Turbine Engineering Handbook, Butterworth-Heinemann, Oxford, 2006.

[5] Ganapathy, V., Industrial Boilers and Heat Recovery Steam Generators, Marcel Dekker,Inc., New York, 2003.

[6] Petchers, N., Combined Heating, Cooling and Power Handbook, Marcel Dekker, Inc., New York, 2003.

[7] Lechner, C., Seume, J., Stationäre Gasturbinen, Springer, Berlin, 2003.

[8] Wengenmayr,R., Bührke, T., Renewable Energy, Wiley-VCH, Weinheaim, 2008 .

[9] Abengoa Solar, www.abengoasolar.com, 2010.

[10] Birnbaum, J., Eck M., Fichtner, M., Hirsch, T., Lehman, D., Zimmermann, G., A Direct Steam Generation Solar Power Plant with Integrated Thermal Storage, 2008.

[11] Herrmann, U., Nava, P., Performance of the Skal-et Collectors of the Andasol Power Plants

[12] Zarza, E., López, C., Cámara, A., Martínez, A., Burgaleta, J. I., Martín, J. C., Fresneda, A., Almería GDV The first Solar Power Plant with Direct Steam Generation.

[13] General Electric Energy, www.gepower.com, 2010

[14] Hartl, M., Ponweiser, K., Haider, M., Tiefenbacher, F., Comparison of a Prestressed Pneumatic Concentrator CSP System with Conventional Systems.

[15] Willinger, R., Thermische Turbomaschinen, Lecture notes, TU Wien, 2008.

[16] Dolezal, R., Kombinierte Gas und Dampfkraftwerte, Springer Verlag, Berlin, 2001

[17] Steiner, A., Numerische Prozesssimulation von Thermischen Energieanlagen, Lecture Notes, 2009.

[18] Elsaket G., Simulating the Integrated Solar Combined Cycle for Power Plants Application in Libia, Cranfield University, 2007.

[19] Desertec-UK, www.trec-uk.org.uk, 2010

[20] Kreuzer D., Dynamic Simulation of a Combined Cycle Power Plant, ITE Department of Thermodynamics and Thermal Engineering, TU Vienna, 2008.

[21] Effenberger, H., Dampferzeugung, Springer Verlag, Berlin, Heidelberg, New York, 2000.

[22] Wikipatents, www.wikipatents.com, 2010.